

HOCHSCHULE LUZERN

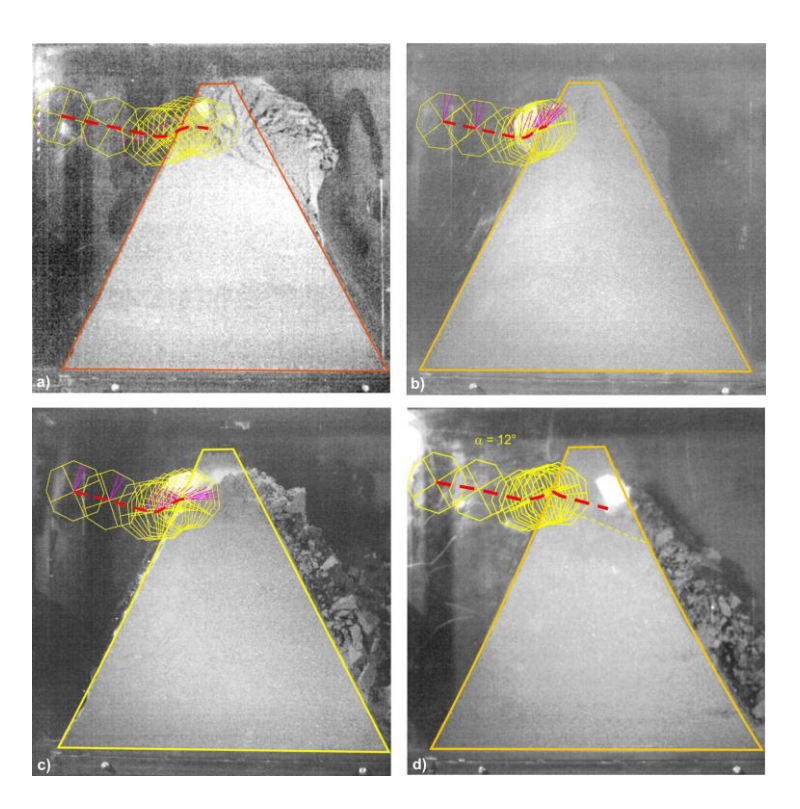
Technik & Architektur

Analysis of Existing Rockfall Embankments of Switzerland (AERES)

Part C: Small-scale experiments

Bernd KISTER¹ and Stéphane LAMBERT²

- ¹ Lucerne University of Applied Sciences and Arts, Technikumstrasse 21, CH 6048 Horw, Switzerland. Current position: kister geotechnical engineering & research, Neckarsteinacher Str. 4 B, D Neckargemünd, +49 6223 71363, kister-ger@t-online.de
- ² Irstea, 2 rue de la papeterie, 38402 Saint Martin d'Hères cedex, France, + 33 4 76 76 27 94, stephane.lambert@irtsea.fr



Commissioned by the Federal Office for the Environment (FOEN)

July 2017 2/90

Analysis of Existing Rockfall Embankments of Switzerland (AERES), part C

Imprint

Commissioned by

Federal Office for the Environment (FOEN), Hazard Prevention Division, CH-3003 Bern. The FOEN is an agency of the Federal Department of the Environment, Transport, Energy and Communications (DETEC).

Contractors

Lucerne University of Applied Sciences and Arts, CH-6048 Horw Irstea, F-38402 Saint Martin d'Hères

Authors

Bernd Kister Stéphane Lambert

FOEN support

Bernard Loup, Hazard Prevention Division Arthur Sandri, Hazard Prevention Division

Notes

The AERES report consists of three parts:

- Part A: State of knowledge
- Part B: Analysis of the collected data and comparison with up-to-date knowledge
- Part C: Small-scale experiments

This study/report was prepared under contract to the Federal Office for the Environment (FOEN). The contractor bears sole responsibility for the content.

Suggested form of citation for Part C

Kister B., Lambert S. 2017: Analysis of Existing Rockfall Embankments of Switzerland (AERES); Part C: Small-scale experiments. Federal Office for the Environment, Bern, 90 p.

Content

1.	1. Introduction		
2.	Quasi-	-2D-Experiments	7
	2.1.	Experimental set-up	7
	2.2.	Embankment material	9
	2.3.	Preparation of embankment models	12
	2.4.	Geometry of embankment models	13
	2.5.	Scaling factor	15
	2.6.	Executed tests	16
3.	Test re	esults	19
	3.1.	Impact angle, block velocity and energy before impact	19
	3.2.	Block movement after contact	
	3.3.	Block deceleration due to impact	41
	3.4.	Drop of energy due to impact	61
	3.5.	Direct measurement of deceleration	65
	3.6.	Displacement inside the embankment due to impact	70
4.	Conclu	usions	75
	4.1.	Influence of embankment's uphill slope inclination	75
	4.2.	Influence of block rotation	79
	4.3.	Influence of block shape and freeboard	80
	4.4.	Embankments with rockery on both slopes	80
	4.5.	Dissipation of energy	83
	4.6.	General remarks	83
	47	Need for further research	84

Appendix

- C1 Block data: Velocities and energies
- C2 Block deceleration with time due to impact opposed to embankment's destruction

1 Introduction

Hofmann & Mölk (2012) have done small scale tests on embankments with and without riprap at the uphill slope (Fig. 1.1a). They stated that the impacting sphere will not move upward in case of riprap on the slope while the impacting sphere was rolling or jumping towards the embankment's crest in the case of pure-earth embankments as well as in the case of reinforced embankments with geogrids. Fig. 1.1 shows the riprap used by Hofmann & Mölk in their experiments in comparison to a real embankment in Switzerland with rockery at the uphill slope. It seems to be that the relative surface roughness of the riprap used by Hofmann & Mölk (2012) shows a larger unevenness than that one of the real embankment, especially in the context of the corresponding block diameter.





Fig. 1.1: a) riprap used in the tests of Hofmann & Mölk (2012), b) rockery surface of embankment Gretla, Canton Grisons (Photo: Tiefbauamt Graubünden).

The statements of Hofmann & Mölk concerning the freeboard have been transferred to the Austrian technical guideline ONR 24810:2013 and it is said that the freeboard for an embankment with riprap and a slope angle of 50° or more should be at least one block diameter while for an embankment without riprap or geogrid reinforcement the freeboard should be at least two block diameters. For an embankment with geogrid reinforcement and a slope angle of 60° or more the freeboard should be at least 1.5 block diameter, for an embankment with geogrid reinforcement and a slope angle of 70° or more the freeboard should be at least one block diameter. Fig.1.2 shows a comparison for the embankment height for an example of a block with a 2 m diameter and an impact height of 2 m. The impact height is measured from the block center to the ditch level.

According to Fig. 1.2 the embankment height in this example may vary between 3.8 m and more than 5 m depending on what kind of construction will be selected. The smallest embankment height is achieved using rockery at the uphill slope and a slope angle of 50° . But Kister (2015) has shown by small-scale and half-scale experiments that the uphill slope of a rockfall protection embankment should be constructed at least with an angle of 60° . However no riprap had been used in those tests, the embankment models had been constructed by pure soil. Moreover in practice an embankment slope made of rockery will not be constructed with a slope angle of about 50° , but with a slope angle in the range of 60° to 80° (see part B of the report).

July 2017 5/90 Analysis of Existing Rockfall Embankments of Switzerland (AERES), part C

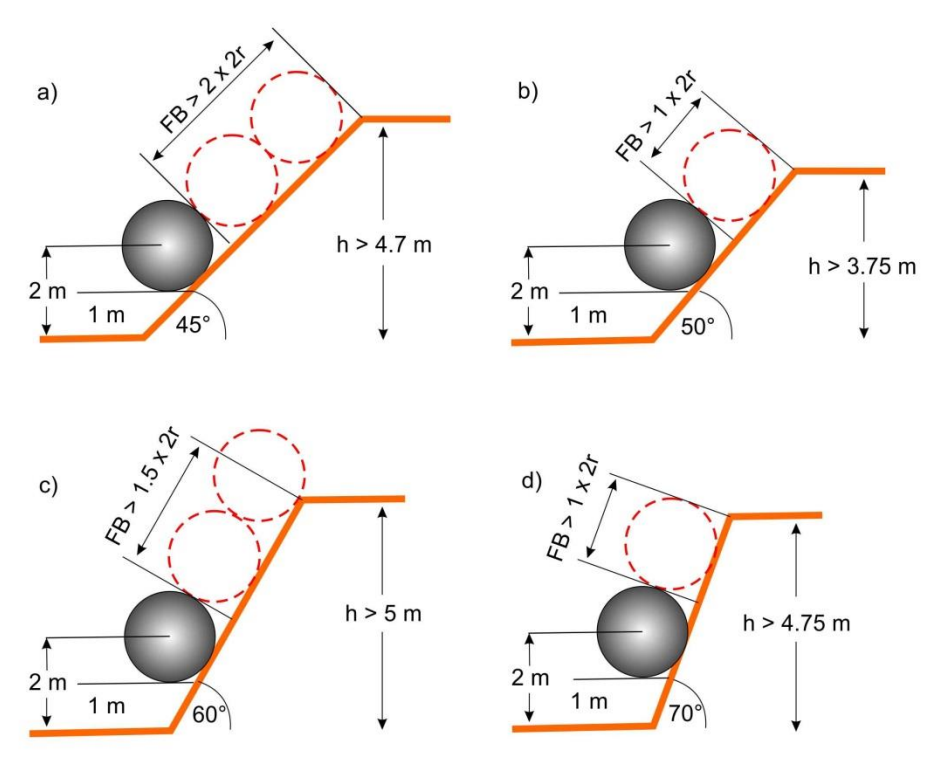


Fig. 1.2: Minimum height of a rockfall protection embankment according to ONR 24810:2013 for a block with diameter 2 m and an impact height of 2 m (based on the block center), a) pure earth embankment without riprap / rockery and slope angle approx. equal to debris friction angle of about 45° , b) embankment with riprap / rockery and a minimum slope angle of at least 50° , c) embankment reinforced with geogrids and slope angle 60° , d) embankment reinforced with geogrids and slope angle 70° .

In Switzerland rockfall protection embankments with rockery at the uphill slope is a very common construction type (see part B of the report). There are examples with rockery up to the crest while other designers preferred a construction where the upper part of the embankment had been made only of soil. Whereas at the first construction type the slope follows a straight line, at the second construction type the slope has a bi-linear profile. Both types of slopes have been investigated by small-scale quasi-2D-impact experiments (Fig. 1.3).

To investigate the influence of roughness of the rockery in the small-scale quasi-2D-impact tests two types of stone arrangement had been used:

- Stones had been placed parallel to the slope angel. This resulted in a relatively smooth slope surface (Fig. 1.3a).
- Stones had been placed with its largest dimension horizontally. This resulted in a stepped surface for the slope, i.e. in a rough slope surface (Fig. 1.3b).

Due to limit available place some embankments had been constructed with rockery at both slopes. The behavior of such a construction under impact load was also investigated.

July 2017 6/90 Analysis of Existing Rockfall Embankments of Switzerland (AERES), part C

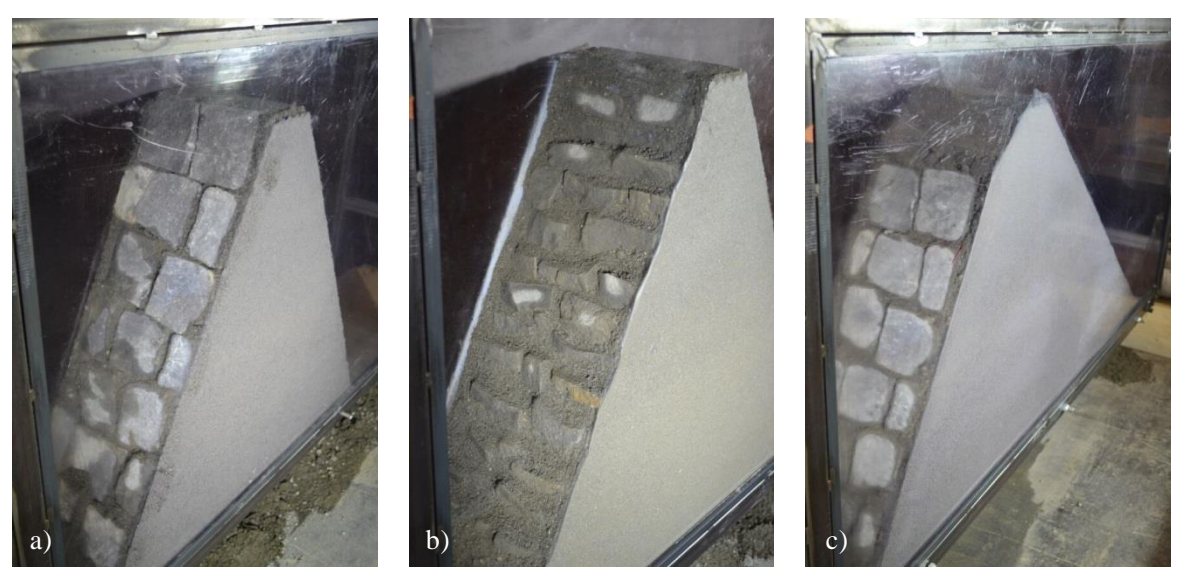


Fig. 1.3: Orientation of stones at the "uphill" slope: a) upright, b) horizontal, c) upright, upper part of the slope without stones, but with a reduced slope angle.



Fig. 1.4: Example of a rockfall protection embankment in Canton Valais with rockery placed in the lower part and soil at the upper part of the uphill slope. The surface roughness of the rockery may be described as smooth and is comparable with the surface roughness in Fig. 1.3a) and c) (Photo: S. Lambert).

2 Quasi-2D-Experiments

2.1 Experimental set-up

Quasi-2D-embankment models made of sand and with a thickness of 20 cm have been constructed in a box with one side made of acrylic glass to observe the impact by a high-speed camera (Fig. 2.1, on the left). The impact process was recorded with a frame rate of 500 Hz that is 1 picture every 2 x 10⁻³ s. To analyze the displacement field inside the embankment the Particle Image Velocimetry (PIV) has been used. The procedure the PIV was used is described in Kister (2015).

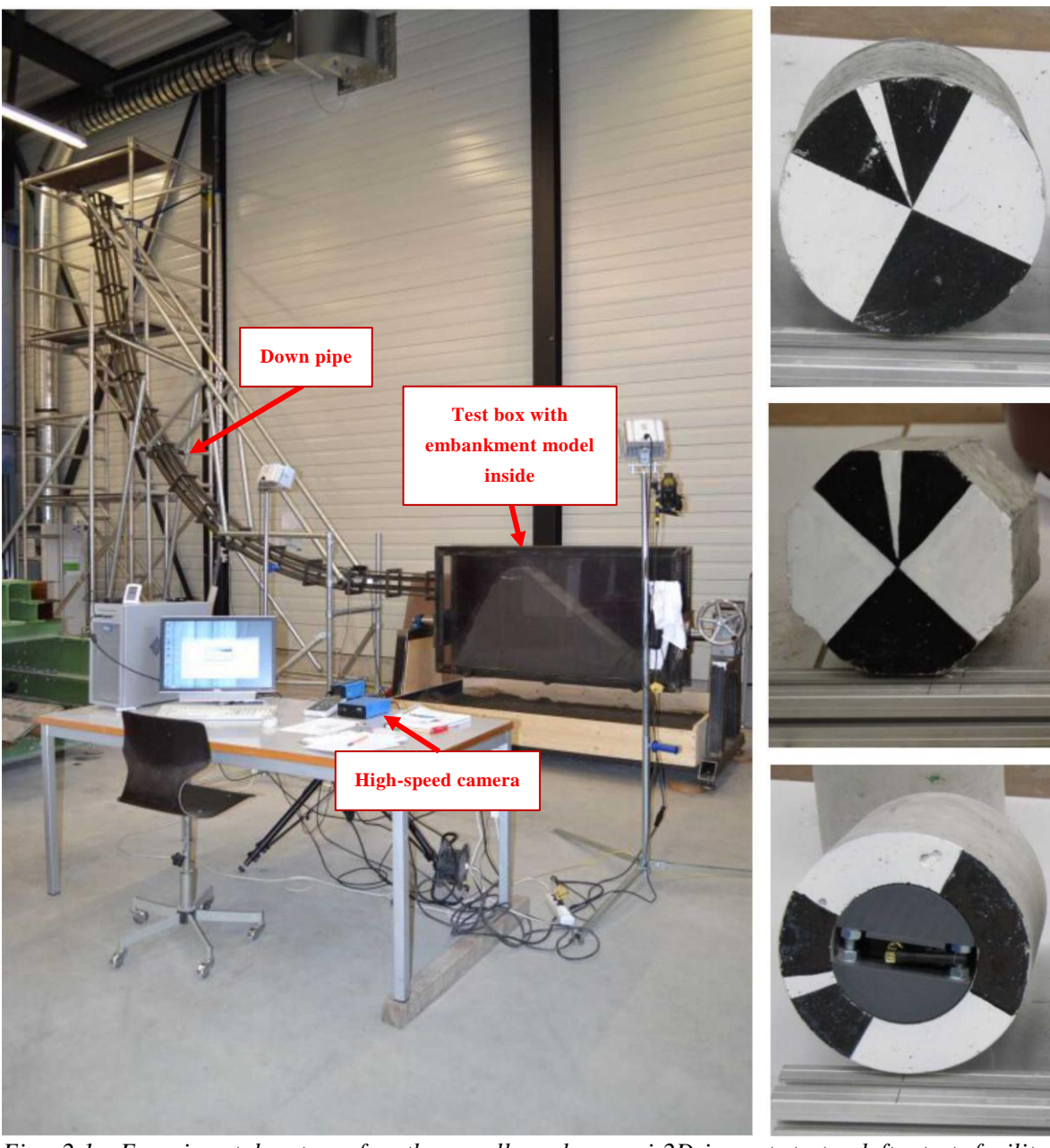


Fig. 2.1: Experimental set-up for the small scale quasi-2D-impact tests, left: test facility, right: impactors G (at the top), OKT (central) and GS with triaxial acceleration sensor (bottom).

July 2017 8/90 Analysis of Existing Rockfall Embankments of Switzerland (AERES), part C

Small scale experiments had been executed with a cylinder G, a hollow cylinder with an acceleration sensor inside GS and an impacting body with octagonal cross-section OKT (Fig. 2.1, on the right). The impactors G and OKT are made totally of concrete. In a first test the impactor GS was also made of pure concrete, but was destroyed in the test on the stony slope. So a new impactor GS with higher capability of resistance had to be built. The new impactor GS has a steel lining as exterior facing and an aluminum lining as inner facing. The annulus space was filled with concrete.

Body	Material	caliber	weight
Cylinder G	Concrete	Diameter: 16 cm	7.44 kg
	Jacket: Steel	External diameter: 16 cm	
Hollow cylinder	Body: concrete		6.76 kg
GS	Core retainer: Aluminum	Inner diameter: 9.4 cm	
Body OKT	Concrete	Distance between 2 sides: 14.8 cm	6.77 kg

Table 2.1: Material, dimensions and weights of the impactors used in the tests. Height of all impactors: 16 cm.

The sensor used inside the impactor GS was a triaxial acceleration sensor with measurement range \pm 200 g. The sensor was placed together with a mini data logger inside the hollow cylinder (Fig. 2.2).



Fig. 2.2: Triaxial acceleration sensor and mini data logger inside impactor GS.

The impacting bodies have been accelerated by gravitational acceleration and with the help of a kind of down pipe with a rectangular cross section (Fig. 2.1). Because of friction between the impacting bodies and the down pipe the impacting bodies start to rotate when moving down the down pipe.

The down pipe was mounted at a framework in such a manner that the complete down pipe could be rotated to a certain extent. This rotation results in a modification of the angle of impact. Tests have been done with two different adjustments of the down pipe. In most tests of this test series an inclination at the exit of 9.3° was used. Additional a few tests have been done with an inclination at the exit of approx. 1.3° (Fig. 2.3).

July 2017 9/90 Analysis of Existing Rockfall Embankments of Switzerland (AERES), part C



Fig. 2.3: Inclinations of the down pipe exit used in the tests.

2.2 Embankment material

The construction material for the embankments was made by mixing 2 different sands and fine gravel. The mix was done in such a way, that the resulting soil was very similar in its grain-size distribution to that one used by Blovsky (2002). Fig. 2.4 shows the grain-size distribution of both soils for comparison and also the grain-size distribution of the construction material of a prototype embankment specified by Blovsky (2002).

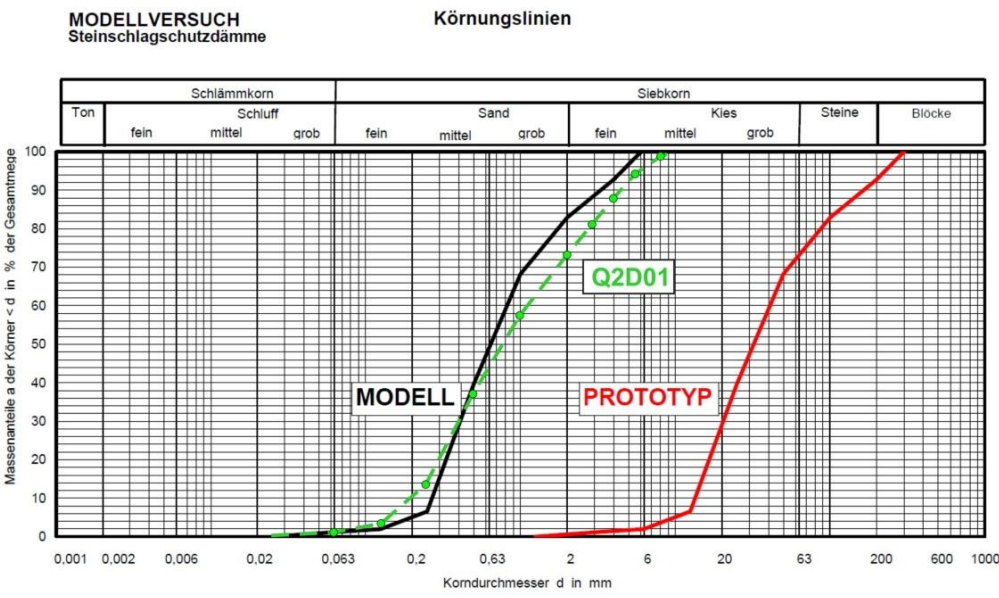


Fig. 2.4: Comparison of the grain-size distribution of the material Q2D01 used in the tests with the grain-size distribution of the model sand used by Blovsky (2002) and the grain-size distribution of the construction material specified by Blovsky for a prototype embankment.

While constructing the embankment models the mass of soil, which was used for the construction, was measured to determine the soil density. If no stones are used in the model to represent the rockery, the embankment volume could be easily calculated. But if stones had been used it was necessary to subtract the volume of the stones from the total embankment volume to get a proper estimation of the soil volume for density calculation. To simplify matters also the weight of the stones had been determined and the stone volume was calculated using the stone density. This stone volume was subtracted from the total embankment volume and with the remaining volume the soil density was determined. Fig. 2.5 shows the frequency distribution of the determined densities, the average density of the soil had been determined to 1840 kg/m³.

July 2017 10/90 Analysis of Existing Rockfall Embankments of Switzerland (AERES), part C

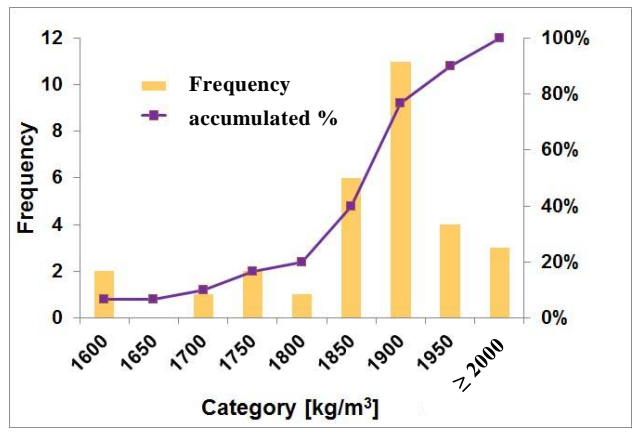


Fig. 2.5: Frequency distribution of the measured density.

At the end of a test, 3 soil samples had been extracted to determine the water content. The minimum value of the water content in the test series was determined to 4.3%, the maximum value of the water content in the test series was determined to 9.1%. As average value over all tests a water content of 6.3% has been determined. The frequency distribution of the water content of all measurements is shown in Fig. 2.6.

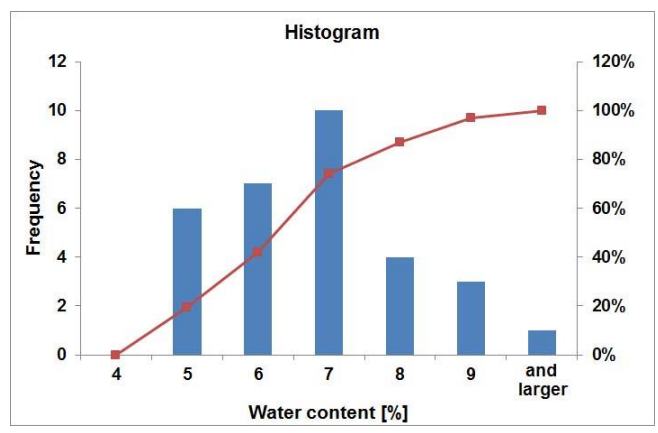


Fig. 2.6: Frequency distribution of the water content of all measurements.

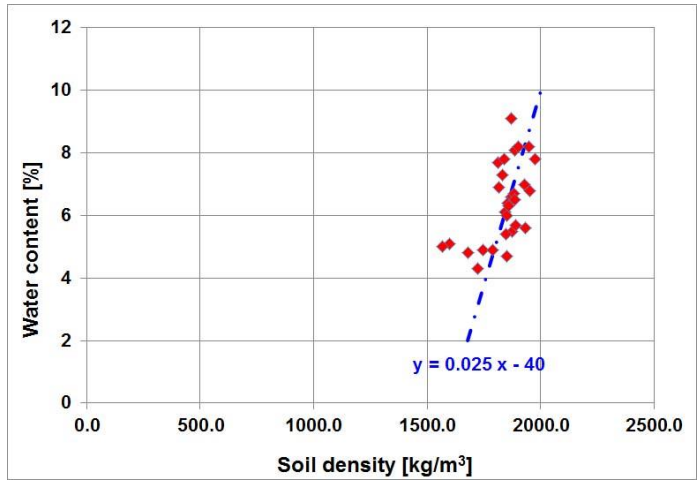


Fig. 2.7: Water content versus soil density of soil Q2D01 in the test series.

Fig. 2.7 shows the water content versus soil density for soil Q2D01. The graph shows that the relationship between soil density and water content may be described approximately by the linear function y = 0.025 x - 40 for the test conditions.

Additional to the tests shown before, the soil Q2D01 was filled in layers into a barrel and compacted. The same procedure was used as for the construction of the embankments. Then a dynamic cone penetrometer test was carried out and CBR values as well as resilient modulus M_R were determined (Fig. 2.8). The resilient modulus M_R was determined according to the formula given by George & Uddin (see TRB, 2008):

$$M_R = 235.3 \cdot DCPI^{-0.48}$$

The resilient modulus is a stiffness parameter, which describes the soil's ability to store and to release elastic energy during a dynamic load and unload process. But it is not a parameter to describe failure. With the formula of George & Uddin the resilient modulus for soil Q2D01 was determined to be in the range of 50 to 70 MPa (Fig. 2.8, left hand). The first 3 measurement points in the diagram had been neglected because of insufficient overburden at the beginning of the test.

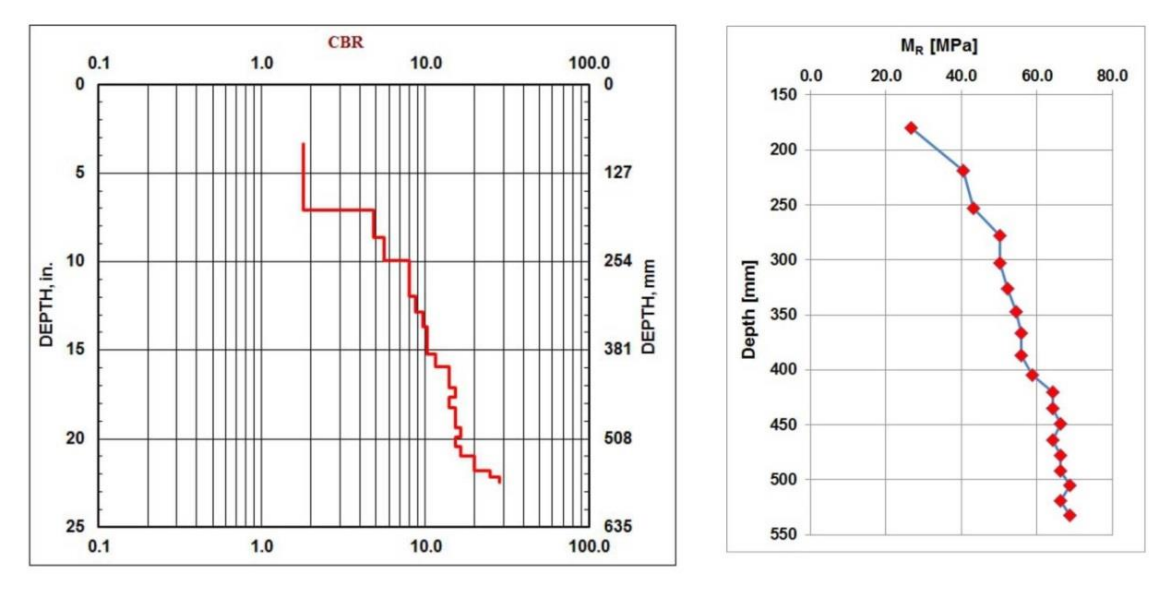


Fig. 2.8: Results of dynamic cone penetrometer test on soil Q2D01

The friction angle of soil Q2D01 was estimated by applying Dhawan's method on the grain-size distribution shown in Fig. 2.4. A friction angle of 39° was estimated for a middle degree of compactness and 45° for a high degree of compactness.

The "rockery" used in the models have been constructed with a local siliceous sandstone called Guber-Quarzsandstein. This material is mined at the stone quarry Guber near Alpnach and shows a real high toughness. To determine the rock density, the static elastic parameters and the uniaxial compressive strength two specimens had been drilled out of a larger block (Fig. 2.9, left). The mean value of the rock density was determined to be $\rho_{St} = 2617 \text{ kg/m}^3$. The results of the laboratory tests on the 2 specimens are shown in table 2.2.

July 2017 12/90 Analysis of Existing Rockfall Embankments of Switzerland (AERES), part C

Specimen	Uniaxial compressive strength	Young's modulus	Poisson's ratio
	σ_{ucs}	$\mathrm{E}_{\mathrm{stat}}$	v_{stat}
	$[MN/m^2]$	[GPa]	[-]
P1	190	47 (40 – 100 MPa)	0.28 (40 – 100 MPa)
P2	172	63 (40 – 100 MPa)	0.34 (40 – 100 MPa)

Table 2.2: Uniaxial compressive strength, Young's modulus and Poisson's ratio of Guber-Quarzsandstein, load range 40-100 MPa.





Fig. 2.9: Left: Block of Guber-Quarzsandstein and specimens P1 and P2, which had been used for uniaxial compression test, right: Selected pieces of Guber-Quarzsandstein before placed in the model embankment.

2.3 Preparation of embankment models

The geometry of the model embankments was constructed by using two panel sheets, which had been placed inside the box (Fig. 2.10, on the left). To construct the embankment the box was turned upside down (Fig. 2.10, on the right) and the soil and stones had been placed in the box by layers. Every soil layer has been carefully compacted. Joints between the masonry stones have been filled with soil.





Fig. 2.10: Left hand: Test box in horizontal position with already installed panel sheets. Right hand: Test box in upside down position ready for filling with soil material. Insulating wall panels (in yellow) had been used for varying the crest's dimension without changing the slope inclination.

After completion of the embankment construction the bottom plate was mounted and then the box was turned in upright position (Fig. 2.11, on the right). Now the cover plate and both panel sheets were removed and the embankment was ready for a test.

July 2017 13/90 Analysis of Existing Rockfall Embankments of Switzerland (AERES), part C





Fig. 2.11: Left hand: Planing of the embankment's base before the bottom plate is mounted. Right hand: Test box in upright position. Cover plate and both panel sheets are still in place.

2.4 Geometry of embankment models

The main scope of work was to study the impact onto an embankment slope with rockery. Due to this the slope angle at the "uphill side" of the embankment was chosen to be rather steep. Most tests have been done with a batter of 2:1 (approx. 63°). A few tests have been done with a steeper slope, i.e. a batter of 5:2 (approx. 69°) resp. 5:1 (approx. 80°).

At the "downhill slope" most tests have been done with a batter of 2:1. But for comparison with the tests described by Kister (2015) also embankments with a batter of 4:5 have been used in the tests. Fig. 2.12 gives an impression of the used cross sections of the model embankments.

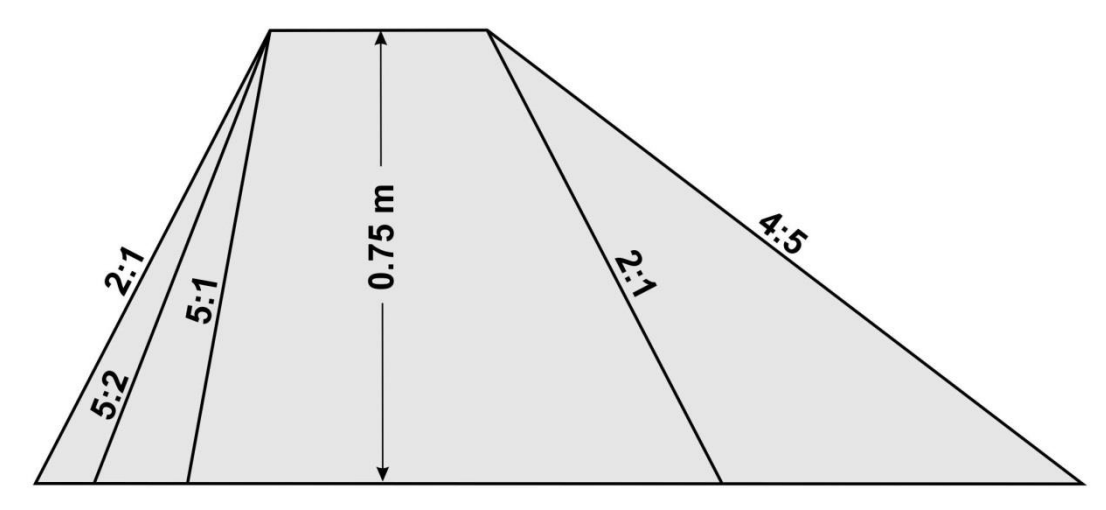


Fig. 2.12: Different slope angles used in the tests.

The visible height of the model embankments in the test box was in all tests 0.75 m. For the total height of the embankments 2 cm have to be added at the basement. This part is hidden by the framework of the test box.

As already shown by Kister (2015) the relationship between the size of the impacting block and the embankment's crest is very significant. The impact tests on pure soil model embankments showed that the embankment crest should be at least 1.2 times the diameter of the dimensioning bloc. Hereby it is assumed that the freeboard is at least 0.8 times the block diameter.

Because of the significance of the relationship between the size of the impacting block and the width of the embankment's crest on one hand and the assumption that the "rockery" will increase the capability of resistance of the embankments on the other hand, two classes of tests on embankments with "rockery" have been executed. In class 1 the crest width was chosen to be smaller than the block diameter. The mean value of the ratio crest width a_c to block diameter 2r is approximately 0.5. In class 2 the crest width a_c was chosen to be larger than the block diameter 2r. In this case the mean value of the ratio $a_c/2r$ is approximately 1.1.

Additional to the embankment geometry described in Fig. 2.12, an embankment cross-section had been used in the tests, which was constructed with a bi-linear slope at the "uphill side". At the slope's lower part stones had been placed, while the upper part of the "uphill side" was made of soil (Figures 2.13 and 1.3c). The use of this type of geometry in the test series was a result of the interviews done with representatives of the cantons and consulting engineers.

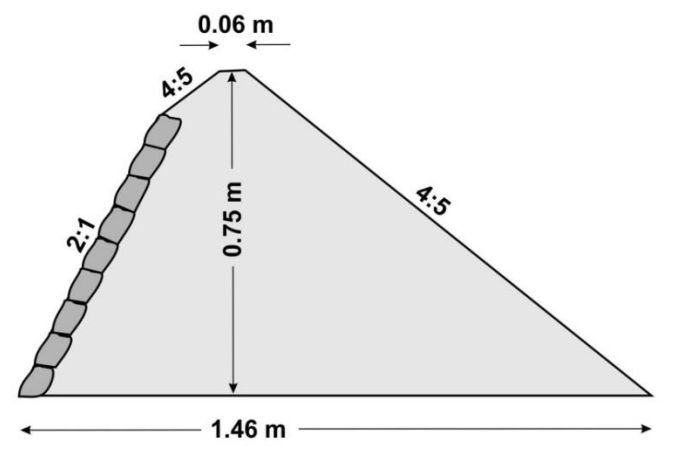


Fig. 2.13: Embankment cross-section with a bi-linear slope at the "uphill side".

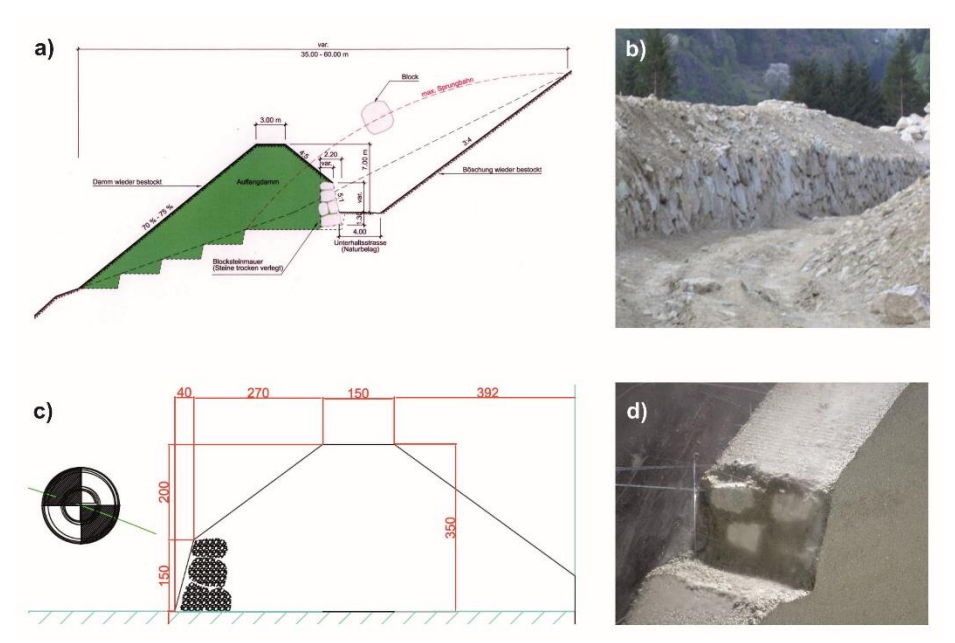


Fig. 2.14: Embankment Gurtnellen: a) design of embankment Gurtnellen North (Kälin, 2006), b) rockery at embankment Gurtnellen South (Photo: B. Kister), c) cross section of the model embankment on a scale of 1:20, dimensions are in mm, d) rockery of the model embankment.

July 2017 15/90 Analysis of Existing Rockfall Embankments of Switzerland (AERES), part C

In addition to the geometry with a bi-linear slope shown in Fig. 2.13 an embankment model was used which represents the cross section of the rockfall protection embankment Gurtnellen North on a scale of 1:20 (Fig.2.14).

2.5 Scaling factor

Blovsky (2002) as well as Hofmann & Mölk (2012) used model embankments with a height of 0.5 m. But the prototype which was taken as a basis in the two investigations is not the same. While Blovsky used a prototype with a height of 25 m as basis for defining the geometrical scaling factor λ ($\lambda = 25/0.5 = 50$), the prototype of Hofmann & Mölk has only a height of 16.5 m, which results in a geometrical scaling factor $\lambda = 33$. Taking into account the prototype height used by Hofmann & Mölk and the model height shown in Fig. 2.12 this will result for the tests of this report in a scaling factor λ of approx. 22.

But in Switzerland most rockfall protection embankments do not reach a height like the prototypes defined by Blovksy or Hofmann & Mölk. The survey of existing rockfall protection embankments in Switzerland showed that an embankment height of 8 m or more is rather rare (part B of the report, Fig. 2.15).

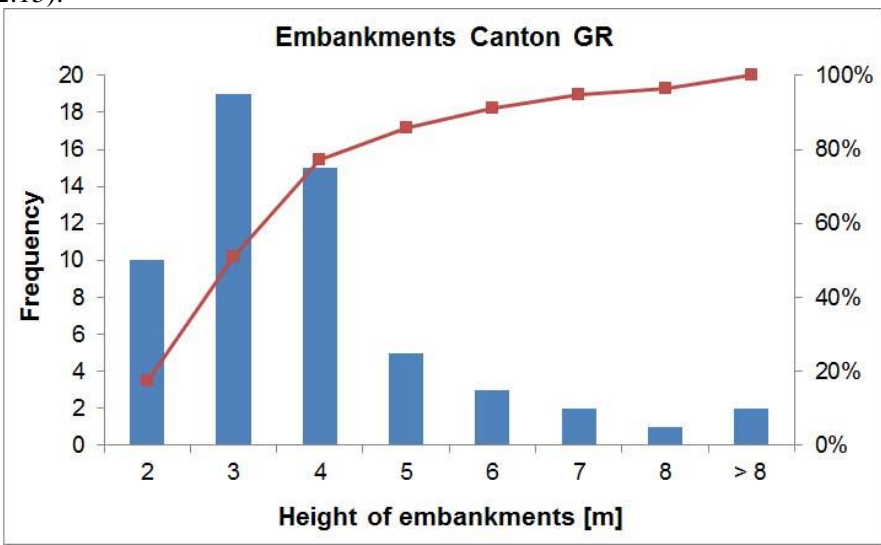


Fig. 2.15: Bar chart of the height of 57 embankments in Canton Grisons

So as a prototype an embankment with a height of 7 m was defined for the models presented in Figures 2.12 and 2.13. This will result in a scaling factor λ of about 9 for the geometry. In case of the Gurtnellen model the scaling factor for the geometry is $\lambda = 20$. The scaling factors for geometry, block velocity and energy are summarized in Table 2.3.

physical quantity	model Gurtnellen	all others
geometrical data	$\lambda = 20$	$\lambda = 9$
block velocity	$\lambda^{1/2} = 4.47$	$\lambda^{1/2}=3$
energy	$\lambda^4 = 160'000$	$\lambda^4 = 6.561$

Table 2.3: Scaling factors for geometrical data, block velocity and energy.

July 2017 16/90 Analysis of Existing Rockfall Embankments of Switzerland (AERES), part C

2.6 Executed tests

Within the framework of this project totally 34 experiments with quasi-2D-embankment models have been done. But not all of these tests could be analyzed in full. So, during two tests a blackout of the high-speed camera occurred. As a consequence of this the first impact in one test and the second impact in another test were not recorded. The test, where the first impact was not recorded, was repeated. Because of the minor significance of the second impact, the other test was not repeated. When doing the first test with impactor GS, made completely of concrete, this impactor was fragmented, when it hits the "rockery" and so no analysis of this test could be done.

The 34 executed tests may be subdivided as follows:

According to the used impactor:

- 9 tests had been done using block G.
- 12 tests had been done using block OKT.
- 13 tests had been done using block GS with the sensor inside.

According to the differences in slope construction:

- 8 tests had been done with the geometries shown in Fig. 2.12 with masonry stones placed parallel to the slope as shown in Fig. 1.3 a).
- 2 tests had been done with the geometry shown in Fig. 2.13 with masonry stones placed parallel to the slope as shown in Fig. 1.3 c) and no stones at the upper part of the slope.
- 12 tests had been done with the geometries shown in Fig. 2.12, but with masonry stones placed horizontally as shown in Fig. 1.3 b).
- 5 tests had been done with the geometries shown in Fig. 2.12, but with the masonry stones on both embankment slopes. The masonry stones have been placed horizontally, as shown in Fig. 1.3 b) resp. Fig. 2.16.
- 5 tests had been done with the geometries shown in Fig. 2.12, no masonry stones had been used in the tests. These tests complement the test series shown by Kister (2015).
- 2 tests had been done with the Gurtnellen model.



Fig. 2.16: Proportion of stone and soil layer in horizontal sections: a) at the upper third of the embankment, b) at the bottom of the embankment.

July 2017 17/90 Analysis of Existing Rockfall Embankments of Switzerland (AERES), part C

Based on the relationship between the size of the impacting block and the embankment's crest width 16 tests may be assigned to class 1, $a_c/2r \approx 0.5$ and 14 tests to class 2, $a_c/2r \approx 1.1$.



Fig. 2.17: Roughness of the "rockery" with masonry stones placed horizontally for slopes with batter 2:1, 5:2 and 5:1. The roughness is reduced with increase of slope steepness.

One test had been done on an embankment with 3 layers of fly-screen in a vertical distance of 15 cm as a kind of "geogrid reinforcement" in the upper part of the embankment to stabilize the downhill slope. The fly-screen has been used because no geogrid in model scale was available. Because a lateral fixation of the reinforcement is missing in the quasi-2D-experiments the results of this test have been rather poor. Therefore no further experiment with that kind of test arrangement was executed.

To identify a test easily by its name generally a labeling consisting of 4 parts is used:

- The first part of the name denotes the impactor which was used in the test. In this test series this is G, GS or OKT.
- The second part contains information concerning the embankment's slopes. The first two numbers refer to the batter of the uphill slope. The second two numbers refer to the batter of the downhill slope. There is one exceptional case. Three numbers, 251, had been used for batter 5:2.
 - If those numbers are followed by a letter, masonry stones had been used in the test. An H indicates that the stones had been placed parallel to the uphill slope. The letter F indicates the masonry stones had been placed horizontally. If two letters F are used, masonry stones have been placed on both slopes of the embankment.
 - If the letter F or H is followed by a letter G the test has been done while the complete test box was raised to achieve a larger value for the freeboard without doing changes at the down pipe.
- The third part of the name specifies the crest dimension in centimeters.
- The fourth part of the name is an indication of the inclination of the down pipe. For an inclination of 9.3° at the exit the identifier 11 is used. For the lower inclination of approx.1.3° at the exit the identifier 01 is used (Fig. 2.3). Most tests had been done with an inclination of 9.3° at the exit.

July 2017 18/90 Analysis of Existing Rockfall Embankments of Switzerland (AERES), part C

For example, a test named OKT_2121FF_18_11 was done with impactor OKT, the embankment cross section was symmetric with a batter of 2:1 on both sides and masonry stones placed horizontally at both slopes. The crest size was approx. 18 cm and the inclination of the down pipe at the exit was 9.3° as shown in Fig. 2.3 on the left.

For the one experiment, which was done with "geogrid reinforcement" at the downhill slope, a G was added as a fifth part of the name.



Fig. 2.18: Model with the "geogrid reinforcement" at the downhill slope.



Fig. 2.19: Bagginess of the "geogrid reinforcement" after the impact.

Sometimes an additional number is used at the end of the test label. If this number is set to 1, this denotes it was the first impact of the test. Number 2 or higher denotes additional impacts on the same model. To shorten the test name the number 1 has been omitted, if only the first impact was of interest or no further impact was done.

3 Test results

3.1 Impact angle, block velocity and energy before impact

The impact angle α is a significant parameter for the impact process as shown by Kister (2015). The impact angle is the angle between the perpendicular to the embankment slope and the block's trajectory. By definition, the angle is positive, if the trajectory is below the perpendicular (Fig. 3.1a) and negative, if the trajectory is above the perpendicular.

A positive impact angle leads to an upward directed velocity component during the impact process (Fig. 3.1b). The larger the positive impact angle, the larger is the upward directed velocity component and with it a force which pushes the block towards the embankment's crest. On the other hand, if the impact angle is negative, the velocity component parallel to the slope will be directed downward and is therefore opposite to the rolling direction of the block.

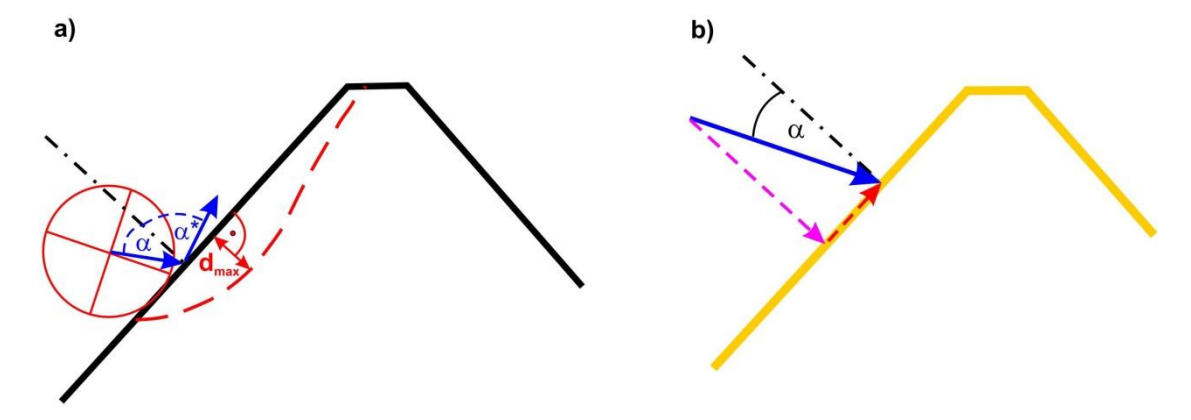


Fig. 3.1: a) Definition of impact angle α , exit angle α^* and maximum penetration depth d_{max} . b) A positive impact angle leads to an upward directed velocity component during the impact process.

Impact angle as well as translational and rotational block velocities had been determined by using 3 pictures just before the impact with different positions of the impactor (Fig. 3.2). The distance and angle of rotation of the block had been measured, the time difference of the pictures was given by the frame rate of 500 Hz of the high speed camera recording.

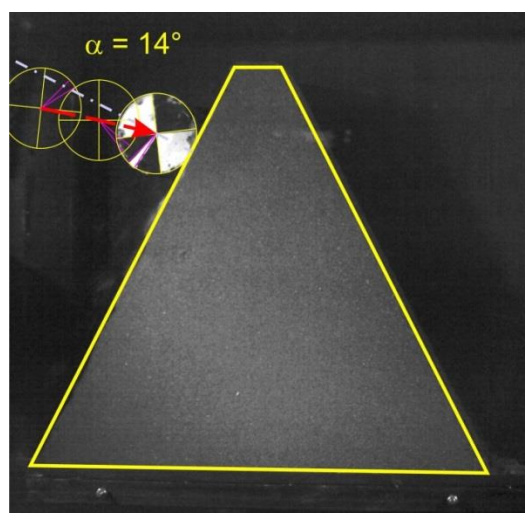


Fig. 3.2: Impact angle α as well as the translational and rotational block velocities have been determined by measurement of three positions of the impacting block.

July 2017 20/90 Analysis of Existing Rockfall Embankments of Switzerland (AERES), part C

For a batter of 2:1 on the "uphill" slope 27 tests have been done in total with all three types of impactors. The minimum impact angle was determined to be 8°, the maximum impact angle was determined to be 15°. Both values were received in tests with impactor GS. The mean value of the impact angle of all 27 tests in round figures is 12°. Fig. 3.3 shows the frequency distribution vertical-bar graph of the impact angle.

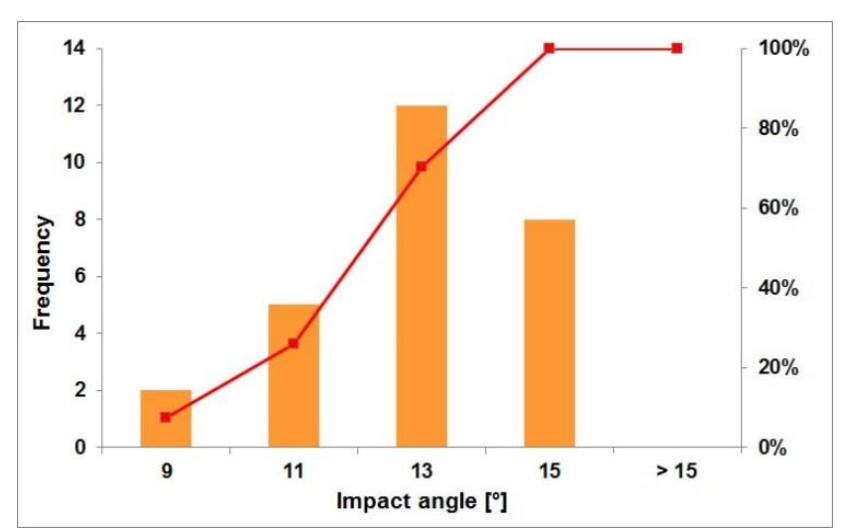


Fig. 3.3: Bar chart of the frequency of impact angle obtained during 27 tests on a slope with batter 2:1.

Two tests had been done on a slope with a batter 5:2, one with impactor G and the other with impactor OKT. In both tests the impact angle has been determined to be 8° . Increasing the batter of the slope to a value of 5:1 resulted in a negative value for the impact angle of -4° (G) respective -5° (OKT). In that case the trajectory is above the perpendicular and this result in a downward directed velocity component, which is contrary to the rolling movement of the block.

The translational block velocity v was determined according to Fig. 3.2 for 31 tests. The mean value of the translational velocity just before the impact had been determined to 6.5 m/s. Taking into account the scaling factor $\lambda^{1/2} = 3$ of Table 2.3 this result in a block velocity in the "prototype world" of 19.5 m/s, which is a quite realistic value for block velocities in rockfall events.

The minimum value of the velocity v = 5.6 m/s was received with that block GS, which was made solely of concrete and which was broken during the first test (test GS_2145H_9_11). The highest velocity v = 7.1 m/s was reached with a block GS too, but now with the new block with a steel lining as exterior facing (GS_2121FF_18_11). Having regard to the 3 different block types, one may see a slight difference in the translational velocities. With a mean value for the velocity v = 6.3 m/s the block G was the most slowly impactor. The block OKT was a little bit faster with v = 6.5 m/s. The highest mean value for the velocity v = 6.7 m/s was achieved for block GS with the steel lining as exterior facing. But the differences in these values for the translational velocities are all within the error of measurement, which has been determined to be about 0.5 m/s.

In the tests with the Gurtnellen model translational velocities of 6.1 m/s and 6.9 m/s had been determined with impactor GS. This is in the same range as determined in the other tests with impactor GS.

Much more significant are the differences concerning the rotational velocity of the 3 kinds of impactors. The block OKT was sliding on its edges in the down pipe at least during the last third of this way. Therefore the rotational velocity at the impact was very slow and in the range of 0 to 13 Hz. The concrete block G got the highest values for the rotational velocities. The mean value here was $\omega = 79$ Hz. In test GS_2145H_9_11 with the pure concrete block the rotational velocity was $\omega = 74$ Hz, which is in the range of the values received with block G. With a mean value for the rotational velocity of $\omega = 39$ Hz the block GS with the steel lining as exterior facing achieves just half the value of the rotational velocity of the concrete block G. The tests done on the Gurtnellen model achieved similar results for the rotational velocity. The lower rotational velocity of impactor GS with a steel facing is a result of the lower friction between steel facing of the block and steel of the down pipe. Fig. 3.4 shows rotational versus translational block velocity of the three impactors. In the graph the differences in rotation is obvious.

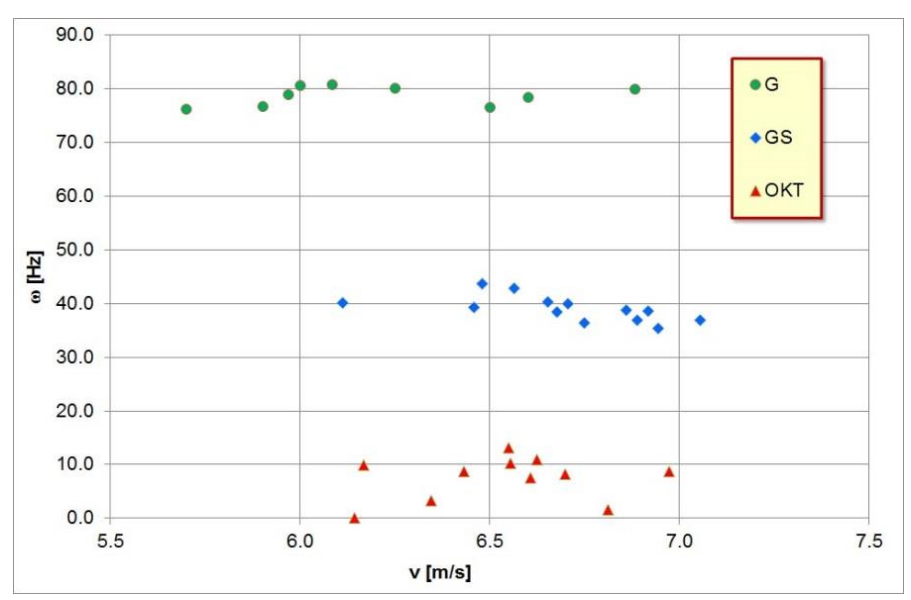


Fig. 3.4: Rotational versus translational block velocity

Fig. 3.5 shows rotational and translational energy determined in the different tests. All data points received with the impactor GS are located between the lines $E_{rot}/E_{trans} = 0.1$ and $E_{rot}/E_{trans} = 0.2$. Due to the very low rotation of impactor OKT all data points of these tests are below the line $E_{rot}/E_{trans} = 0.025$. All tests results received with impactor G show high values for the ratio of rotational and translational energy in the range of 0.5.

A graph concerning the ratio of rotational to translational energy of blocks can be found in the Japanese Rockfall Protection Handbook (JRA, 2000) as well as in the paper of Yoshida (1998). In this graph the most data pairs of rotational and translational energy are located between the upper boundary line with the value 0.2 and the lower boundary line with the value 0.02. Usiro et al. (2006) had done real scale tests on a 41 m high slope to determine the ratio of rotational to translational energy in rockfall events. They had done tests with concrete bodies (sphere: 200 kg, cube: 520 kg) as well as tests with 10 natural rock blocks (120 kg up to 2060 kg). According to these tests a lower and an upper boundary value for the ratio of rotational to translational energy of natural blocks during rockfall can be given. The lower boundary value is 0.025, while the upper boundary value is 0.2. But larger values than 0.4 had been achieved for the ratio of rotational to translational energy for the concrete sphere.

July 2017 22/90 Analysis of Existing Rockfall Embankments of Switzerland (AERES), part C

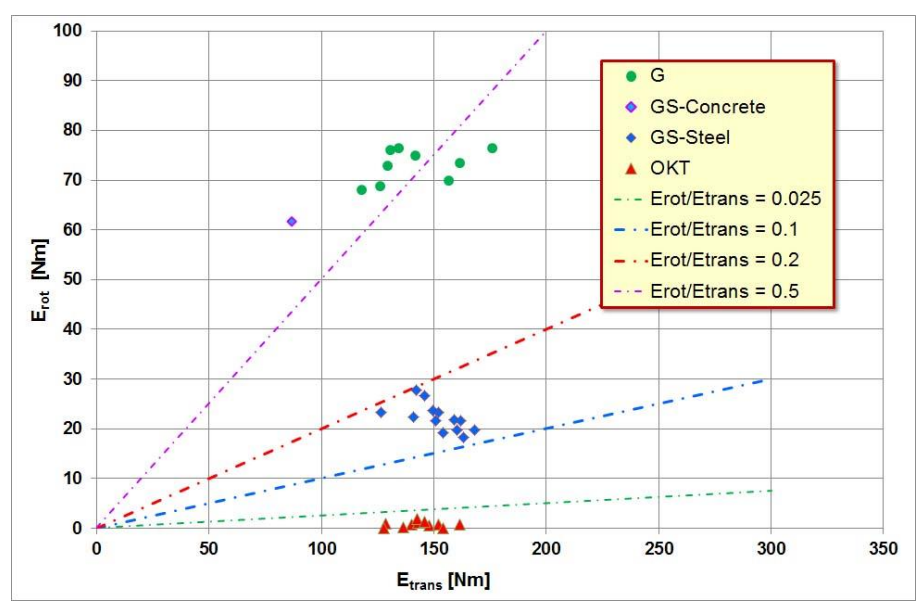


Fig. 3.5: Comparison of rotational and translational energy data of the impacting blocks G, GS and OKT.

The test results concerning the ratio of rotational to translational energy received with impactor GS with the steel lining as exterior facing fits very well with data of the ratio of rotational to translational energy found in real scale tests for natural blocks. On the other hand the ratio of rotational to translational energy, received in tests with impactor G, seems to be too high in comparison to the real scale tests with natural blocks, but are in the range of the tests done by Usiro et al. (2006) with a concrete sphere (see also Kister, 2015).

Using the scaling factor for the energy $\lambda^4=6561$ in Table 2.3 the impact translational energy of the tests may be transformed to the "prototype" size. This leads to a mean value for the impact translational energy of about 0.95 MJ (without consideration of tests on model Gurtnellen). Fig. 3.5 shows the frequency distribution vertical-bar graph of the transformed energy values. The minimum value of 0.57 MJ was achieved for test GS_2145H_9_11 with the hollow concrete cylinder, which was broken in the first test. The test GS_2145H_9_11 differs also significant from other tests because a very high ratio $E_{\text{rot}}/E_{\text{trans}}=0.7$ was achieved.

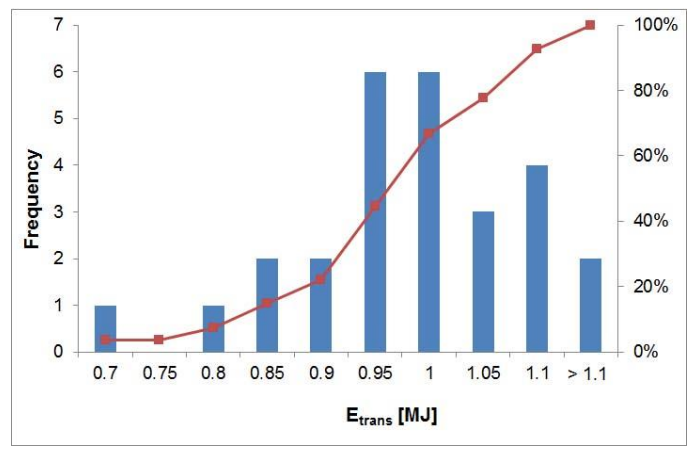


Fig. 3.6: Bar chart of the frequency of transformed translational energy values of the impacting blocks G, GS and OKT. Total number of tests: 31

July 2017 23/90 Analysis of Existing Rockfall Embankments of Switzerland (AERES), part C

For the Gurtnellen model the scaling factor for the energy is $\lambda^4 = 160^{\circ}000$ in Table 2.3. So the transformed translational energy in this case is in the range of 20 MJ to 26 MJ. For the Gurtnellen embankments two block sizes, 50 t and 160 t, had been taken into account for the design. The impact velocity for both blocks was assumed to be 25 m/s. This will result to impact energies of 15.6 MJ respective 50 MJ taking into account only the translational energy as was done for the design of the Gurtnellen embankments. So the transformed translational energies are within the two values used for the design of the Gurtnellen embankments and may be interpreted in energy values as a block of about 70 to 85 t with a velocity of 25 m/s.

3.2 Block movement after contact

The tests had been recorded by a high-speed camera with 500 fps i.e. a picture was done every 2 milliseconds. In a first impact analysis step these pictures were used to determine the block's trajectory after the contact with the embankment. The following determining factors had been investigated with that method:

- Block shape and rotational velocity resp. rotational energy
- Shape of the embankment
- Crest width
- Slope facing.

Because of the used experimental set-up the parameters block shape and rotational velocity resp. rotational energy cannot be analyzed independent. If the impactor is a cylinder, this block will have rotation when impacting the embankment due to friction between the cylinder barrel and the down pipe. Otherwise the block with the octagonal cross section is sliding on two edges at the lower part of the down pipe and therefore this block has no or only minor rotation when the block hits the embankment. So a regulation of the rotational velocity respectively the rotational energy of a block is not possible with that kind of experimental set-up.

For the purpose of comparison of embankments with rockery facing and soil facing some of the test results shown in Kister (2015) had been used again in this chapter. Those test results can be identified by their name, because instead using the crest width in cm in these names the letters A or B are used to describe the crest width.

Fig. 3.7 shows the tests results for an embankment with an asymmetric cross section with a slope inclination 2:1 (62.6°) at the "uphill" side and a slope inclination 4:5 (37.3°) at the "downhill" side. On three pictures on the left the trajectories of cylinder G are shown, while on three pictures on the right the trajectories of block OKT are shown. In the tests of the two upper pictures a) and b) the crest width was 8.5 cm resp. 9.5 cm (identification mark B for the crest width). This equates to the crest width used in the new tests shown in the pictures e) and f) with stones placed parallel to the embankments slope (see Fig. 1.3a). In the middle the pictures c) and d) show the trajectories of tests with crest width 18.5 cm resp. 19 cm (identification mark A for the crest width) but no stones on the slopes.

In all three tests with rotating cylinder G the embankment was surmounted during the first impact, but there are differences in the curve progression of the trajectories. In picture a) the relationship of crest width to block diameter is approximately 0.53 and the block punched through the embankment's crest because of low resistance. The trajectory of the block center runs partly inside the contour of the embankment (Fig. 3.7 a).

July 2017 24/90 Analysis of Existing Rockfall Embankments of Switzerland (AERES), part C

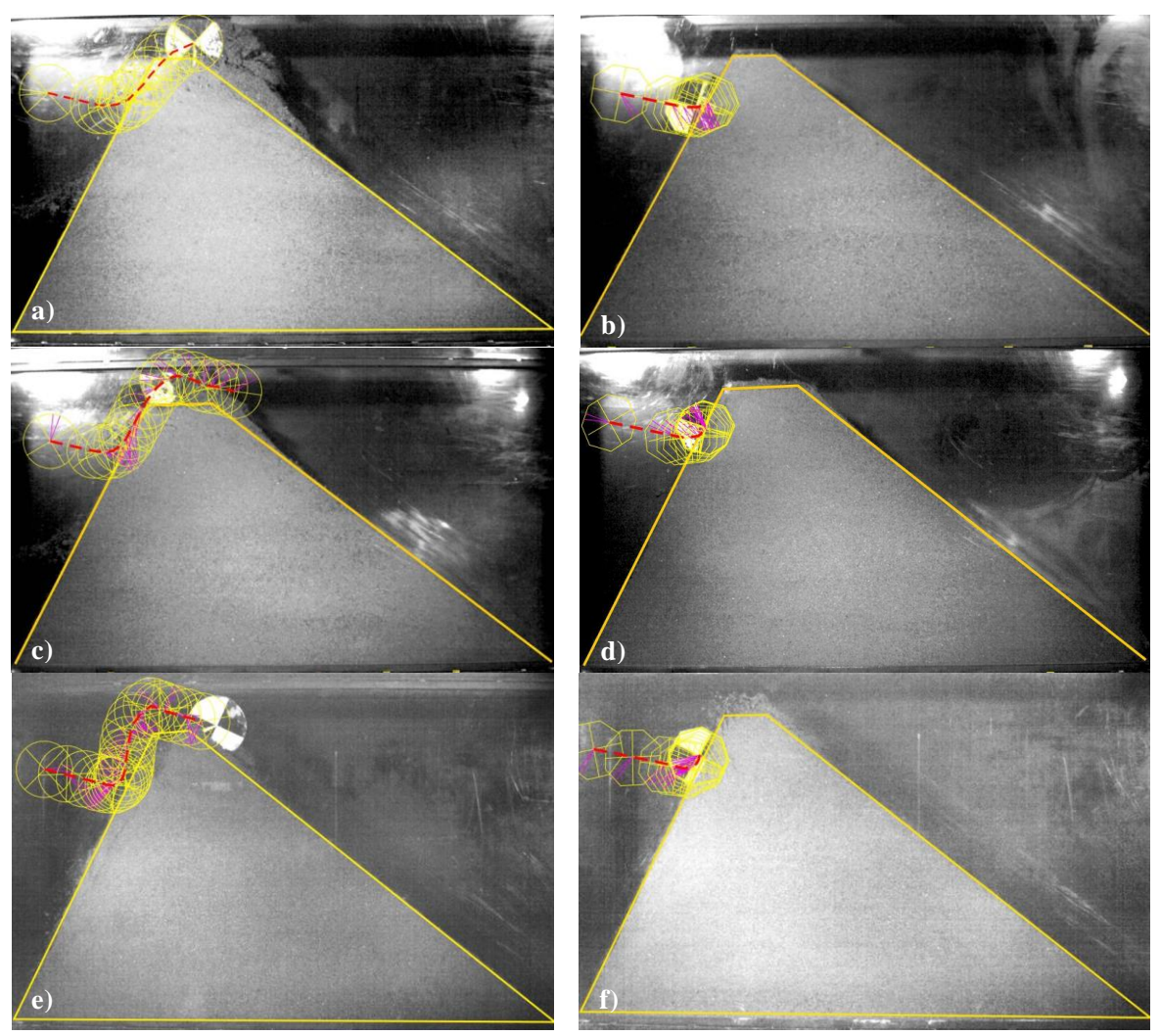


Fig. 3.7: Comparison of the block trajectories after the contact with an embankment with asymmetric cross section: a) G_2145_B_11-1, b) OKT_2145_B_11-1, c) G_2145_A_11-1, d) OKT_2145_A_11-1, e) G_2145H_9_11-1, f) OKT_2145H_9_11-1.

In picture Fig. 3.7 c) the relationship of crest width to block diameter is approximately 1.15 and therefore the impacting block is faced by a larger activated volume of the embankment resp. a larger activated mass. This results in an increase of the resistance of the embankment against the impacting block and so the trajectory of the block center runs along the contour of the embankment but not inside the contour of the embankment.

Fig. 3.7 e) shows the trajectory of a test with an embankment where stones had been placed parallel to the embankment's slope. Even though the relationship of crest width to block diameter in this test is only approximately 0.53, the block G in this case is not able to punch through the embankment's crest. The stones increase the resistance of the embankment and the trajectory of the block center runs outside of the contour of the embankment. But nevertheless the embankment was surmounted by the block G also in this test.

The tests done with the same embankment cross section but now impacted by the block OKT with no or only very low rotation show a very different behavior. The embankment was not surmounted by block OKT due to the first and second impact and the block was neither able to punch through the embankment in those tests. Only with a third impact in test OKT_2145_B_11 the block OKT was able to surmount the embankment. During this third impact the crest was completely destroyed. Furthermore the trajectories of the three tests with block OKT look very similar as shown in Fig. 3.7 b), d) and f).

Table 3.1 summarizes data and results of the tests shown in Fig. 3.7.

Description	Cylinder G	Body OKT
β _{us} : 62.6°	G_2145_B_11	OKT_2145_B_11
β_{ds} : 37.3°	FB approx. 0.6 * 2r	FB approx. 0.6 * 2r
a _c : 9 cm	1 st impact: block jumped over	embankment not surmounted
OS: no rockery	embankment	1 st impact: crest heavily damaged.
	crest with violent damage	2 nd impact: crest with violent damage
		3 rd impact: crest completely destroyed
		embankment surmounted
β_{us} : 62.6°	$G_2145_A_11$	OKT_2145_A_11
β _{ds} : 37.3°	FB approx. 0.6 * 2r	FB approx. 0.6 * 2r
a _c : 18.5 cm	1 st impact: block jumped over	embankment not surmounted
OS: no rockery	embankment	1 st impact: crest slightly damaged.
	crest with violent damage	2 nd impact: crest heavily damaged
	2 nd and 3 rd impact: block jumped	3 rd impact: crest with violent damage
	over embankment	embankment not surmounted
β_{us} : 62.6°	G_2145H_9_11	OKT_2145H_9_11
β _{ds} : 37.3°	FB approx. 0.7 * 2r	FB approx. 0.6 * 2r
a _c : 8.5 cm	block jumped over embankment	embankment not surmounted
OS: upright	crest with violent damage	1st impact: crest slightly damaged.
	stones are completely separated and	2 nd impact: crest damaged, but not
	fell down	completely destroyed
Explanation:	β_{us} : slope angle uphill side	OS: orientation of stones
	β_{ds} : slope angle downhill side	2r: block diameter
	ac: crest width	FB: Freeboard

Table 3.1: Summary of the results of the tests shown in Fig. 3.7.

The embankment with an asymmetric cross section with a slope inclination 2:1 (62.6°) at the "uphill" side and a slope inclination 4:5 (37.3°) at the "downhill" side has also been used for impact tests with impactor GS with the steel lining and a triaxial acceleration sensor inside. One test with stones placed parallel to the embankment's slope (Fig. 1.3a) had been done as well as one test with stones placed horizontally to get a rough slope surface (Fig. 1.3 b). The relationship of crest width to block diameter was approximately 0.5. The difference of the translational energies in both tests was approx. 2.6%. The difference of the rotational energies in both tests was less than 4%. The relationship of rotational to translational energy was 0.18 resp. 0.19, which is below the upper boundary of 0.2 found by Usiro et al. (2006) for natural blocks. In both tests the block GS was not able to surmount the embankment, even though the freebord in the tests does not fulfills the requirements of ONR 24810:2013 and was smaller than one block diameter (Table 3.2).

The main difference in the two tests is the impact angle α . In the test GS_2145F_7_11 an impact angle of about 8° was determined while in the test GS_2145H_9_11 the impact angle was larger and reached a value of 13°.

July 2017 26/90 Analysis of Existing Rockfall Embankments of Switzerland (AERES), part C

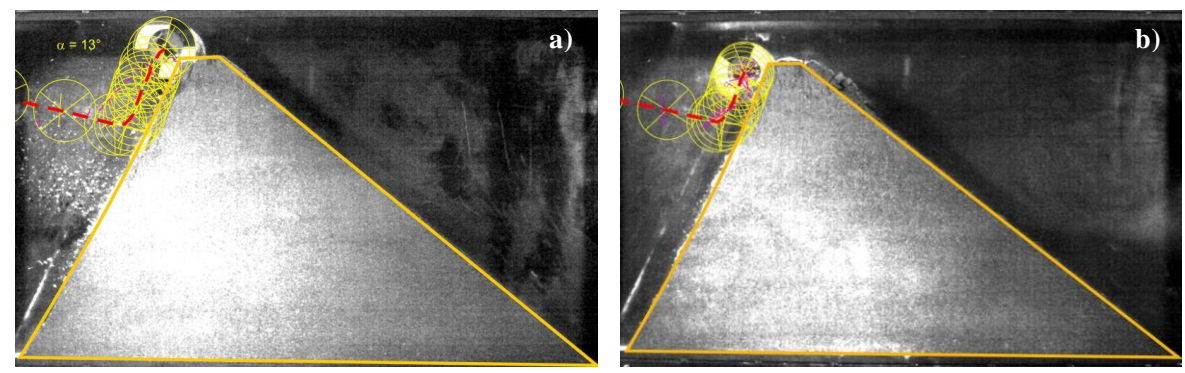


Fig. 3.8: Comparison of the block trajectories after the contact with the embankment with asymmetric cross section and "rockery": a) GS_2145H_9_11-1, b) GS_2145F_7_11-1

The larger value of the impact angle as well as the smoother surface of the "rockery" in test GS_2145H_9_11-1 may explain why block GS reached a higher level in test GS_2145H_9_11-1 than in test GS_2145F_7_11-1 (Fig. 3.8). The larger deformation at the top of the downhill slope with intensive formation of cracks during test GS_2145F_7_11-1 is a result of the horizontally placed stones, which are not able to reduce energy by compaction but transfer the energy to the smaller soil body behind the stones. A summary of the test data and results is given in Table 3.2.

Description	GS_2145H_9_11	GS_2145F_7_11
β _{us} : 62.6°	FB approx. 0.85 * 2r	FB approx. 0.75 * 2r
β_{ds} : 37.3°	embankment was not surmounted,	embankment was not surmounted, but
a _c : 8.5 cm resp. 7 cm	but center of block above crest level	center of block at crest level
	1st impact: crest slightly damaged.	1st impact: crest damaged and
		intensive formation of cracks
	2 nd impact: crest damaged, large	2 nd impact: crest material was pushed
	joints during impact process	to the "downhill" slope

Table 3.2: Summary of the results of the tests shown in Fig. 3.8.

Two tests had been done with an embankment with a bi-linear slope at the "uphill side". At the lower part with a batter of 2:1 stones had been placed parallel to the embankment's slope. The upper part was solely made of soil and had an inclination of approx. 37° (4:5). One test had been done with cylinder G and the other test with block OKT. In both tests the block hit the embankment immediate under the break of the bi-linear slope at the "rockery" (Fig. 3.9). The impact angle was 13° resp. 14° and therefore more or less the same.

The block mass of block OKT is 7% lower than the mass of block G and block G got a translational velocity at the impact point which is approx. 7.25% higher than the velocity of block OKT at this point. This results in a difference of the translational energy of about 26%. But the comparison of the rotational energy of both blocks showed approximately a factor 100 (block G: 76.3 Nm, block OKT: 0.79 Nm). This led to a completely different behavior of the blocks during the impact process. While block G jumped high over the embankment, block OKT was not able to surmount the embankment and fell back on the "uphill" side. Fig. 3.9 shows the trajectory of both blocks during the tests.

Three additional impact tests had been done with block OKT on the already damaged embankment. This resulted in an increasing penetration depth for block OKT, but the embankment was neither punched through nor was the block able to surmount the embankment. A second impact with block G on the embankment damaged the crest and the stones had been separated and fell down.

July 2017 27/90 Analysis of Existing Rockfall Embankments of Switzerland (AERES), part C

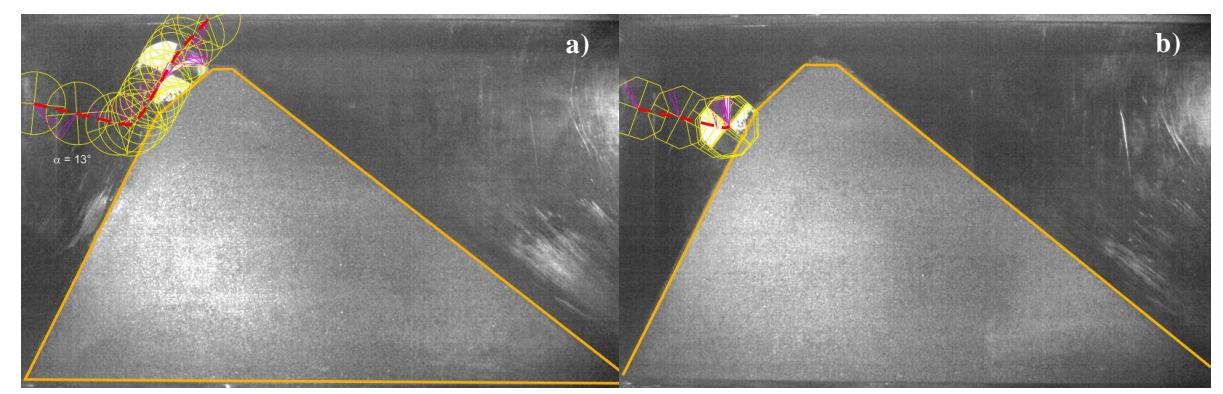


Fig. 3.9: Comparison of the block trajectories after the contact with a bi-linear slope at the "uphill side" of an embankment, "rockery" at the lower part, soil at the upper part: a) G_2145H_4K_11, b) OKT_2145H_6K_11, first impacts.

A summary of the test data and results of the tests G_2145H_4K_11 and OKT_2145H_6K_11 is given in Table 3.3.

Description	Cylinder G	Body OKT
β_{us} : 62.6°	G_2145H_4K_11	OKT_2145H_6K_11
β _{ds} : 37.3°	FB approx. 1 * 2r	FB approx. 1 * 2r
a _c : 4.5 cm resp. 6 cm	block jumped over embankment	embankment not surmounted,
OS: upright	1 st impact: crest slightly damaged.	crest damaged, but withstands
	2 nd impact: crest damaged, stones are	additional three impacts
	completely separated and fell down	

Table 3.3: Summary of the results of the tests shown in Fig. 3.9.

Impact tests on embankment models with batter 2:1 at both sides had been done for the following surface conditions of the embankment slopes:

- a) without stones, embankment made solely out of soil
- b) stones placed parallel to the slope at the impact side
- c) stones placed horizontal at the impact side
- d) stones placed horizontal at both slopes.

The tests had been done with block G as well as with block OKT. The crest to block diameter ratio for these tests was chosen to be approx. 0.56.

Fig. 3.10 shows the trajectory of block G for the test conditions a) to d). In all 4 tests the embankment was not able to stop the block, but the trajectories show significant differences.

For the embankment made solely out of soil a part of the crest was chipped and a large amount of material was sliding down at the "downhill" slope. Block G received a maximum jump height above the crest level and this maximum is located at the "downhill side".

The stones placed parallel to the slope at the impact side in case b) increased the resistance of the embankment and therefore the penetration depth is less than in case a). On the other hand the jump height now is higher, but the maximum height is located above the crest, i.e. the length of the jump is shorter than in case a).

July 2017 28/90 Analysis of Existing Rockfall Embankments of Switzerland (AERES), part C

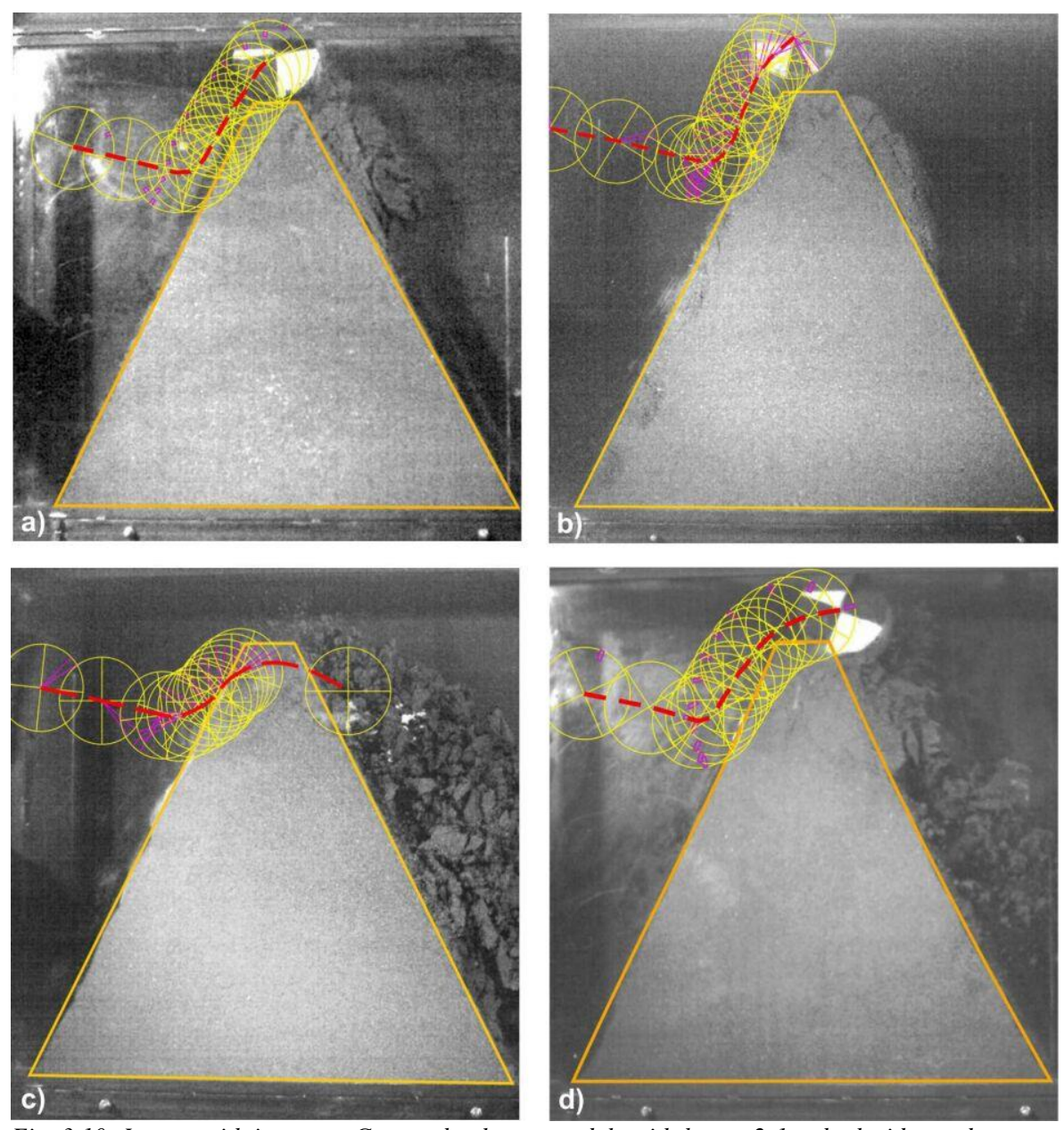


Fig. 3.10: Impact with impactor G on embankment models with batter 2:1 at both sides and crest to block diameter ratio 0.56: a) without rockery $(G_2121_9_11-1)$, b) stones placed parallel to the slope at the impact side $(G_2121H_9_11-1)$, c) stones placed horizontal at the impact side $(G_2121F_8_11-1)$, d) stones placed horizontal at both slopes $(G_2121F_9_11-1)$.

When the stones had been placed horizontally (see Fig. 2.16), the block punched through the embankment's crest (Fig. 3.10 c). An upward movement of the block can also be seen in case c), but the difference between impact point and maximum trajectory level is less in this test compared with the cases a), b) and d). In addition the trajectory of the block center is running within the contour of the embankment (Fig. 3.10 c). As already mentioned the stones are not able to reduce energy by compaction but transfer the energy to the soil body behind the stones. The soil body behind the stones in this case is smaller than in cases a) and b), that means the resistance of the soil is less than in case a) or b), which ends up in the destruction of the crest.

July 2017 29/90 Analysis of Existing Rockfall Embankments of Switzerland (AERES), part C

Additional stones placed horizontal at the "downhill" slope as done in case d) increase the weight and therefore the resistance of the embankment's crest. This resulted in a larger upward movement of the block G and the block cuts the crest and surmounts the embankment.

The same four embankments, but now impacted by block OKT with no or minor rotation, show a very different behavior in comparison to the tests with block G. In all four tests the block OKT was not able to surmount the embankment. But already the first impact destroyed the embankment's crest totally (Fig. 3.11).

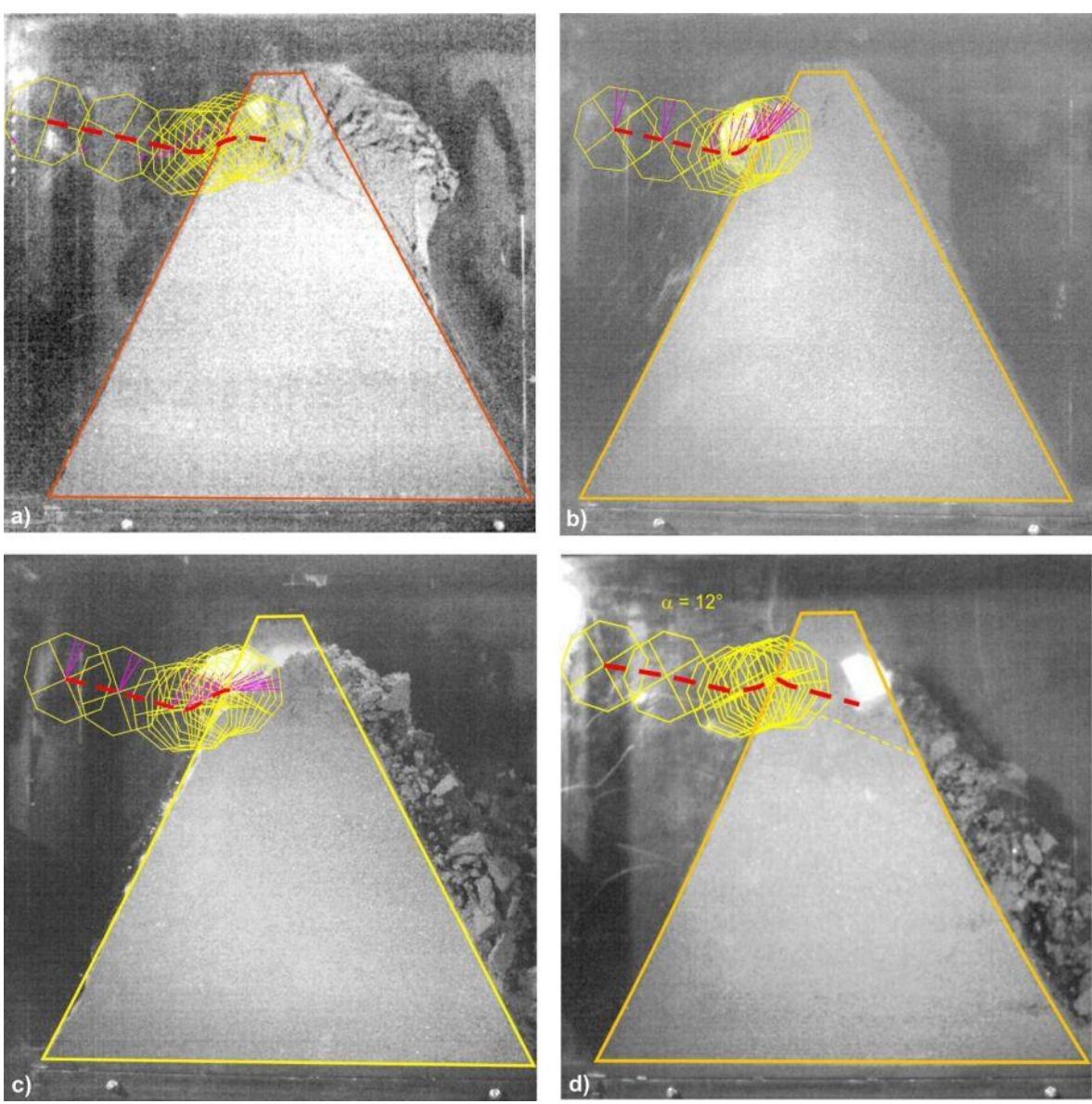


Fig. 3.11: Impact with impactor OKT on embankment models with batter 2:1 at both sides and crest to block diameter ratio 0.56: a) without rockery (OKT_2121_9_11-1), b) stones placed parallel to the slope at the impact side (OKT_2121H_7_11-1), c) stones placed horizontal at the impact side (OKT_2121F_8_11-1), d) stones placed horizontal at both slopes (OKT_2121FF_9_11-1).

July 2017 30/90 Analysis of Existing Rockfall Embankments of Switzerland (AERES), part C

There are significant differences between the four tests. In the tests OKT_2121_9_11-1 (Fig. 3.11a) and OKT_2121FF_9_11-1 (Fig. 3.11d) block OKT produced a shear plane during the test, which is approximately parallel to the perpendicular line to the slope and its extension takes course to the center of block OKT at impact position. The impact angle in the two tests is 13° respective 12°. So the shear plane is not parallel to the impact direction. During the tests OKT_2121H_7_11-1 and OKT_2121F_8_11-1 no such shear plane is visible.

The penetration depth of block OKT in the tests OKT_2121H_7_11-1 and OKT_2121F_8_11-1 is less than in the two other tests and reached an amount which is only a little bit larger than the outside radius of block OKT. This resulted in a rollback of the block on the "uphill" slope. The penetration depth in the tests OKT_2121_9_11-1 and OKT_2121FF_9_11-1 is much deeper. The block reaches the "downhill" slope with its contour, i.e. the block punched through the embankment's crest. Additional in both cases the block OKT remains at the top of the destroyed embankment crest.

So it can be stated that for block OKT the stones increase the resistance of the embankment in the tests OKT_2121H_7_11-1 and OKT_2121F_8_11-1 while an additional stone layer, which was used in test OKT_2121FF_9_11-1 at the "downhill" slope for that slender construction, is counterproductively and may led to secondary rockfall produced by stones, which will be pushed out of the rockery. A summary of the test data and results of the tests is given in Table 3.4.

Description	Cylinder G	Body OKT
β_{us} : 62.6°	G_2121_9_11	OKT_2121_9_11
β_{ds} : 62.6°	FB approx. 0.6 * 2r	FB approx. 0.7 * 2r
a _c : 8.5 cm resp. 7 cm	block jumped over embankment	embankment not surmounted,
OS: no rockery	crest with violent damage	but crest totally destroyed
β_{us} : 62.6°	G_2121H_9_11	OKT_2121H_7_11
β_{ds} : 62.6°	FB approx. 0.6 * 2r	FB approx. 0.7 * 2r
a _c : 8 cm	block jumped over embankment	embankment not surmounted,
OS: upright	crest with violent damage	but crest totally destroyed
β_{us} : 62.6°	$G_2121F_8_11$	OKT_2121F_8_11
β_{ds} : 62.6°	FB approx. 0.6 * 2r	FB approx. 0.7 * 2r
a _c : 8 cm	embankment was punched through,	embankment not surmounted,
OS: horizontal	crest totally destroyed	but crest totally destroyed
β_{us} : 62.6°	G_2121FF_9_11	OKT_2121FF_9_11
β_{ds} : 62.6°	FB approx. 0.6 * 2r	FB approx. 0.6 * 2r
a _c : 8 cm	block jumped over embankment	embankment not surmounted,
OS: horizontal	crest with violent damage	but crest totally destroyed

Table 3.4: Results of tests with an embankment model with batter 2:1 at both sides and crest to block diameter ratio of approx. 0.5.

To analyze the influence of crest thickness, another test series had been done with an embankment model with batter 2:1, but now with a crest to block diameter ratio of approx. 1.1. In this test series block GS was used instead of block G. Block GS has a little bit less weight (GS: 6.76 kg, G: 7.28 kg), but the values for the ratio of rotational to translational energy received with impactor GS in these tests correspond very well with the data found by Usiro et al. (2006) for natural blocks. The ratio of rotational to translational energy determined for block GS was in the interval 0.12 to 0.16 (Fig. 3.5).

July 2017 31/90 Analysis of Existing Rockfall Embankments of Switzerland (AERES), part C

Tests had been done for the following surface conditions of the embankment slopes:

- a) without stones, embankment made solely out of soil
- b) stones placed horizontal at the impact side
- c) stones placed horizontal at both slopes.

But even though the ratio of rotational to translational energy of block GS agrees very well with the data of Usiro et al. (2006), the embankment was surmounted by block GS. There was just one exceptional case: In test GS_2121FF_18_11-1 the block GS changed its rotational axis when climbing up to the crest level (Fig. 3.12c). Due to this change of the rotational axis and the corresponding loss of energy, the block was not able to surmount the embankment. Therefore this test was repeated. The repeated test was named GS_2121FF_18_11_B and in this test the embankment was surmounted again. Fig. 3.12 shows the trajectories of block GS for the test conditions a) to c) presented above.

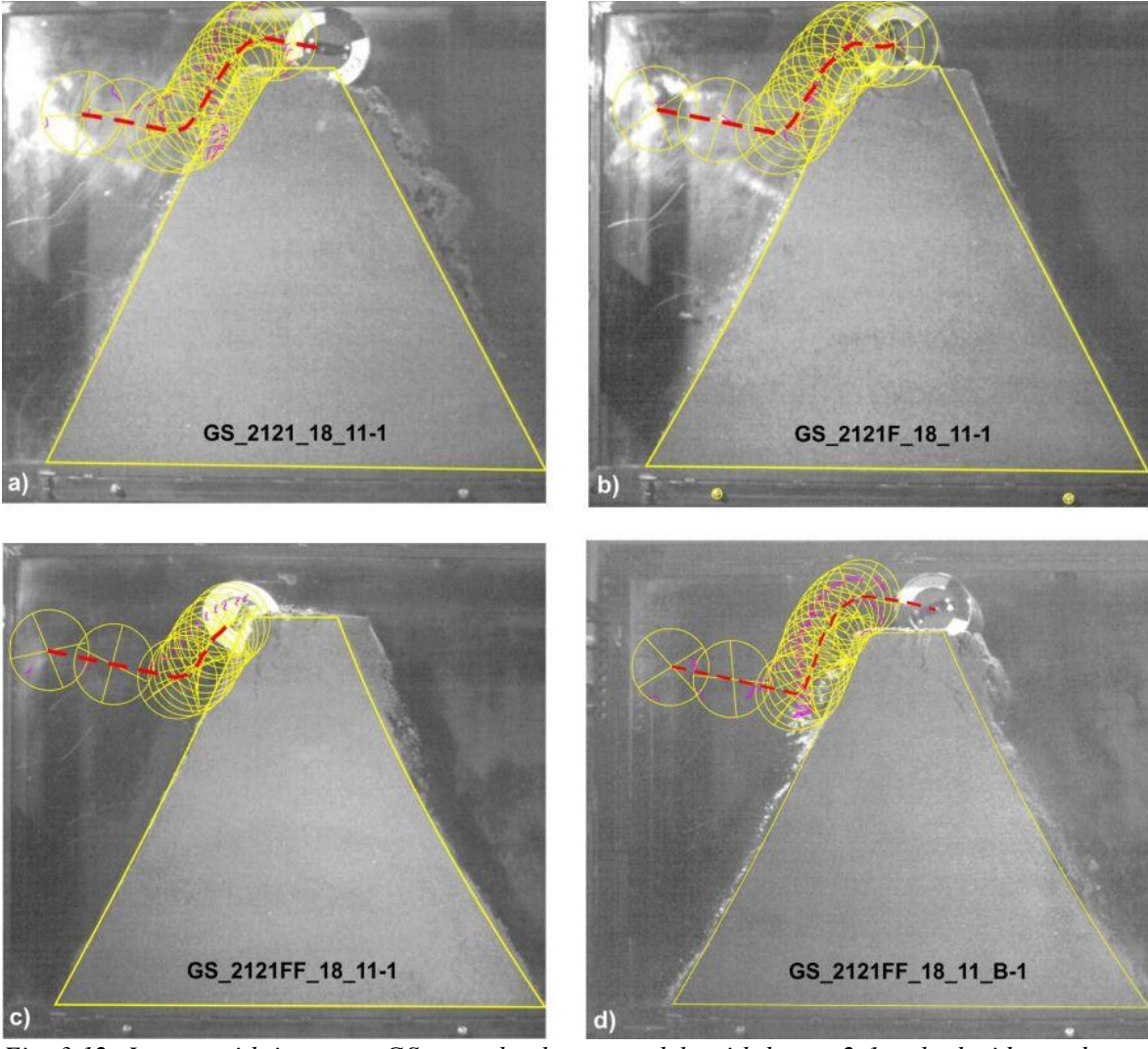


Fig. 3.12: Impact with impactor GS on embankment models with batter 2:1 at both sides and crest to block diameter ratio approx. 1.1: a) without rockery, b) stones placed horizontal at the impact side, c) and d) stones placed horizontal at both slopes, FB approx. 0.5*2r. Only in test GS_2121FF_18_11-1, shown in picture c), the embankment was not surmounted.

Embankment models with batter 2:1 at both sides and crest to block diameter ratio approx. 1.1 had also been used for impact tests with body OKT. During the test OKT_2121_18_11-1 a malfunction of the high speed camera occurred and no pictures had been recorded for the first impact. Therefore the test was repeated and the repeated test is named as OKT_2121_18_11-B1 for the first impact and OKT_2121_18_11-B2 for the second impact (Fig. 3.13 a, b).

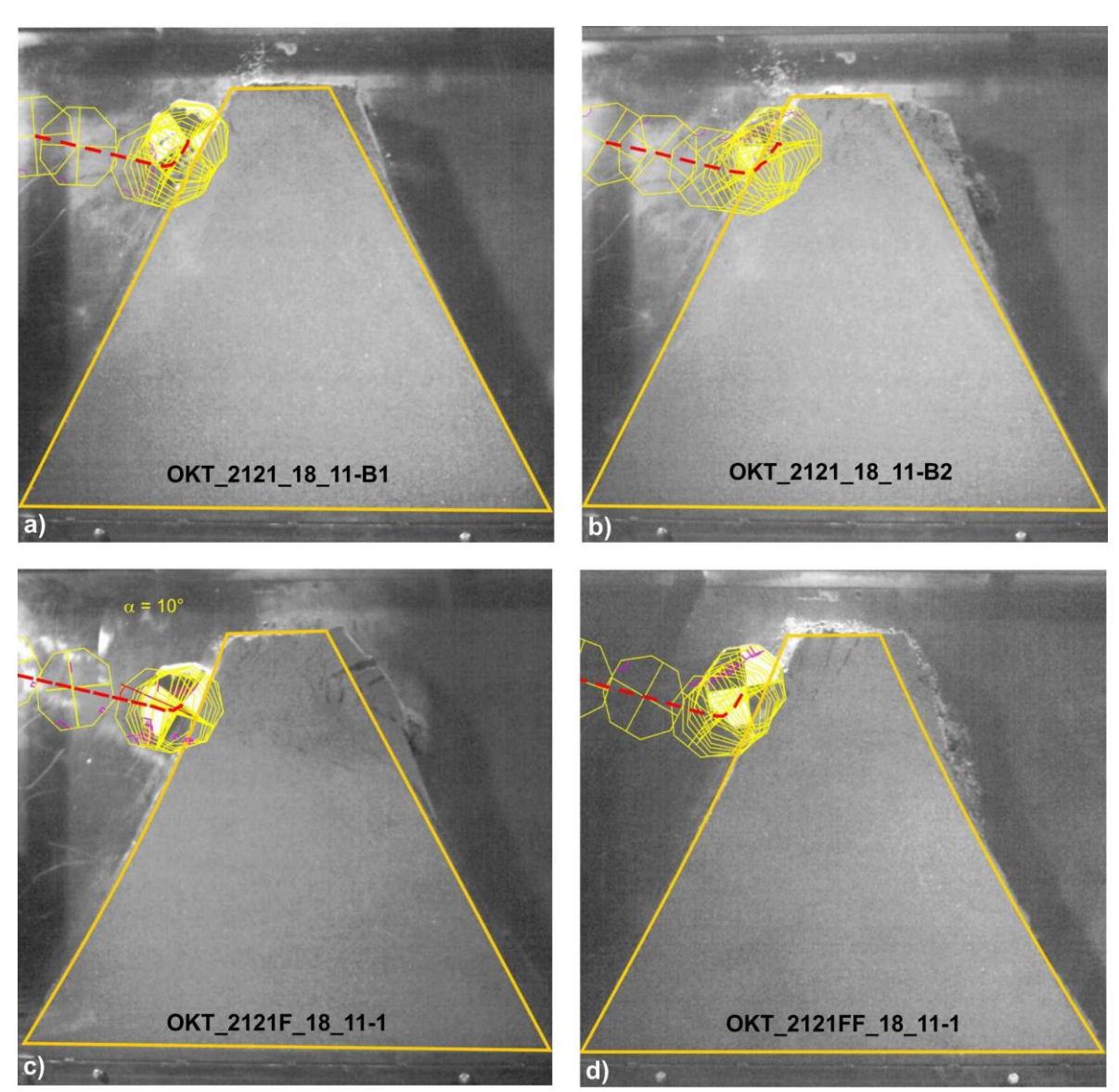


Fig. 3.13: Impact with impactor OKT on embankment models with batter 2:1 at both sides and crest to block diameter ratio approx. 1.1: a) and b) without rockery, first and second impact, c) stones placed horizontal at the impact side, d) stones placed horizontal at both slopes, $FB: 0.7*2r \dots 0.8*2r$.

In all tests there is a movement of block OKT upwards to the crest. The penetration depth of block OKT is less than the block radius for all first impacts (Fig. 3.13 a, c, d). As expected the penetration depth reached its largest amount in test OKT_2121_18_11-B1, without any stones. Only for the second impact of test OKT_2121_18_11-B2 the penetration depth is larger, but there was loosening of the embankment material due to the first impact.

July 2017 33/90 Analysis of Existing Rockfall Embankments of Switzerland (AERES), part C

The penetration depth in tests OKT_2121F_18_11-1 and OKT_2121FF_18_11-1 is approx. the same (Fig. 3.13c and d). So the "rockery" at the "downhill" slope seems to have no significant influence on the resistivity of the embankment and the penetration depth for a crest to block ratio of approx. 1.1 or larger.

Even though the freeboard in those tests shown in Fig. 3.13 was less than one block diameter, the minimum dimension, which is recommended by the standard ONR 24810:2013, the block OKT was neither be able to punch through the embankment's crest nor to surmount the embankment. But it has to be taken into account that block OKT has no or only very low rotation in the tests.

For all three surface conditions a), b) and c) of the embankment slope, the embankment withstands a second impact too. The penetration depth of the block OKT due to the second impact is deeper (cf. Fig. 3.13, a and b) because the embankment material has been already loosened and displaced by the first impact. The embankment had been heavily damaged or even destroyed due to the second impact, but the task to retain the block was fulfilled in the tests. Test data and results of the tests shown in Fig. 3.13 are summarized in Table 3.5.

Description	Cylinder GS	Body OKT
β _{us} : 62.6°	GS_2121_18_11-1	OKT_2121_18_11
β _{ds} : 62.6°	FB approx. 0.5 * 2r	FB approx. 0.8 * 2r
a _c : 18 cm	only one impact	embankment not surmounted
OS: no rockery	embankment surmounted	1st impact: crest damaged.
	crest with significant damage	2 nd impact: significant damage
	shear plane visible	
β _{us} : 62.6°	GS_2121F_18_11-1	OKT_2121F_18_11
β_{ds} : 62.6°	FB approx. 0.5 * 2r	FB approx. 0.7 * 2r
a _c : 17.5 cm / 18 cm	only one impact	embankment not surmounted
OS: horizontal	embankment surmounted	1 st impact: significant damage.
	crest with significant damage	2 nd impact: massive damage,
		shear plane visible
β_{us} : 68.6°	GS_2121FF_18_11-1	
β_{ds} : 62.6°	FB approx. 0.55 * 2r	
a _c : 18 cm	only one impact	OKT_2121FF_18_11
OS: horizontal	rotational axis changed at crest	FB approx. 0.75 * 2r
	embankment not surmounted	embankment not surmounted
	crest with significant damage	1 st impact: significant damage.
β_{us} : 68.6°	GS_2121FF_18_11_B	2 nd impact: crest totally destroyed,
β_{ds} : 62.6°	FB approx. 0.55 * 2r	block rolled back
a _c : 18 cm	embankment surmounted	
OS: horizontal	1 st impact: crest with large cracks	
	2 nd impact: shear planes visible, crest	
	destroyed	
Explanation:	β_{us} : slope angle uphill side	OS: orientation of stones
	β_{ds} : slope angle downhill side	2r: block diameter
	a _c : crest width	FB: Freeboard

Table 3.5: Results of tests with an embankment model with batter 2:1 at both sides and crest to block diameter ratio of approx. 1.1.

July 2017 34/90 Analysis of Existing Rockfall Embankments of Switzerland (AERES), part C

As shown before, a freeboard less than one block diameter is sufficient to stop the non-rotating or slow-rotating block OKT with edges at an embankment with batter 2:1, even though the impact angle is as large as 10° to 14°. On the other hand the same embankment was not able to stop the rotating block GS, even though the ratio of rotational to translational energy agrees very well with the data of Usiro et al. (2006) found for natural blocks.

To determine the maximum climbing height of block GS during an impact and to get information about the influence of the roughness of the "rockery" surface two impact tests on embankment models with a batter 2:1, but with different "rockery roughness", had been done (Figures 3.14 and 3.15):

- a) With stones placed parallel to the slope at the impact side (GS_2121HG_18_11) and
- b) With stones placed horizontally at the impact side (GS_2121FG_18_11).

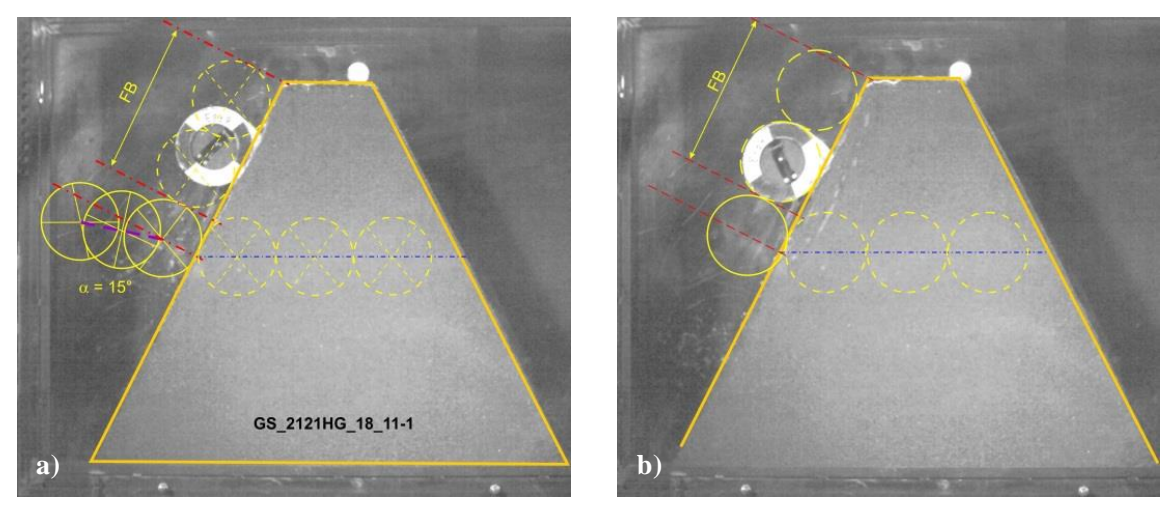


Fig. 3.14: Test GS_2121HG_18_11: a) first impact, FB = 2*2r, climbing height approx. 1.3*2r, b) second impact, FB = 1.9*2r, climbing height approx. 1*2r.

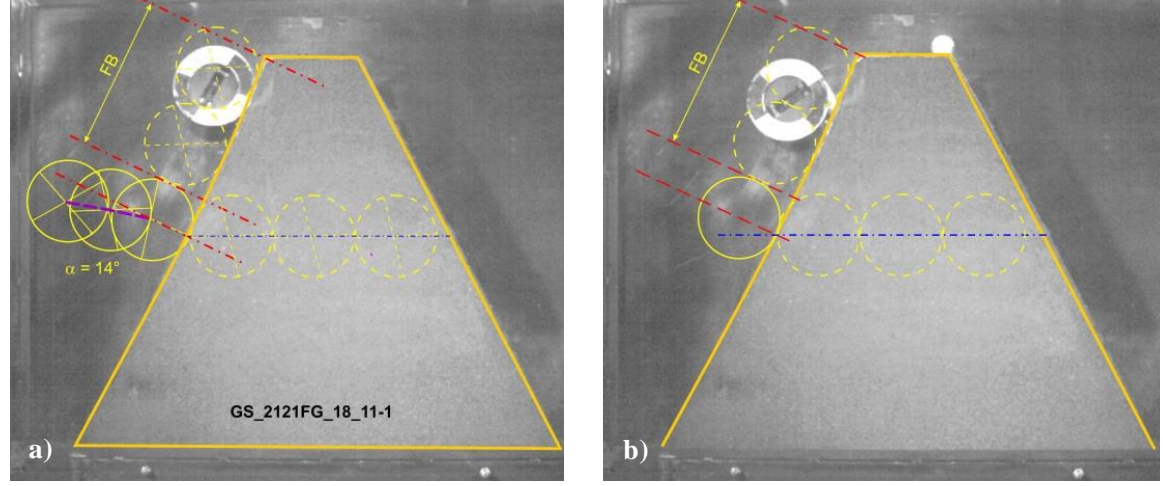


Fig. 3.15: Test GS_2121FG_18_11: a) first impact, FB = 1.9*2r, climbing height approx. 1.8*2r, b) second impact, FB = 1.9*2r, climbing height approx. 1.55*2r.

July 2017 35/90 Analysis of Existing Rockfall Embankments of Switzerland (AERES), part C

For these tests the freeboard was chosen to be approximately 1.9 block diameter. This value is a little bit less than the value of 2 block diameters specified in standard ONR 24810:2013 as minimum value for the freeboard of pure soil embankments, but significantly larger than the minimum value specified for embankments with rockery. The crest to block diameter ratio was chosen again to be approx. 1.1. The impact point is at a level, where the embankment thickness is larger than three block diameter (Fig. 3.14 and Fig. 3.15) and therefore according to Kister (2015) there was no risk that the embankment will be punched through. On each embankment type a first and a second impact with block GS had been done. In no test the embankment was surmounted by block GS but the experiments showed some remarkable results:

- a) The rough surface of the rockery in test GS_2121FG_18_11 led to a larger climbing height for block GS than the "smooth" surface in test GS_2121HG_18_11, although the block velocities had been very similar (see Appendix C1, difference in translational velocity: 1.5%, difference in rotational velocity: 6%). If the climbing height is measured in the same way as the freeboard, i.e. parallel to the slope, the first impact on the rough surface led to a climbing height which is 1.8 the block diameter while the first impact on the smooth surface led to a climbing height of 1.3 block diameter. So the climbing height for the first impact at the rough surface is 28% higher than the climbing height at the smooth surface. For the second impact the climbing height of block GS at the rough surface is approx. 35% higher than the climbing height at the smooth surface. The maximum climbing heights received in the tests are shown in Figure 3.14 respective Fig. 3.15.
- b) The first impact of block GS resulted in a larger climbing height than the second impact for both surface roughness types. For the smooth surface the factor for the climbing height between first and second impact is 1.3. For the rough surface this value is a little bit less and approx. 1.2.

These results may be interpreted as follows:

- a) In the test with the stepped rough slope surface impactor GS and rockery surface have less contact points than in the test with the "smooth" surface. Additional during the impact process the block GS bounced off the embankment's slope in both tests, but the time without a contact was larger in test GS_2121FG_18_11 than in test GS_2121HG_18_11. Therefore friction losses between impactor and embankment slope are smaller in test GS_2121FG_18_11 than in test GS_2121HG_18_11.
- b) Due to the first impact the stones are pushed into the soil and a kind of depression is produced (Fig. 3.16b, Fig. 3.17a and b). When the impactor hits this depression again during the second impact, energy is needed to get out of this depression. This amount of energy is missing, when the impactor is climbing up. Therefore the climbing heights of the second impacts are smaller than the climbing heights of the first impact.

Fig. 3.16a and b show the rockery before and after the first impact. Only little damage is visible to the naked eye and the damage seems to be restricted to the impact area. But at the embankment's crest a crack occurred between rockery and soil (Fig. 3.16 c). This is already an indication for dissolution. In consequence of the second impact a separation between rockery and soil occurred and all stones dropped down. On the other hand, a golf ball, which was placed on the crest of the embankment, showed only a small displacement. But a horizontal crack at the "downhill" slope was detected after the second impact.

July 2017 36/90 Analysis of Existing Rockfall Embankments of Switzerland (AERES), part C

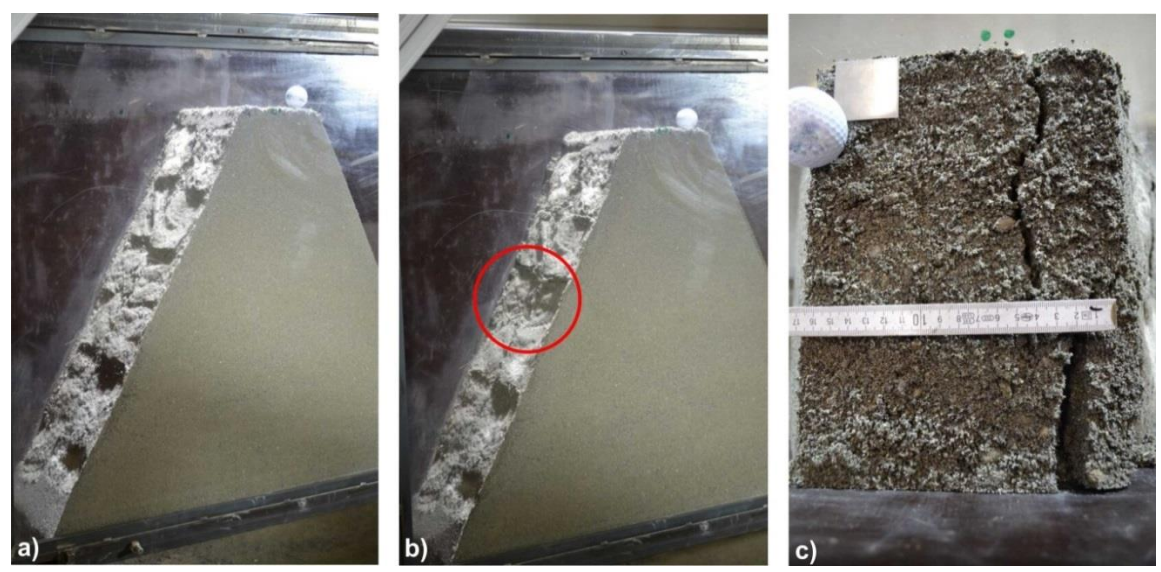


Fig. 3.16: Test GS_2121HG_18_11: a) rockery before first impact, b) rockery after first impact, red circle marks impact position, c) dissolution of stones due to the first impact at the crest, only a small shift of the golf ball at the top occurred due to the impact.

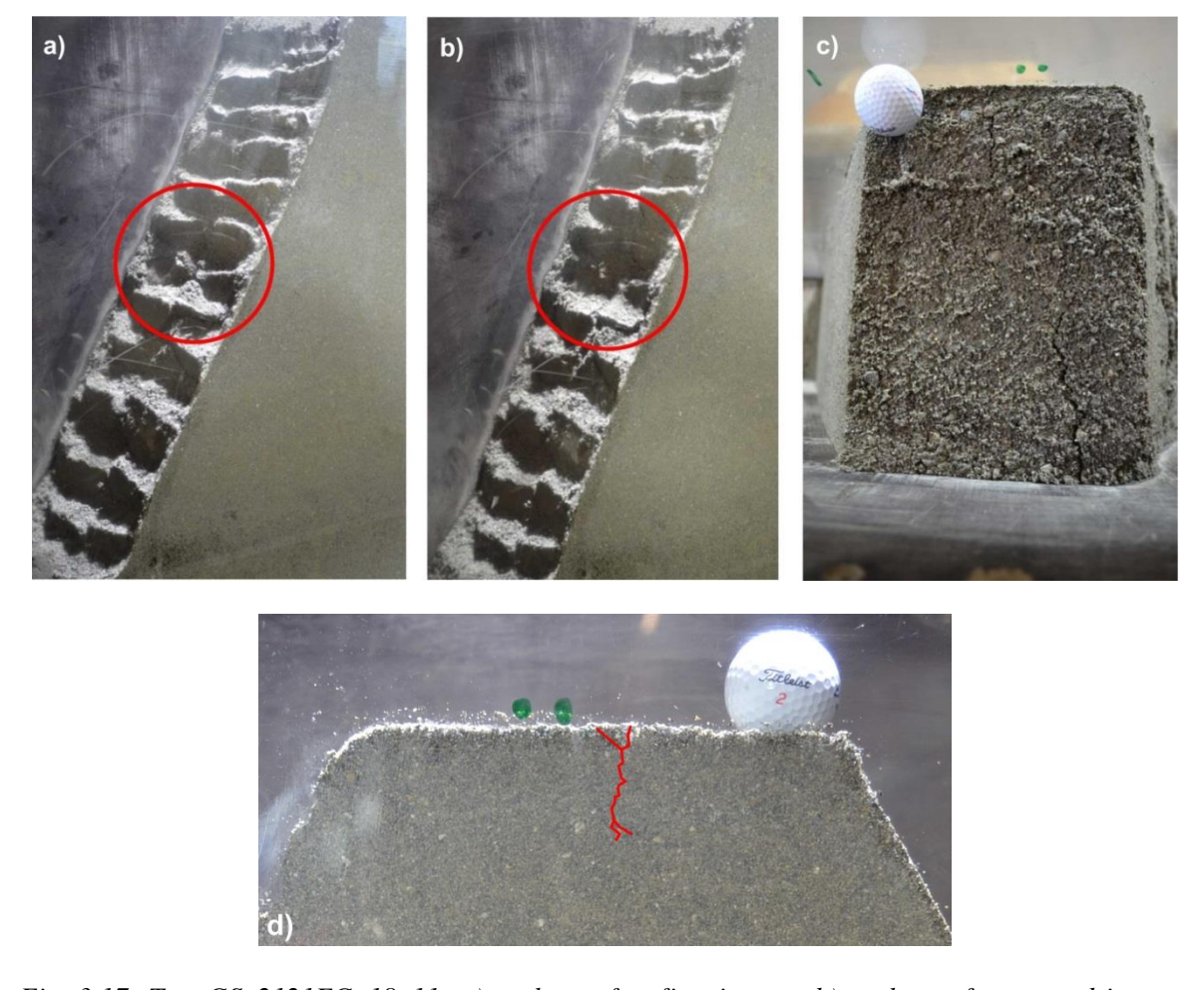


Fig. 3.17: Test GS_2121FG_18_11: a) rockery after first impact, b) rockery after second impact, c) and d) crack formation due to the second impact at the crest; red circle marks impact position.

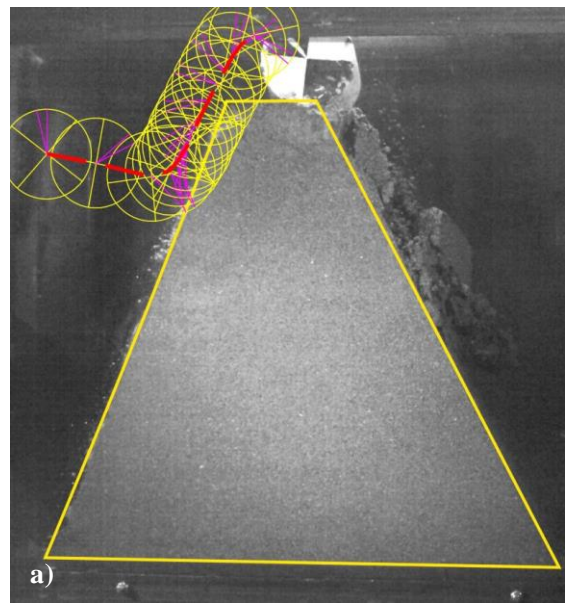
Fig. 3.17a and b show the rockery made of stones placed horizontally (GS_2121FG_18_11) after the first and second impact. Also in these tests the damage seems to be restricted to the impact area and relatively small. A crack occurred at the crest as a result of the second impact, but was smaller than that one in test GS_2121HG_18_11-1. The crack could be identified visual up to a depth of about 4 cm at the forefront of the test box (Fig. 3.17 d). No crack was visible at the "downhill" slope after the second impact.

To check the influence of the slope angle additional tests had been done with a batter 5:2 and 5:1. For each slope angle a test had been done with block G as well as with block OKT. For a batter of 5:2 in both tests the impact angle has been determined to 8°. For the tests with a batter of 5:1 the impact angle was -4° respective -5°. Taking into account the error of measurement these values can be considered to be identical.

Each test had been done with a crest to block diameter ratio of approx. 1.1. The freeboard in the tests was about 0.5 block diameter (see Table 3.6). But only in test G_25121F_17_11-1 the embankment was surmounted by block G (Fig. 3.18a). The trajectory in this test looks very similar to the trajectory of test G_2121_9_11-1 without rockery (Fig. 3.10a).

The block trajectories of both blocks, G and OKT, determined in the tests with an embankment with a batter of 5:2 are shown in Fig. 3.18. The penetration depth of block G is less than the radius of the block. The block moved upward and removed part of the crest. At the maximum jump height the lower contour line of the block is higher than the crest level (Fig. 3.18a). Cracks occurred during the impact process, but had been closed and destroyed when the block fell back onto the crest.

Block OKT had a translational velocity v, which is close to the translational velocity of block G (G: v = 5.9 m/s, OKT: v = 6.3 m/s, difference: approx. 7%, this is still within the measurement error). Block OKT moved also towards the crest and reached a penetration depth of approx. $\frac{1}{2}$ block diameter (Fig. 3.18b).



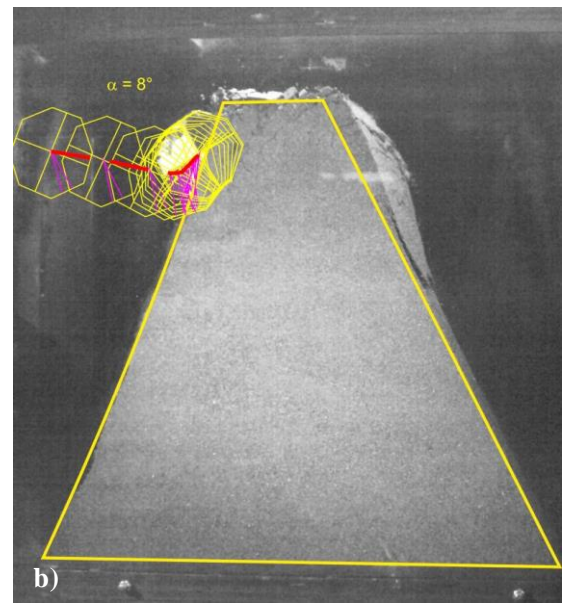


Fig. 3.18: Influence of block shape and block rotation on the trajectory: Embankment with batter 5:2, i.e. slope angel approx. 69° , a) test $G_25121F_17_11-1$, FB approx. 0.6*2r b) test $OKT_25121F_17_11-1$, FB approx. 0.5*2r.

The embankment's crest was deformed and pushed towards the "downhill" direction by block OKT. Slope instability occurred and a large part of the crest material slid down at the "downhill" slope, but the block was not able to surmount the embankment (Fig. 3.19a). Even a second impact onto the already heavily damaged embankment with block OKT was not able to surmount the embankment. Now the embankment's crest was totally destroyed and block OKT remained on the destroyed embankment (Fig. 3.19b).

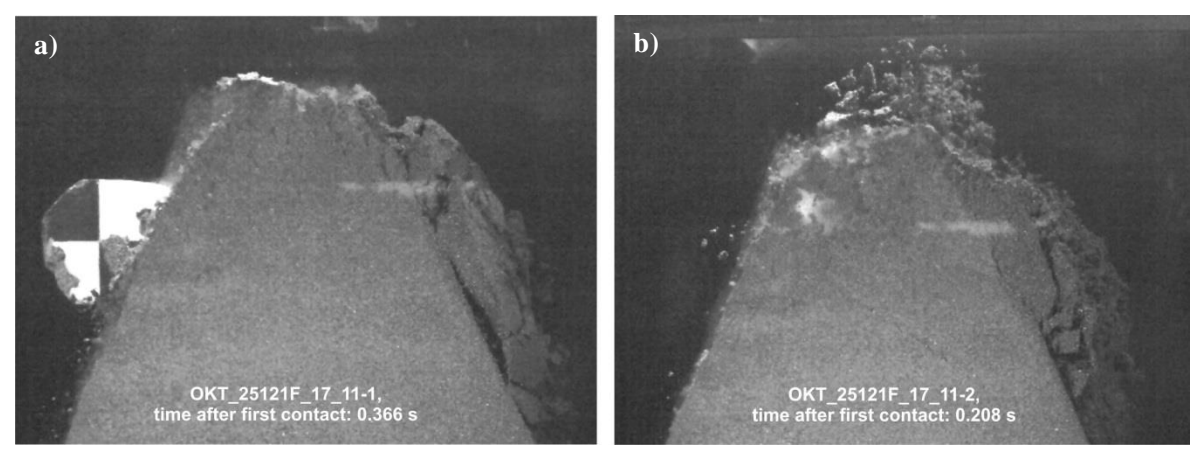


Fig. 3.19: Test OKT_25121F_17_11: a) slope instability due to first impact, block fell back on the "uphill" side, b) slope instability due to second impact, block remain on the destroyed crest.

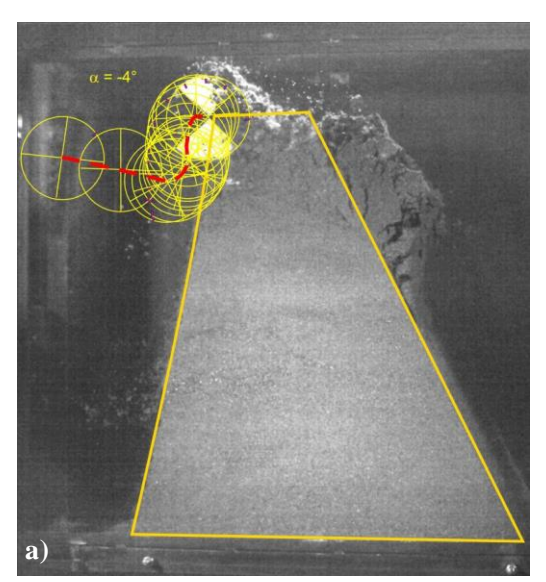
Beside the difference in the cross section of the two blocks G and OKT there is another parameter which differs significant in the two tests: the rotational velocity. While the rotational velocity of block G is approx. 77 Hz, the rotational velocity of block OKT is only 3.4 Hz just before the impact. From this follows that the rotational energy of block OKT is less than 0.2% of the rotational energy of block G when the block is impacting the embankment.

For the tests G_5121F_17_11 and OKT_5121F_17_11 with a batter 5:1 the block trajectory is above the vertical to the embankment's slope. By definition the impact angle now is negative and the translational velocity component parallel to the slope (see Fig. 3.1b) acts in opposition to the direction of block movement. Neither block OKT nor block G is able to surmount the embankment (Fig. 3.20). In both tests the block fell back to the "uphill" side, but the embankment was totally damaged.

The comparison of Figures 3.20a and 3.18a shows an upward movement of block G, which is significantly less in test G_5121F_17_11-1 than in test G_25121F_17_11-1. But the translational velocities just before the impact are nearly identical (5.9 m/s resp. 6.0 m/s) and the rotational velocities are very similar (77 Hz, 79 Hz). So because in both tests the same block G was used, this difference is traced back to the increased batter 5:1.

Block OKT shows also a lower upward movement in Fig. 3.20b of test OKT_5121F_17_11-1 than in Fig. 3.18b of test OKT_25121F_17_11-1, even though the rotational velocity ω in test OKT_5121F_17_11-1 is more than twice the rotational velocity in test OKT_25121F_17_11-1 (8.1 Hz resp. 3.4 Hz). However it has to be taken into account that the rotational velocity in both tests is very low. A summary of the test data and results of the tests shown in Figures 3.18 and 3.20 is given in Table 3.6.

July 2017 39/90 Analysis of Existing Rockfall Embankments of Switzerland (AERES), part C



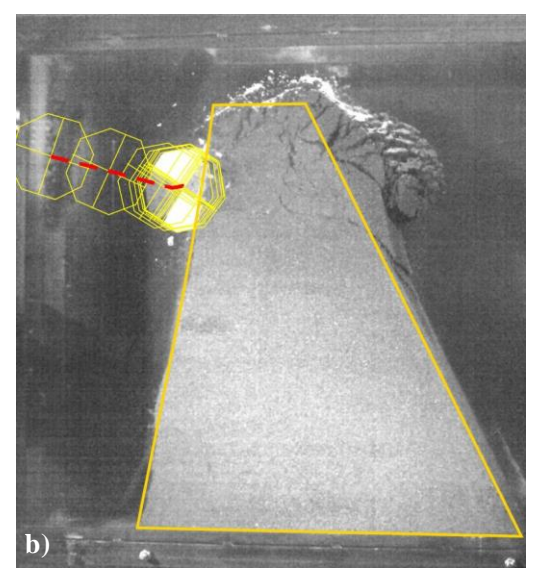


Fig. 3.20: Influence of block shape and block rotation on the trajectory: Embankment with batter 5:1, i.e. slope angel approx. 79.5° , a) test $G_5121F_17_11-1$, FB approx. 0.4*2r b) test $OKT_5121F_17_11-1$, FB approx. 0.5*2r.

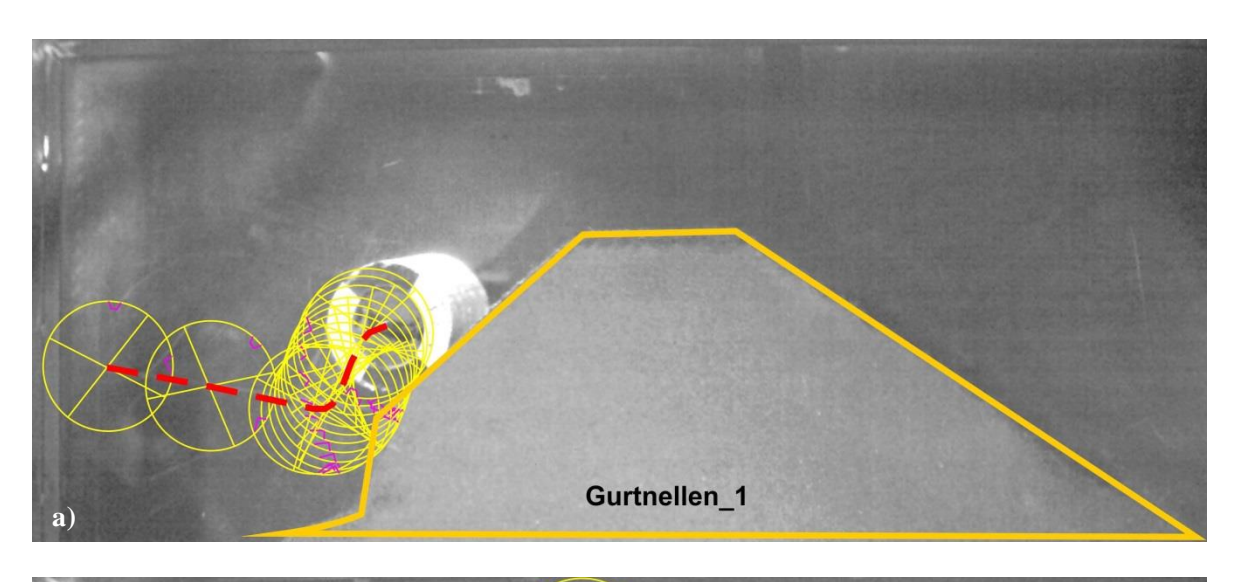
β _{us} : 68.6°	G_25121F_17_11	OKT_25121F_17_11
β_{ds} : 62.6°	FB approx. 0.6 * 2r	FB approx. 0.5 * 2r
a _c : 16.5 cm	block jumped over embankment	embankment not surmounted
OS: horizontal	crest with significant damage	1 st impact: significant damage.
		2 nd impact: crest totally destroyed
β _{us} : 79.5°	G_5121F_17_11	OKT_5121F_17_11
β_{ds} : 62.6°	FB approx. 0.4 * 2r	FB approx. 0.5 * 2r
a _c : 17.5 cm	embankment not surmounted,	embankment not surmounted,
OS: horizontal	but crest totally destroyed	but crest totally destroyed.
Explanation:	β_{us} : slope angle uphill side	OS: orientation of stones
	β_{ds} : slope angle downhill side	2r: block diameter
	a _c : crest width	FB: Freeboard

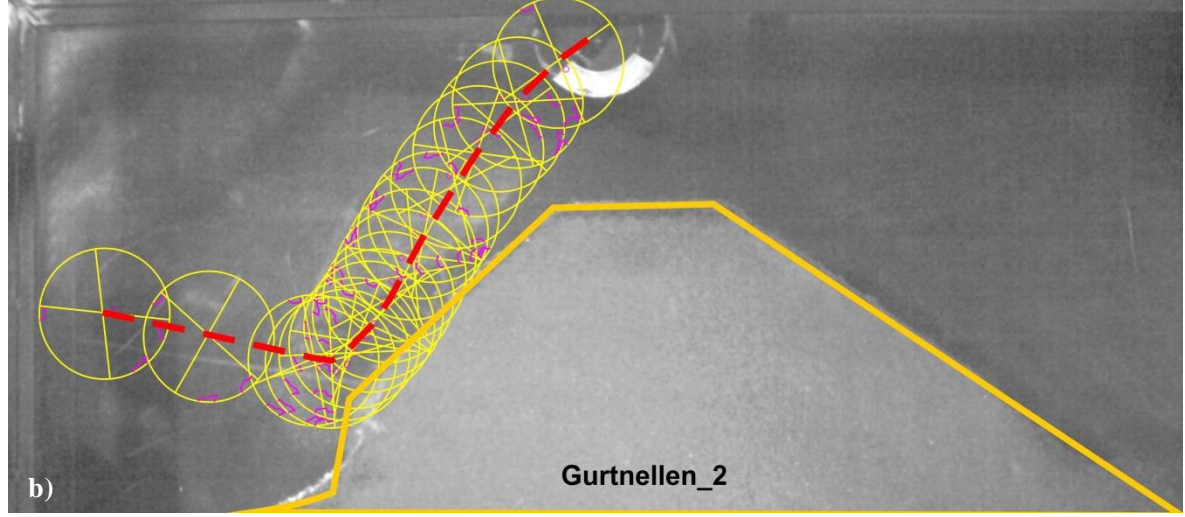
Table 3.6: Results of tests with an embankment model with batter 5:2 respective 5:1 at the "uphill" slope and crest to block diameter ratio of approx. 1.1.

With the impactor GS three tests, two first impacts and one second impact, had been done on a model on a scale of 1:20 of the Gurtnellen Embankment North (Fig. 2.14). For the first test named as Gurtnellen_1 the embankment model and the down pipe had been arranged in such a way, that the impact point was just below the kink of the bi-linear slope. So the impactor hits the rockery surface of the slope and pushed the topmost stones into the soil body of the embankment. Then the block moves upward the flat-angle soil part of the slope. But the energy loss of the block due to that impact was large enough so that the block was not able to surmount the embankment. Fig. 3.21a shows the block trajectory of this test.

A second impact test had been done on the same model, but now the model was lowered for a few centimeters. This lowering resulted in an impact point, which was now located a little bit above the kink of the bi-linear slope. Now the impactor hits the stones on the top. Because the stone were placed on other stones underneath, neither a large deformation nor a large displacement of the topmost stones was possible. A large amount of energy remained at the block and the embankment was now surmounted with a large jump (Fig. 3.21b).

July 2017 40/90 Analysis of Existing Rockfall Embankments of Switzerland (AERES), part C





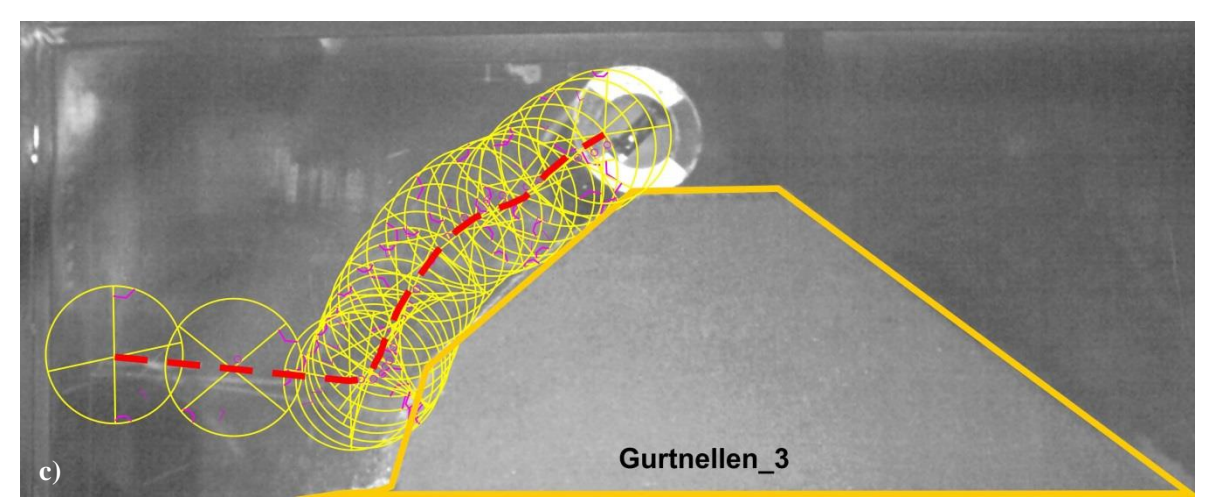


Fig. 3.21: Trajectories received with the embankment model Gurtnellen and impactor GS

July 2017 41/90 Analysis of Existing Rockfall Embankments of Switzerland (AERES), part C

The model embankment was constructed a second time and now embankment model and down pipe had been again arranged in such a way, that the impact point was below the kink of the bi-linear slope. In this test the block reached the top of the embankment, but the embankment was not surmounted. Fig. 3.21 c) shows the block trajectory.

3.3 Block deceleration due to impact

The data received with the high speed camera had also been analyzed with the open source program Tracker. The program Tracker is a video analysis tool and was used for center of mass tracks to get information about the translational velocity of a block during the impact process. To do this in the pictures of a test the position of the center of mass has to be visible. For each test a series of about 350 to 450 pictures had to be analyzed.

Additional the block rotation was determined and the rotational block velocity had been evaluated. This was done by hand and on the basis of the trajectory pictures shown in the chapter before. Therefore the number of data points for those analyses are significantly lower.

Impact tests with the same embankment cross section with a batter of 2:1 and stones placed parallel to the embankment's slope at the uphill side had been analyzed for the three impactors G, GS and OKT. The mean value of the translational velocity v of the blocks G and GS before the impact was approx. 6.6 m/s resp. 6.7 m/s. For block OKT the mean value of the velocity was a little bit less, that is to say 6.1 m/s. Within the first 6 ms of the impact process the translational velocity was reduced to a value less than 3 m/s and the graphs for the three impactors look alike (Fig. 3.22). Within the next 16 ms the translational velocity is still reduced, but the amount of deceleration is significantly smaller and differences appear for the 3 impactors G, GS and OKT. 22 ms after the contact the velocity is reduced furthermore, but now the graphs in Fig. 3.22 show only a very small decrease for the mean value of the velocities. The scattering of the data points in Fig. 3.22 gives an idea about the measurement error of that type of analysis with the program Tracker.

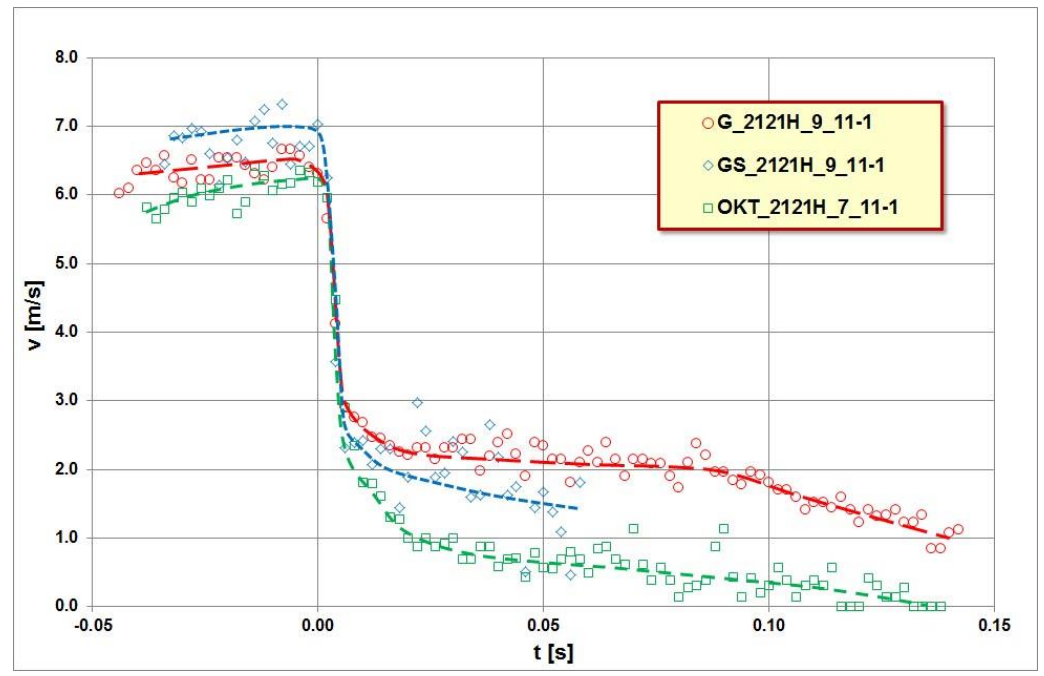


Fig. 3.22: Decrease of translational velocity v of the three used impactors at the same embankment cross section with batter 2:1 and stones placed parallel to the slope surface.

Fig. 3.22 shows the largest amount of deceleration for block OKT with edges and no rotation before it hit the embankment. Within 22 ms the translational block velocity is reduced to 15% of the value before the impact and the translational energy is reduced to 2.3% of the value before the impact (Table 3.7). On the other hand the velocity v of cylinder G made of concrete and with $E_{rot}/E_{trans} = 0.45$ just before the impact, is only reduced to 35% of the value before the impact in the same period. The translational energy is also reduced, but is still 12% after 22 ms. Block GS with the steel jacket and with $E_{rot}/E_{trans} = 0.15$ lies in between the values of the two other blocks (Table 3.7).

Impostor	Impact	v(t=0)	v(t=6 ms)	v(t=22 ms)	E _{trans,0}	E _{trans,6}	E _{trans,22}
Impactor	angle	[m/s]	[m/s]	[m/s]	[Nm]	[Nm]	[Nm]
0	120	6.6	2.9	2.3	162	31	19
G	13°	(100%)	(44%)	(35%)	(100%)	(19%)	(12%)
CS	12°	6.7	2.4	1.9	152	19.5	12
GS	12	(100%)	(36%)	(28%)	(100%)	(13%)	(8%)
OVT	1.40	6.1	2.9	0.9	128	28.5	3
OKT	14°	(100%)	(48%)	(15%)	(100%)	(22%)	(2.3%)

Table 3.7: Mean values of translational velocity and translational energy just before the impact process and 6 ms resp. 22 ms after the contact block – embankment.

Fig. 3.23 shows the decrease of the rotational velocity ω with time for the three impactors. The impactor OKT had no rotation before the impact. Rotation of impactor OKT is produced only by the impact itself and only a very low rotation with a maximum less than 10 Hz occurred. The block OKT had not surmounted the embankment and reached its maximum height 156 ms after the contact. Then the block fell back on the "uphill" slope.

The high rotation of cylinder G is a result of the friction between the concrete surface of the block and the steel down pipe. Because the friction between the steel jacket of block GS and the steel down pipe is less than the friction between concrete and steel, the rotation of block GS is lower than the rotation of block G. After 0.04 s the rotational velocity of both blocks is approximately constant, but on different levels (Fig. 3.23).

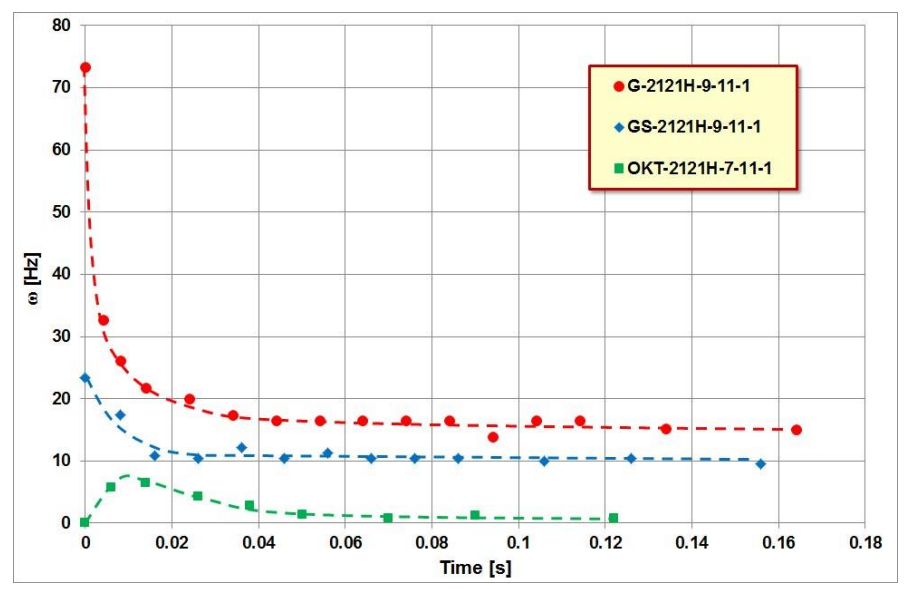


Fig. 3.23: Decrease of rotational velocity ω of the three used impactors at the same embankment cross section with batter 2:1 and stones placed parallel to the slope surface.

July 2017 43/90 Analysis of Existing Rockfall Embankments of Switzerland (AERES), part C

Comparing the graphs in Figures 3.22 and 3.23 it seems to be that the higher the block rotation, the lower is the decrease of the translational velocity v. So the statement "The initial rotational kinetic energy favors an increase of the translational kinetic energy during the impact" given by Plassiard & Donzé (2009) may be converted into: A high rotational block energy leads to less reduction in the translational energy than a low rotational energy.

In Figures 3.24, 3.25 and 3.26 the decrease of translational velocity v of the three used impactors is opposed to the destruction occurred at the embankment due to the impact. It is noteworthy that in all three tests the heaviest damage at the embankment occurred at a time, when the block translational energy has already dropped to a significant low level, i.e. less than 15% for the cylinders and less than 5% for block OKT with edges (Table 3.7). On the other hand the embankment was surmounted by block G as well as by block GS despite of such a low translational and rotational velocity. Only in the test with block OKT, where no rotation occurred before the impact, the embankment was able to retain the block.

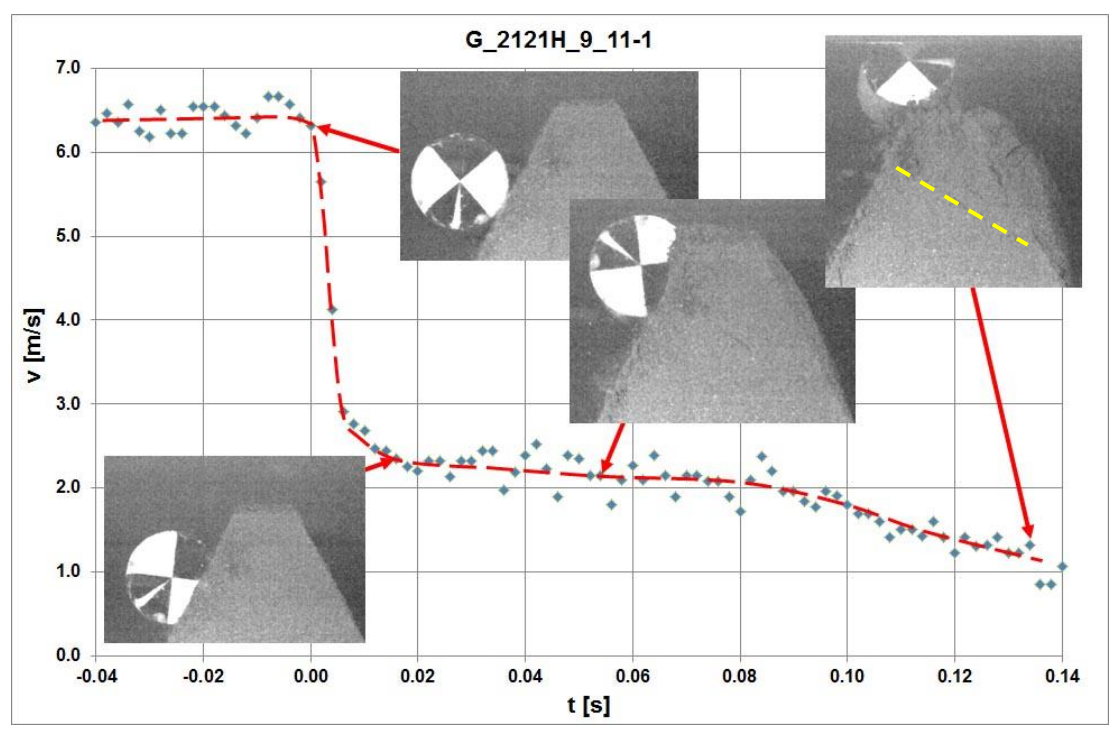


Fig. 3.24: Block deceleration in test $G_2121H_9_11-1$, red line: assumed mean translational velocity, yellow line marks a failure plane with a dip of approx. 30° .

In test G_2121H_9_11-1 as well as in test GS_2121H_9_11-1 a failure plane occurred during the tests. The failure plane showed a downward dip to the "downhill side" but with a different inclination in the two tests (Fig. 3.24 and Fig. 3.25). In the test with impactor G the inclination of the failure plane is approx. 30° while in the test with impactor GS the inclination is just one half. Such a failure plane was not observed in tests for embankment cross sections of type 1111 or type 2145 which had been studied by Kister (2015). Also in test OKT_2121H_7_11-1 with the nonrotating block (Fig. 3.26) such a failure plane was not detected.

Because the embankment material was the same in all tests and also the impact angle was more or less the same in the three tests (Table 3.7), the reason for such a failure plane may be traced back to the combination of block rotation and the slender structure.

July 2017 44/90 Analysis of Existing Rockfall Embankments of Switzerland (AERES), part C

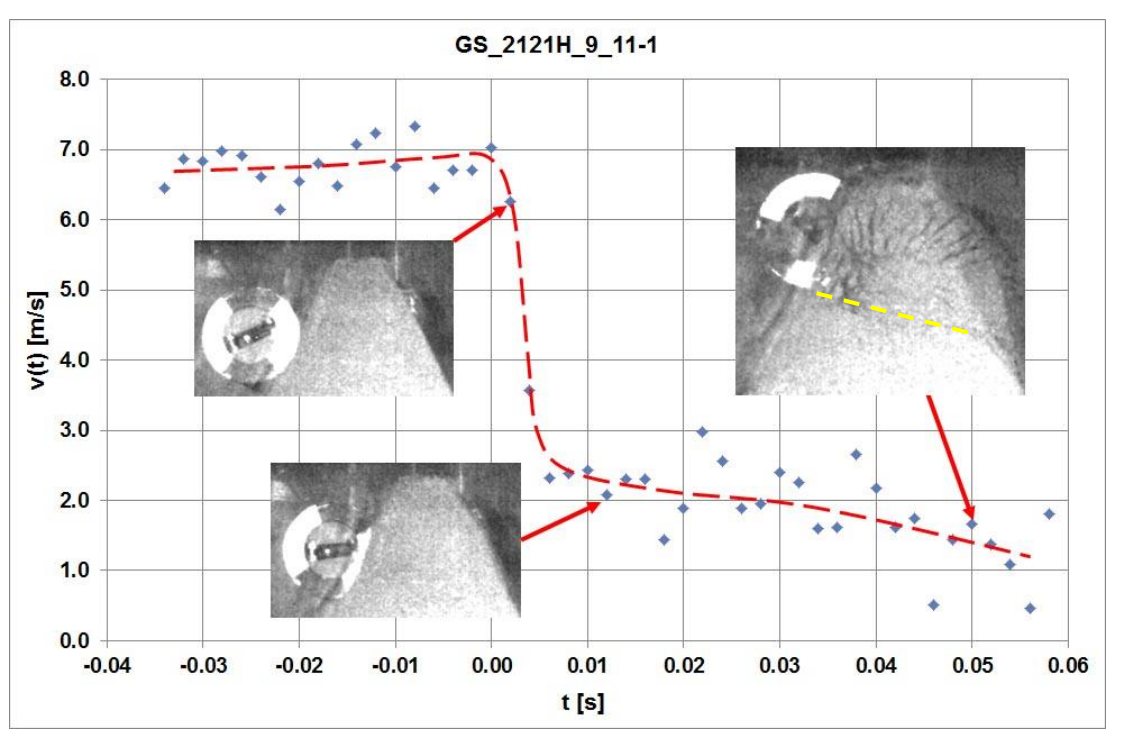


Fig. 3.25: Block deceleration in test GS_2121H_9_11-1, red line: assumed mean translational velocity, yellow line marks a failure plane with a dip of approx. 15°.

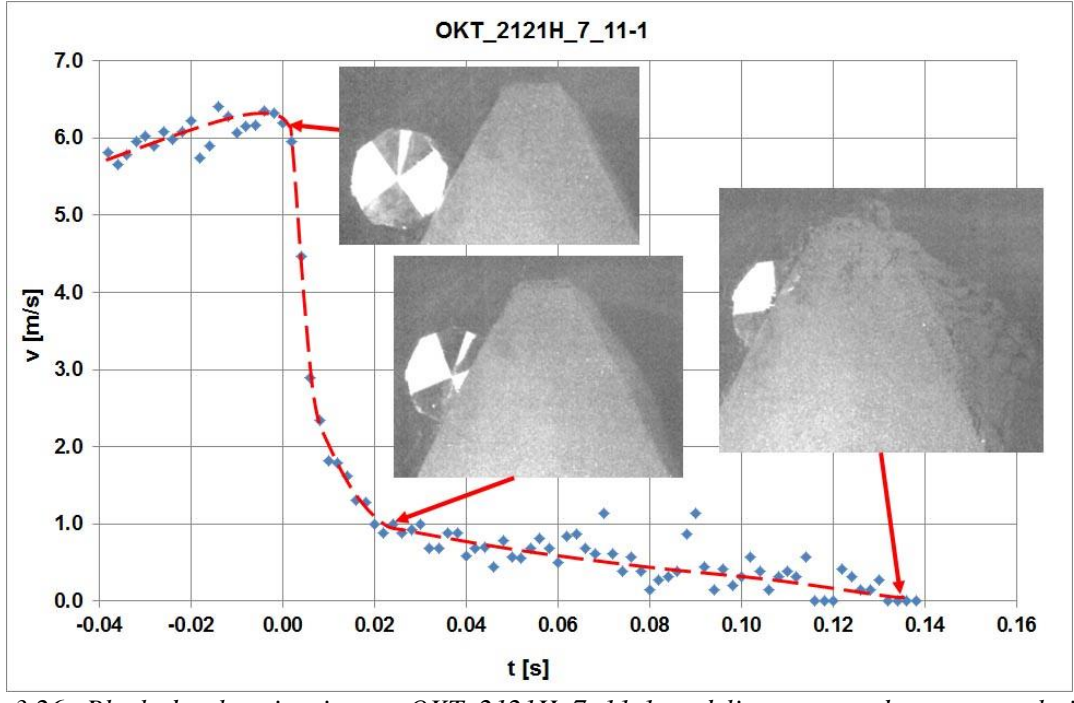


Fig. 3.26: Block deceleration in test OKT_2121H_7_11-1, red line: assumed mean translational velocity

Fig. 3.27 shows the decrease of translational velocity v of impactor G during the impact process at the embankment with cross section with batter 2:1 on both slopes but different surface conditions at the "uphill" slope. For all four tests – without rockery (G_2121_9_11-1), with stones placed parallel to the slope (G_2121H_9_11-1), with stones placed horizontally at the "uphill" slope (G_2121F_9_11-1) and with stones placed horizontally at both slopes (G_2121FF_9_11-1) – the main loss of translational energy occurs within the first 6 to 8 ms after the first contact. The translational velocity v drops from a level of about 6 to 6.5 m/s to a level of 3 m/s or less. This is a translational energy decline of about 75% at least for block G.

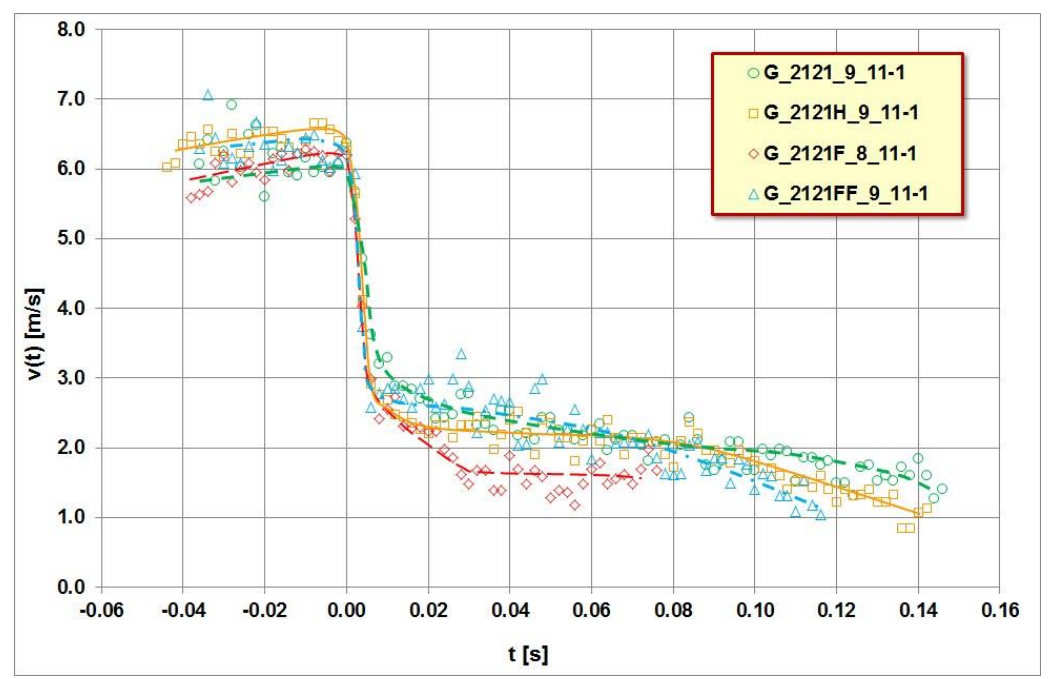


Fig. 3.27: Comparison of translational velocity v versus time t of impactor G for cross section 2121 with different surface conditions at the slope.

Taking into account the measurement accuracy, the data received in the four tests are very close together, especially during the first 6 ms of the impact process. But the curve progression for the period larger than 6 ms shows however some differences (Fig. 3.27). The largest reduction in velocity v is shown for test $G_2121F_8_11-1$ with the rough slope surface. In the interval 0.03 s to 0.07 s the data points of this test show the lowest values for the velocity v. At the last measurement point in this graph block G had penetrated the embankment by its half diameter. No additional analysis could be done because the block center then vanished in an embankment material cloud. In test $G_2121_9_11-1$, without rockery, the penetration depth of block G was less and at the last measurement point shown in the graph, the block was already flying directly above the crest with a velocity v larger than 1 m/s. Looking at the graphs in the interval 0.08 s - 0.14 s in Fig. 3.27 it seems to be, that the decline of the block velocity v increases with slope roughness.

Fig. 3.28 shows the reduction of the rotational velocity during the impact process. The rotational velocity ω before the impact varies only between 78 and 81 Hz in the four tests. This results in a difference of less than 4% between maximum and minimum value of the rotational energy of impactor G. But for a time t > 0.04 s the rotational velocity of block G in test G_2121F_8_11-1 is twice the rotational velocity of block G in test G_2121_9_11-1 without a stony slope surface.

July 2017 46/90 Analysis of Existing Rockfall Embankments of Switzerland (AERES), part C

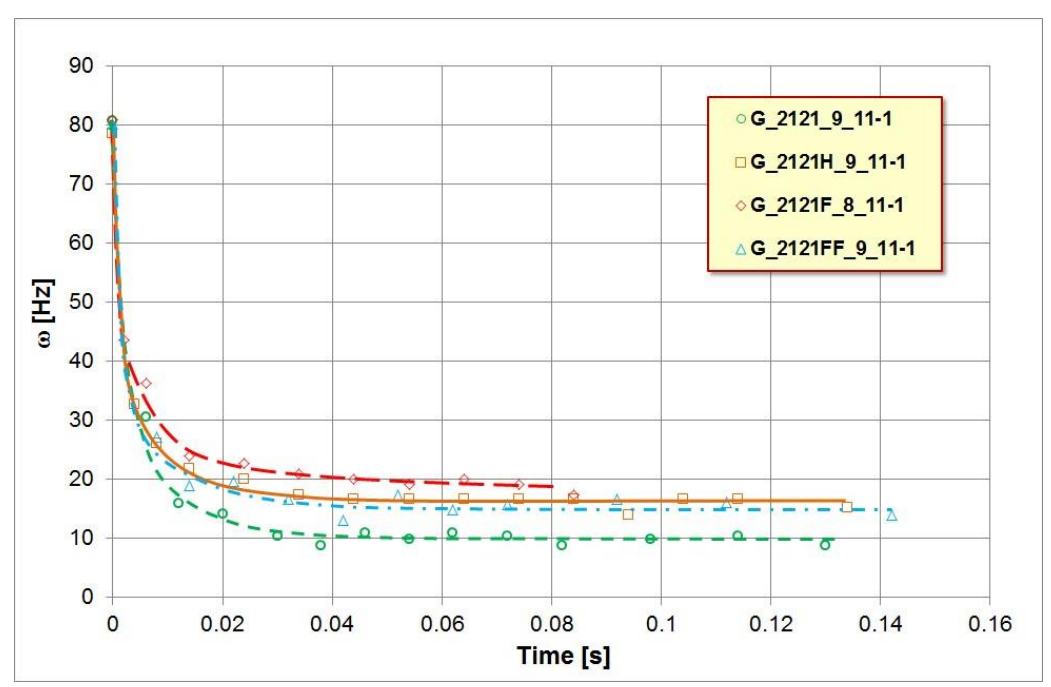


Fig. 3.28: Comparison of rotational velocity ω versus time t of impactor G for cross section 2121 with different surface conditions at the slope.

As shown in Fig. 3.28 the data points of the rotational velocity during the impact process in the tests $G_2121FF_9_11-1$ with stones placed horizontally and $G_2121H_9_11-1$ with the stones placed parallel to the slope are close together. The highest rotational velocities had been observed in test $G_2121F_8_11-1$, even though in this test the slope roughness was the same as in test $G_2121FF_8_11-1$. The difference in both tests is the placing of stones on the "downhill" slope in test $G_2121FF_8_11-1$, which reduced the compressible embankment volume. All four tests have in common that the rotational velocity is approx. constant for t > 0.04 s (Fig. 3.28).

In Figure 3.29 the decrease of translational velocity v of impactor G in test G_2121F_8_11-1 is opposed to the destruction occurred at the embankment due to the impact. Approximately 8 ms after the contact of block and embankment the growth of a bulge at the opposite slope can be recognized. At that moment the block translational velocity was already reduced to less than 42% of the velocity value before the contact and the translational energy was less than 18% of the translational impact energy. The rotational velocity is less than 50% of the rotational velocity before the contact. The penetration depth is about one quarter of the block diameter.

Approximately 60 ms after the contact, a downward failure plane became apparent with a dip of approx. 30°. If the failure plane is elongated by a line, this line goes more or less directly through the center of the block at that time. The penetration depth of the block is now a half diameter (Fig. 3.29, large picture at the right).

Approximately 80 ms after the contact, the bulge had been transformed into a slide. Block G moved through the loosened embankment material respective pushed a part of this material forward and finally the embankment was surmounted by the block (Fig. 3.30).

It is noteworthy that also in this test the heaviest damage at the embankment occurred at a time, where the block translational energy is already very low (8 Nm). The translational energy at this time is less than 7% of the translational energy just before the contact (131 Nm).

July 2017 47/90 Analysis of Existing Rockfall Embankments of Switzerland (AERES), part C

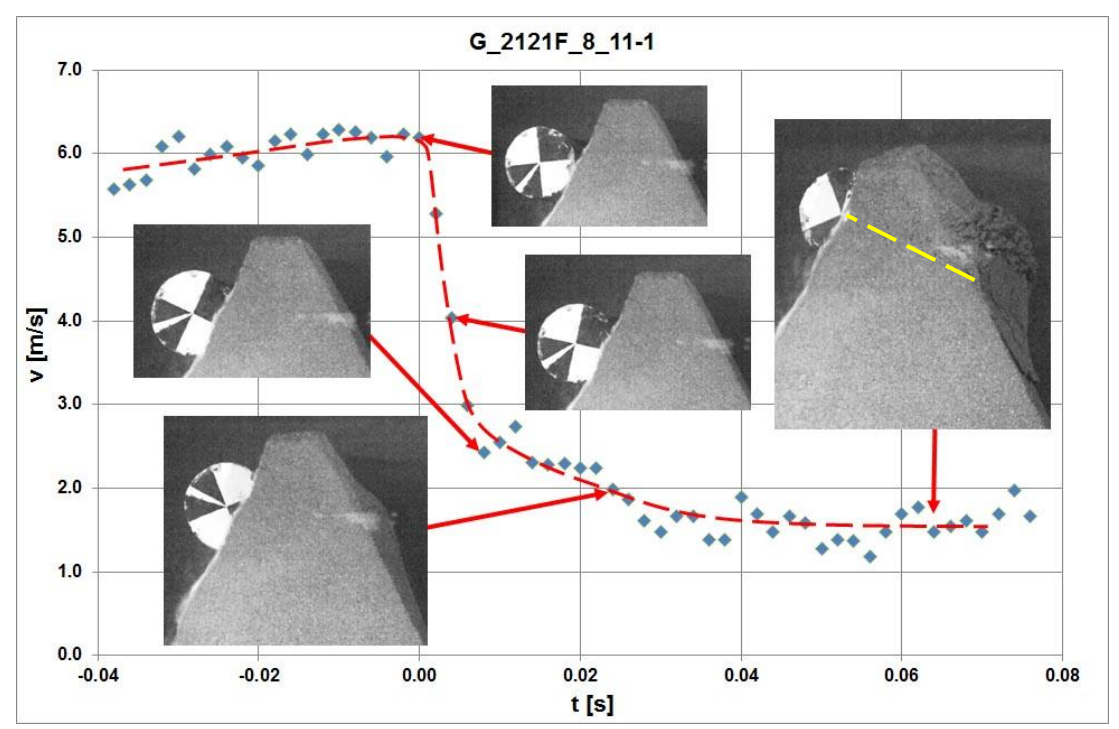


Fig. 3.29: Block deceleration in test $G_2121F_8_{11-1}$, red line: assumed mean translational velocity, yellow line marks a failure plane.

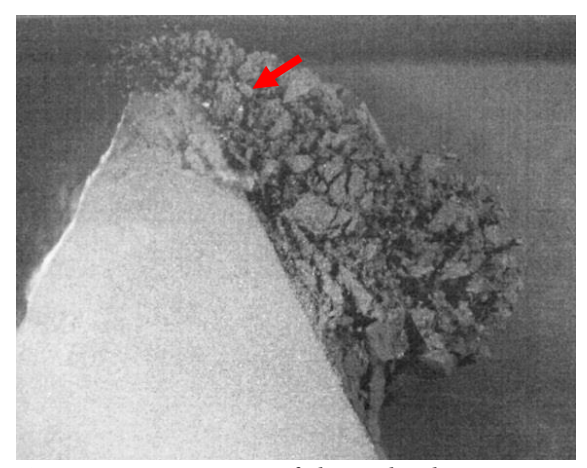


Fig. 3.30: Test $G_{2121F_8_{11-1}}$: Destruction of the embankment's crest by block G (t = 0.224 s after contact). The block is hidden to a very large extent by a cloud of embankment material. Block position marked by the arrow.

The block deceleration determined in tests with block G, but embankment's batter 5:2 resp. 5:1 are shown in Figure 3.31 in comparison to data obtained in the tests with batter 2:1. It is obvious that the translational block velocity v is reduced faster by the steep slope with a batter of 5:1 and to a lower level than in the other three tests. But it has kept in mind that the impact angle for the test with batter 5:1 was -4° (see definition in Figure 3.1). This means there was a velocity component in downward direction of the slope. On the other hand the impact angle in the three other tests was positive (8° for 5:2, 14° for 2:1F and 12° for 2:1 without stones) which results in a velocity component in upward direction.

July 2017 48/90 Analysis of Existing Rockfall Embankments of Switzerland (AERES), part C

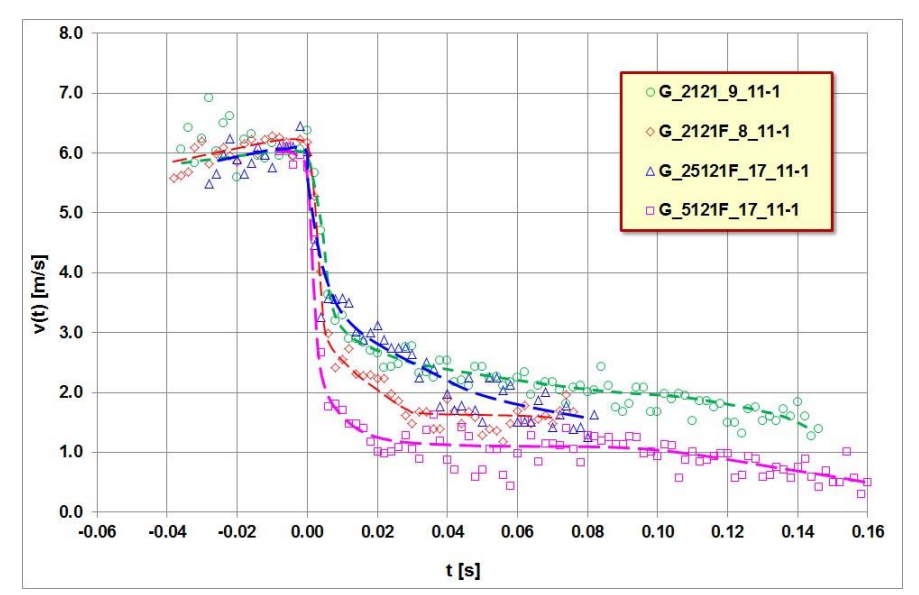


Fig. 3.31: Comparison of translational velocity v versus time t of impactor G for different batter 2:1, 5:2 and 5:1.

For the first 40 ms the graph of test G25121F_17_11-1 with batter 5:2 and rockery is very similar like that one of the test on a slope with batter 2:1 without rockery. But despite the large scattering of the data due to measurement errors it is visible, that the data converges for longer times to the data of the test with batter 2:1 with stones placed horizontally.

20 ms after the first contact in the tests $G_2121_9_11-1$ and $G_25121F_17_11-1$ the block velocity is reduced to less than half of the velocity just before the contact. But for the slope with batter 5:1 the velocity is reduced in the same time interval to a value of only 20% of the velocity just before the contact. Assuming the translational energy of block G in test $G_2121_9_11-1$ is 100% at t=20 ms, then the block in test $G_5121F_17_11-1$ has approx. only 19% of that energy determined for the other test. Even 70 ms after the first contact the block G in test $G_5121F_17_11-1$ has significant lower translational energy than in the other tests. Because the velocity v is nearly identical before the impact for all 4 tests, the steeper embankment slope with batter 5:1 reduces the block energy much better and in a shorter time than the slopes with lower inclination (Table 3.8).

Impactor	Impact angle	v(t=0) [m/s]	v(t=20 ms) [m/s]	v(t=70 ms) [m/s]	E _{trans,20} [Nm]	$\begin{array}{c} E_{trans,70} \\ [Nm] \end{array}$
G_2121_9_11-1	12°	6.0 (100%)	2.7 (45%)	2.1 (35%)	27 (100%)	16 (100%)
G_2121F_8_11-1	14°	5.9 (100%)	2.0 (34%)	1.6 (27%)	15 (55%)	9 (56%)
G_25121F_17_11-1	8°	6.1 (100%)	2.7 (44%)	1.6 (26%)	27 (100%)	9 (56%)
G_5121F_17_11-1	-4°	6.0 (100%)	1.2 (20%)	1.1 (18%)	5 (19%)	4 (25%)

Table 3.8: Mean values of translational velocity and translational energy at 20 ms resp. 70 ms after the contact block – embankment for batter 2:1 without and with "rockery", 5:2 and 5:1.

July 2017 49/90 Analysis of Existing Rockfall Embankments of Switzerland (AERES), part C

In Figure 3.32 the decline of the rotational velocity ω versus time t is shown. Again all four tests have in common that the rotational velocity is approx. constant for t > 0.04 s (cp. Fig. 3.28). It is interesting to see, that the decline of rotational velocity in the two tests G_2121_9_11-1, with batter 2:1 but no "rockery", and G_5121F_17_11-1, with batter 5:1 and stones placed horizontally, is identical to the greatest possible extent for t > 0.025 s. On the other hand the rotational velocity ω in test G_2121F_8_11-1 is twice the value in the tests G_2121_9_11-1 and G_5121F_17_11-1. The graph of test G_25121F_17_11-1 with batter 5:2 lies in between.

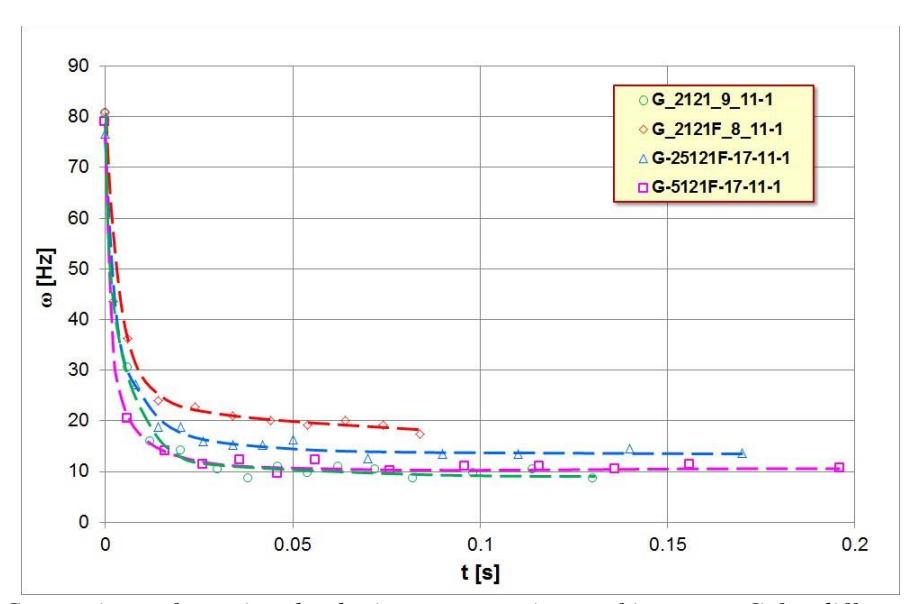


Fig. 3.32: Comparison of rotational velocity ω versus time t of impactor G for different batter 2:1, 5:2 and 5:1.

In Figures 3.33 and 3.34 the decrease of translational velocity v of impactor G is opposed to the destruction occurred at the embankment due to the impact. Again the heaviest destruction of the embankment occurred, when the block already had lost most of its energy. A failure plane with downward dip can clearly be seen again in test G_5121F_17_11-1 (Fig. 3.34).

The Figures 3.35 and 3.36 show the decline of translational and rotational velocity during the impact process in the tests done with impactor GS for the different slope surface conditions. It should be kept in mind, that impactor GS with a steel jacket had a ratio of rotational to translational energy, which is in the same interval as for natural blocks (Usiro et al., 2006, cp. Fig. 3.5).

The measurement error in tests with block GS is larger because of missing cross-lines at the center of the block. As a result a larger scattering of the data points determined with the program Tracker occurred (Fig. 3.35). But also the scattered data shows, that the translational velocity v is less reduced in the test without stones at the embankment's slope than in the tests with stones placed at the embankment's slope.

The differences in the tests with and without stones at the embankment's slope can be seen easier in Fig. 3.36 where the rotational velocity ω versus time is shown for the impact procedure. Here the test without stones on the embankment's slope led to the lowest rotational velocity. The subsidence in the graph of test GS_2121FF_18_11-1 for t>0.05 s corresponds to a twist of the block GS, when it was on its way in upward direction, and this part of the graph is therefore not comparable with the other data.

July 2017 \$50/90\$ Analysis of Existing Rockfall Embankments of Switzerland (AERES), part C

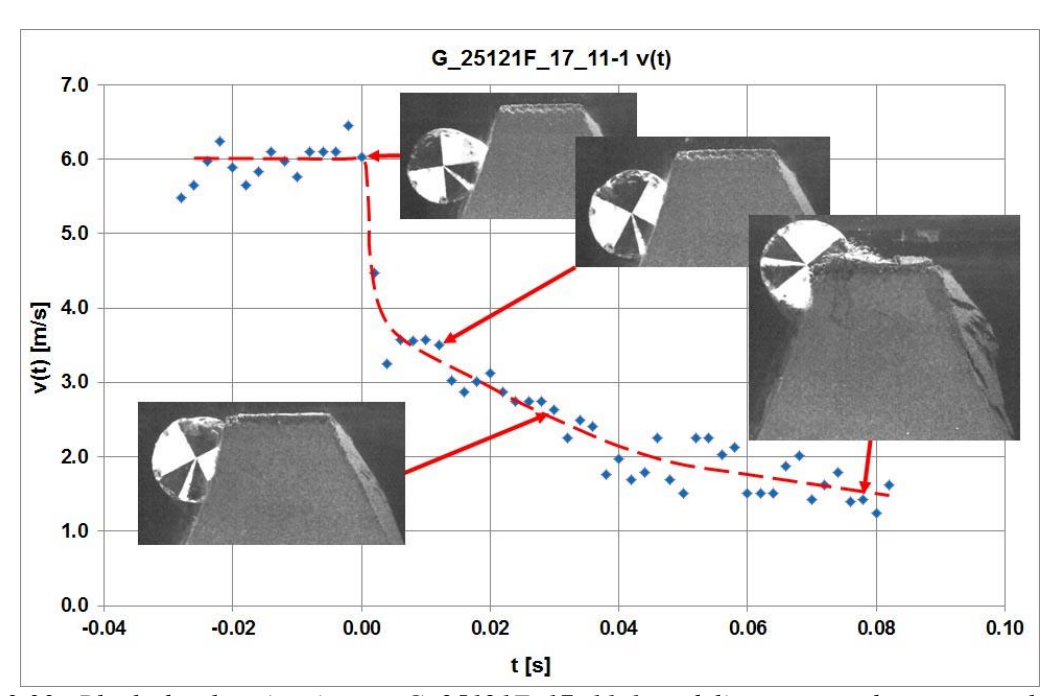


Fig. 3.33: Block deceleration in test $G_25121F_17_11-1$, red line: assumed mean translational velocity.

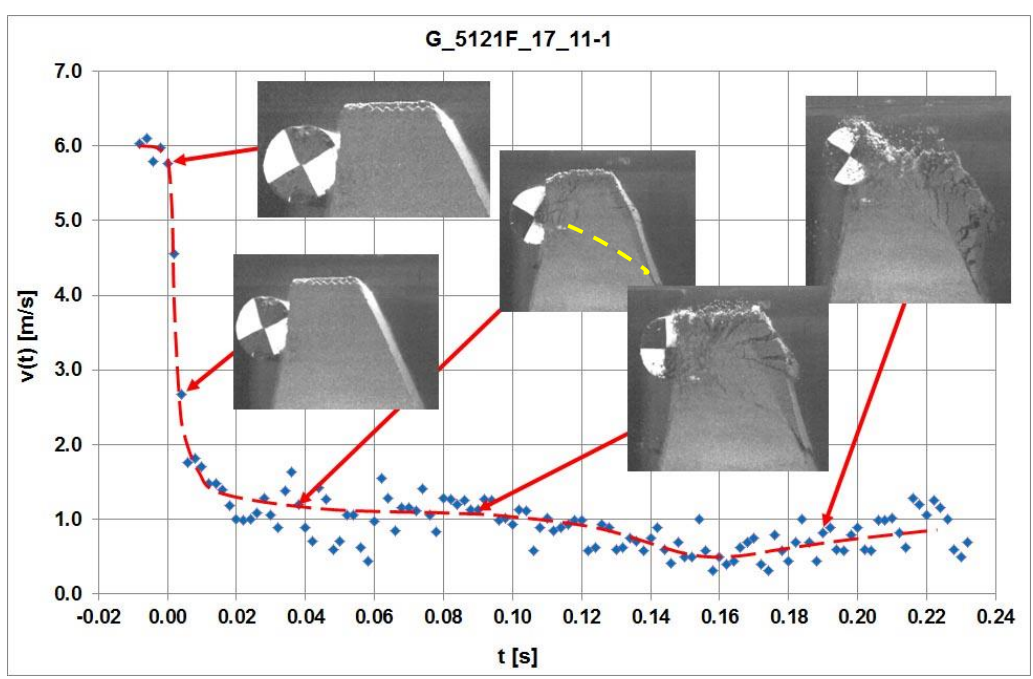


Fig. 3.34: Block deceleration in test $G_5121F_17_11-1$, red line: assumed mean translational velocity, yellow line marks a failure plane.

July 2017 51/90 Analysis of Existing Rockfall Embankments of Switzerland (AERES), part C

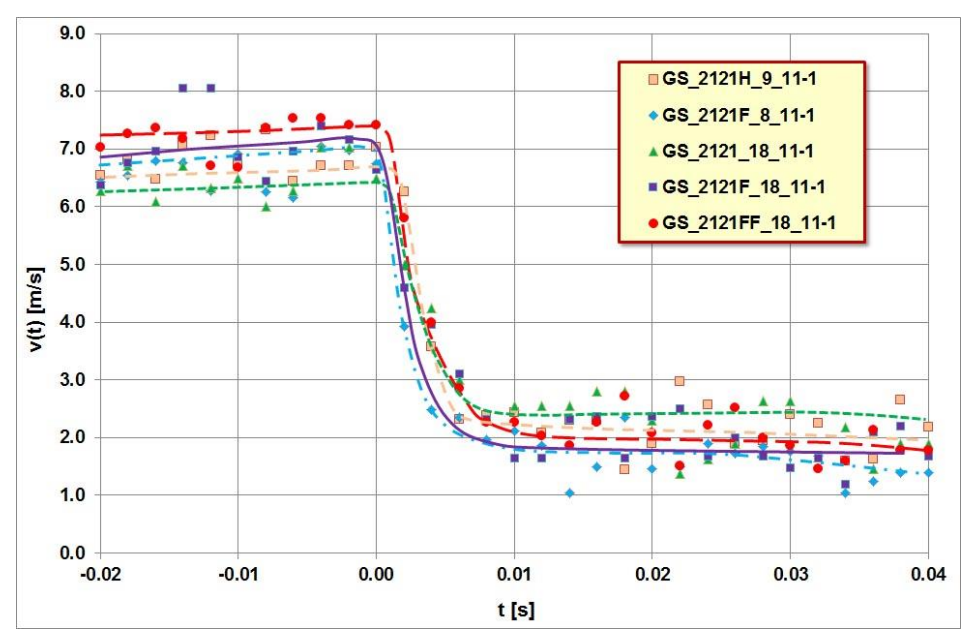


Fig. 3.35: Deceleration of impactor GS at an embankment cross section with batter 2:1, but different surface condition of the slope, lines: assumed mean translational velocity.

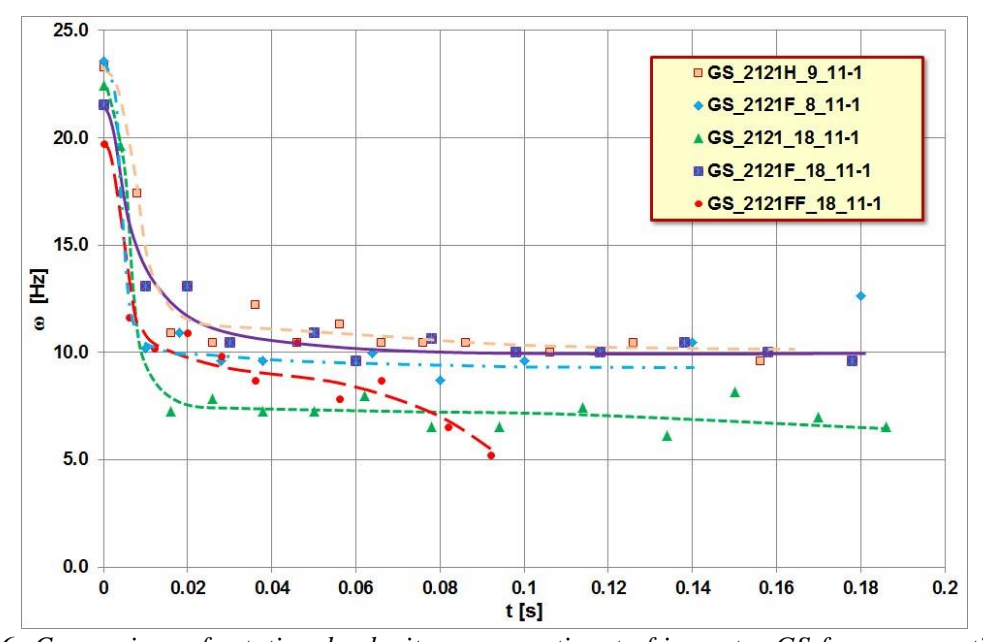


Fig. 3.36: Comparison of rotational velocity ω versus time t of impactor GS for cross section 2121 with different surface conditions at the slope.

In Figure 3.37 the decrease of translational velocity v of impactor GS is opposed to the destruction occurred at the embankment due to the impact. Again the heaviest destruction of the embankment occurred, when the block already had lost most of its energy. A failure plane with downward dip is visible in the right picture of Fig. 3.42 and marked by arrows. The inclination of this failure plane is approx. 25°.

July 2017 52/90 Analysis of Existing Rockfall Embankments of Switzerland (AERES), part C

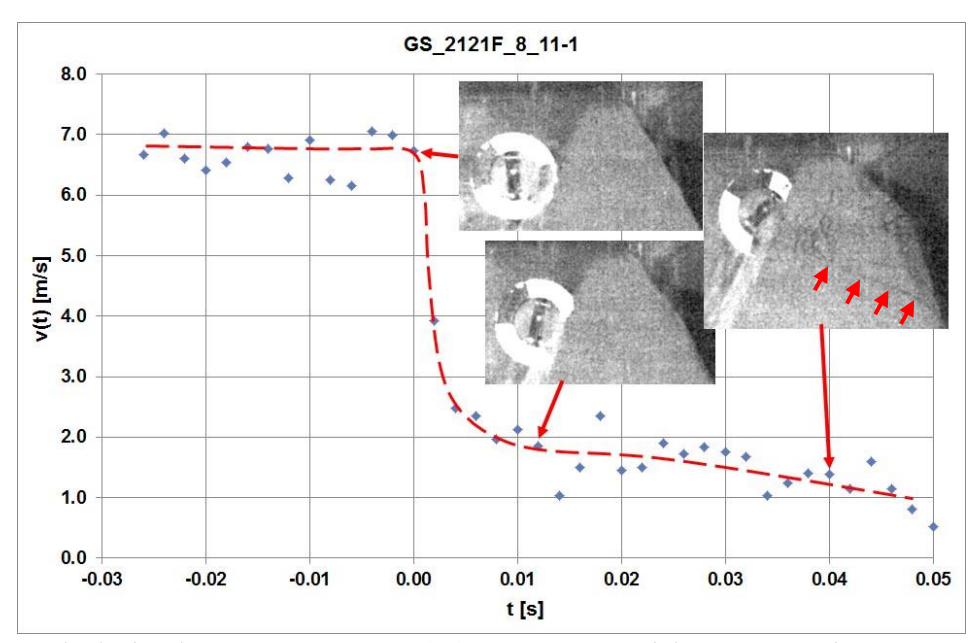


Fig. 3.37: Block deceleration in test GS_2121F_8_11-1, red line: assumed mean translational velocity, arrows mark failure plane.

The tests shown in Figures 3.31 and 3.32 with cylinder G for embankments with different batter had been repeated with the impactor OKT with the octagonal cross section and a low rotational velocity. As mentioned before the block OKT was not able to surmount the embankment in the 4 tests, neither in the three tests with a crest to block ratio of approx. 1.1 nor in test OKT_2121F_8_11-1 with a crest to block ratio of approx. 0.5. But the extent of damage was different and very much larger in test OKT_2121F_8_11-1 with the smaller crest than in the other three tests. Fig. 3.38 shows the decrease of velocity v of impactor OKT at the four embankments with the same surface condition on the slope, but different batter at the "uphill" side.

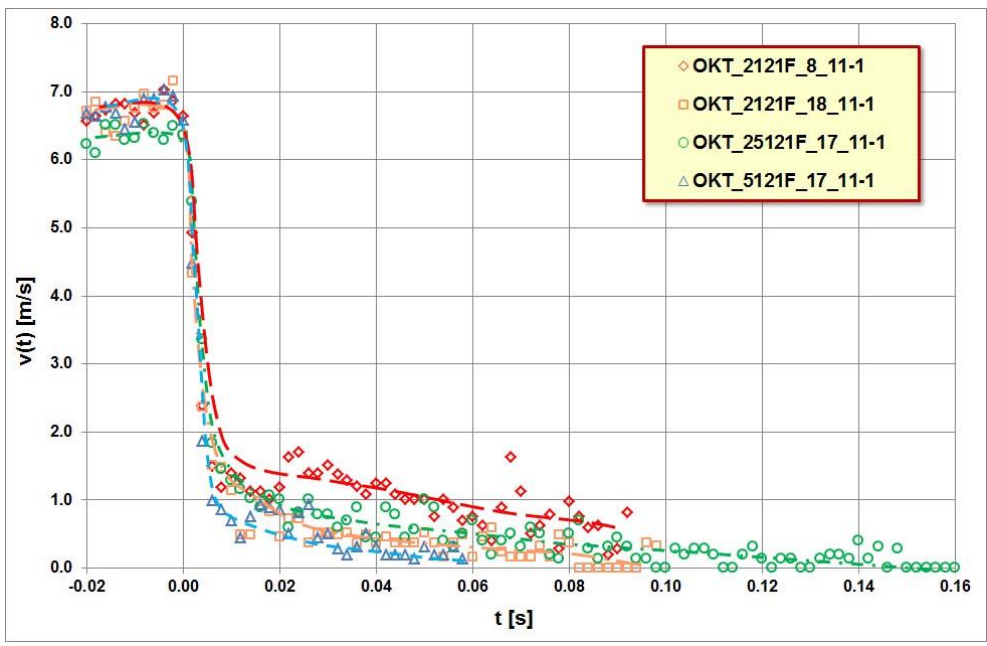


Fig. 3.38: Decrease of velocity v of impactor OKT at embankments with same surface condition on the slope, but different batter at "uphill" side.

July 2017 53/90 Analysis of Existing Rockfall Embankments of Switzerland (AERES), part C

The translational velocity in all four tests drops down from a value larger than 6 m/s to a value smaller than 2 m/s within a time period of approx. 6 ms. The block velocity drop in this time period is very similar for all four tests. After this period Fig. 3.38 shows a kind of splitting of the data. The highest block velocity in this time period is determined for the embankment with the small crest to block ratio of approx. 0.5. This may be an indication that the embankment's resistance against impact in this case is less than for the three other tests with crest to block ratio of approx. 1.1.

The embankment with batter 5:1 reduced the block velocity of block OKT much better and in a shorter time than the embankment slopes with lower inclination. Block OKT is stopped and fell back at approx. 0.06 s after the contact of block and embankment. The embankment with batter 5:2 needs more time, approx. 0.14 s, to stop the block OKT. On the other hand the embankment with batter 2:1 and a crest to block ratio of approx. 1.1 needed only about 0.1 s to stop the block OKT and lies in between the other tests. So there is no clear correlation between slope steepness and time interval for the block to stop.

10 ms after the first contact the block velocity v had been reduced in three of the four tests to a value of approx. 20% of the value just before the impact. The exceptional case is the test OKT_5121F_17_11-1 with batter 5:1, where the reduction is larger and the velocity v at 10 ms is only approx. 10% of the velocity before. The translational energy at 10 ms after the first contact in this test is just a quarter of the translational energy in test OKT_2121F_8_11-1 with batter 2:1 (Table 3.9). So also in the case of a block with edges and very low rotation the embankment with batter 5:1 and a negative impact angle is the combination which is able to reduce the kinetic block energy most effectively.

Impactor	Impact angle	v(t=0) [m/s]	v(t=10 ms) [m/s]	$\begin{array}{c} E_{trans,10} \\ [Nm] \end{array}$
OKT_2121F_8_11-1	11°	6.6 (100%)	1.4 (21%)	6.6 (100%)
OKT_2121F_18_11-1	10°	6.6 (100%)	1.14 (17%)	4.4 (67%)
OKT_25121F_17_11-1	8°	6.4 (100%)	1.3 (20%)	5.7 (86%)
OKT_5121F_17_11-1	-5°	6.7 (100%)	0.7 (10%)	1.7 (26%)

Table 3.9: Mean values of translational velocity and translational energy at 10 ms after the contact block – embankment for batter 2:1, 5:2 and 5:1.

In Fig. 3.39 the decrease of velocity v versus horizontal displacement x of impactor OKT is shown. The horizontal movement of block OKT stops after 4 cm in case of the embankment with batter 5:1 and this is the shortest distance in the 5 tests shown in Fig. 3.39. On the other hand for the embankment with a crest to block ratio of only approx. 0.5 and a batter 2:1 the horizontal displacement x is more than twice. For the embankment with batter 2:1 and a crest to block ratio of approx. 1.1 the horizontal displacement x is approx. 5 cm. This value is approx. 20% larger than the horizontal displacement x in the test with batter 5:1, but significantly smaller than the value of more than 6.5 cm in the test with a batter of 5:2. So again there is no clear correlation between slope steepness and block stopping. Furthermore it is surprisingly that even in the test OKT_2121_18_11-1_B without stones on the embankment slope and a batter of 2:1 the horizontal displacement x is smaller than in the tests OKT_25121F_17_11-1 and OKT_2121F_8_11-1 with stones on the embankment slope.

July 2017 54/90 Analysis of Existing Rockfall Embankments of Switzerland (AERES), part C

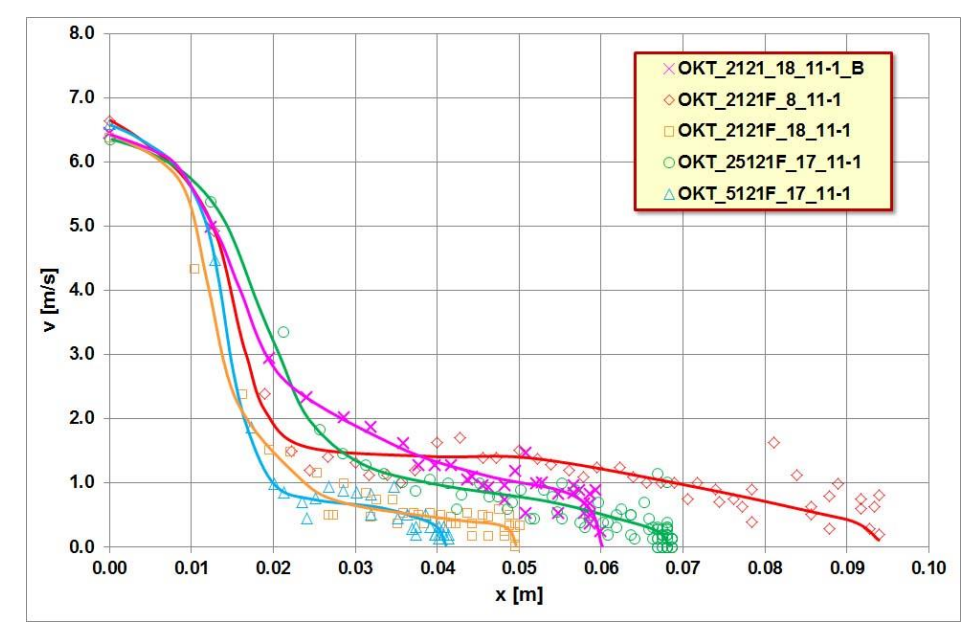


Fig. 3.39: Decrease of velocity v versus horizontal displacement x of impactor OKT at embankments with same surface condition on the slope, but different batter at "uphill" side. For comparison also test OKT_2121_18_11-1_B without stones on the slope is shown.

Fig. 3.40 shows the variation of the rotational velocity ω with time in the four tests with stones placed horizontally at the embankment slope. The rotational velocity of block OKT is low before the impact and in the range of 3 – 13 Hz. Because of the low rotation of block OKT also during the impact process, the measurement of the angle of rotation is difficult. The small changes of the angle of rotation results therefore in a small number of measurement points.

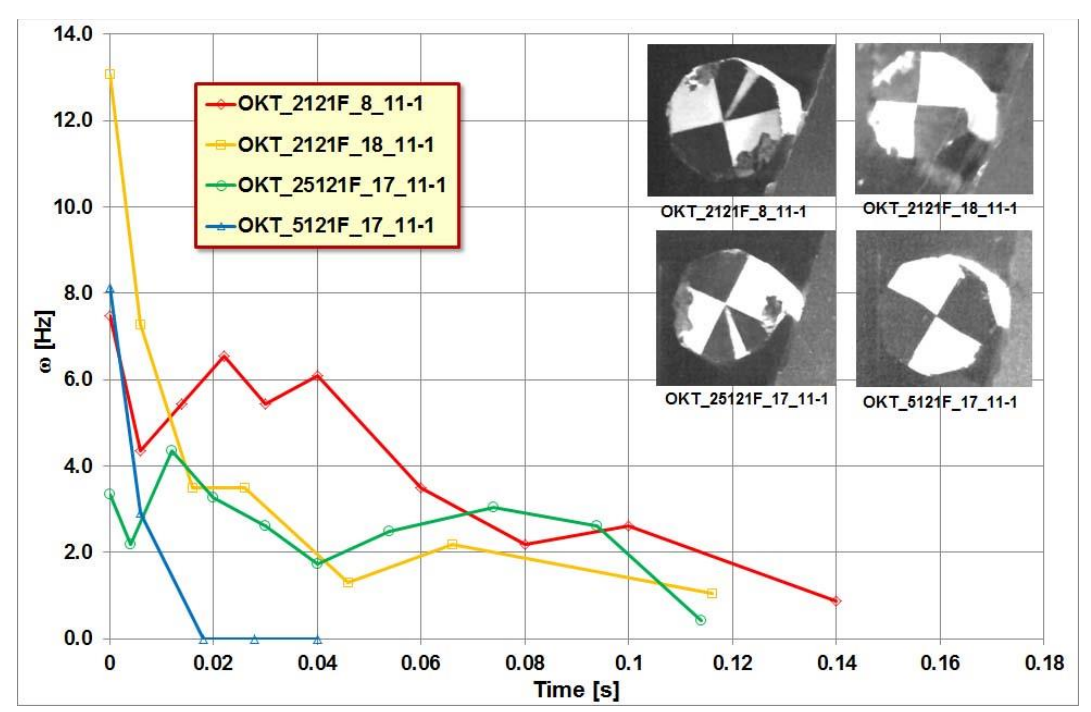


Fig. 3.40: Slowdown of rotational velocity of impactor OKT at embankments with same surface condition of the slope, but different batter at "uphill" side and different crest width.

In all four tests the block OKT hits the embankment with an edge first, but the position of the edge was slightly different when the contact was established (small pictures in Fig. 3.40). This may result in different moments of a torque and may affect the block rotation. So the graphs in Fig. 3.40 did not show a smooth curve but a zigzag line. Nevertheless the fastest stop of block rotation was achieved for the embankment with batter 5:1. For the embankment with a crest to block ratio of only approx. 0.5 and a batter 2:1 the longest time interval was needed for stopping block OKT.

In Figures 3.41 to 3.44 the decrease of translational velocity v of impactor OKT is opposed to the destruction occurred at the embankment due to the impact. Again the heaviest destruction of the embankment occurred, when the block already had lost most of its energy.

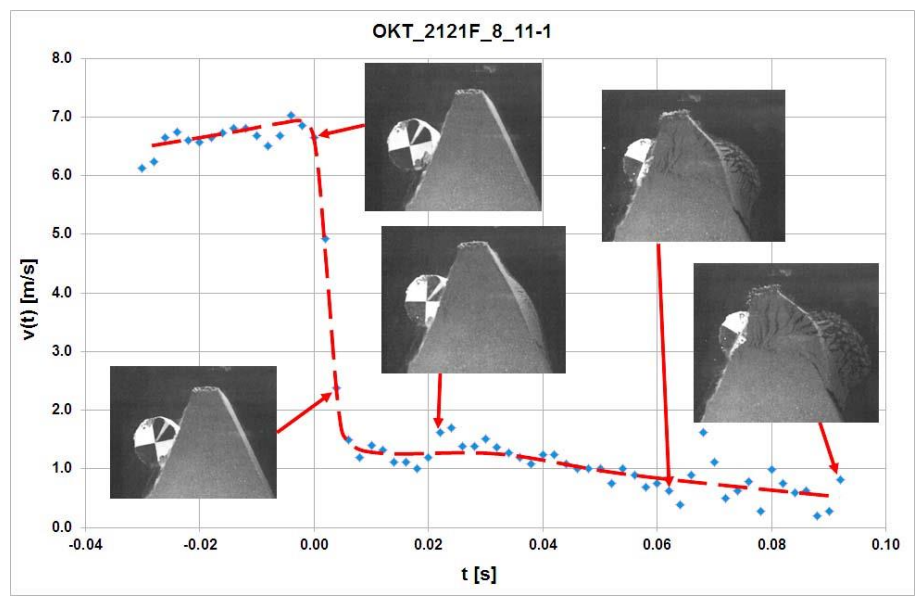


Fig. 3.41: Block deceleration in test OKT_2121F_8_11-1, red line: assumed mean translational velocity.

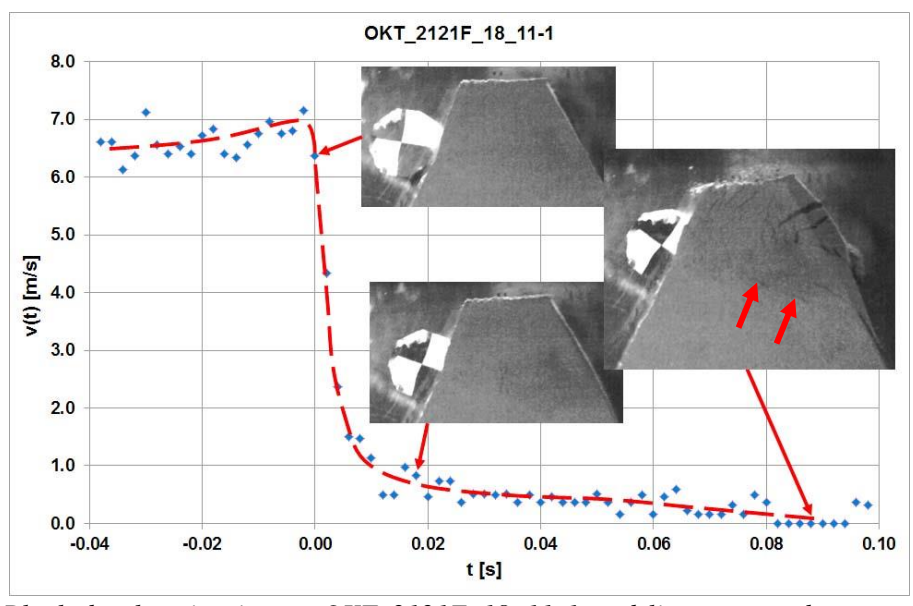


Fig. 3.42: Block deceleration in test OKT_2121F_18_11-1, red line: assumed mean translational velocity, arrows: partly visible shear plane.

July 2017 56/90 Analysis of Existing Rockfall Embankments of Switzerland (AERES), part C

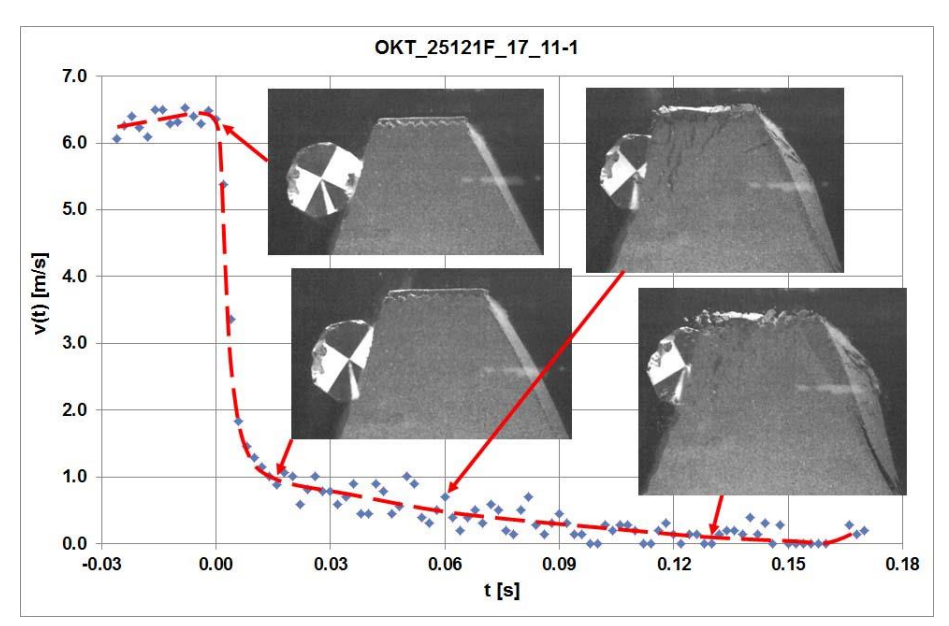


Fig. 3.43: Block deceleration in test OKT_25121F_17_11-1, red line: assumed mean translational velocity.

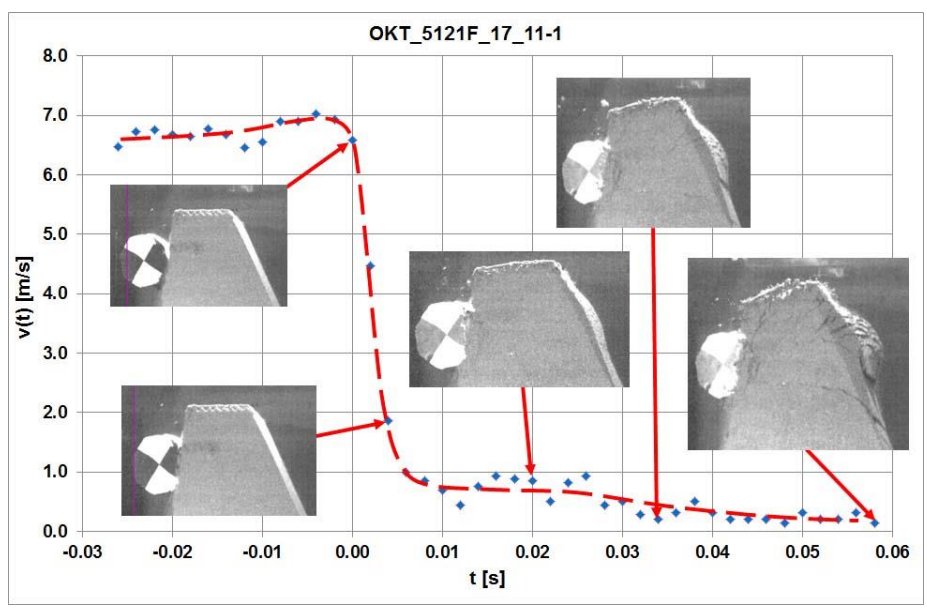


Fig. 3.44: Block deceleration in test OKT_5121F_17_11-1, red line: assumed mean translational velocity.

Due to the impact of block OKT at the opposite slope of the embankment a bulge appears. With increase of the volume of such a bulge tension cracks occur. Those cracks proceed more or less radial to the impact point. A failure plane with downward dip, as it was seen in tests with the rotating cylinders (Figures 3.24, 3.29, 3.37), could not be identified clearly. Only during test OKT_2121F_18_11-1 such a shear plane was visible in parts (Fig. 3.42).

Fig. 3.45 shows the translational velocity versus time for the embankment type 2121 without stones on the slopes, with stones placed horizontally at the "uphill" side and stones placed on both slopes of the embankment. In all three tests the crest width was the same and the crest to block ratio was approx. 1.1.

Just before the impact the velocity of block OKT is very similar in the three tests and is in the interval 6.8 - 7 m/s. During the first 5 ms of the impact process the block velocity graphs show nearly identical curve progression. So the differences in embankment construction seem to be not so important for that part of the impact process. But after the period of 5 ms in test OKT_2121F_18_11-1 the velocity values drop to a lower level than in the two other tests. After 0.02 s the translational block velocity in test OKT_2121F_18_11-1 is reduced to a value of approx. 0.6 m/s while the velocity in the tests OKT_2121_18_11-1 and OKT_2121FF_18_11-1 remains at approx. 1 m/s. During the further test procedure the block velocity is still reduced, but with a significant smaller gradient and the difference between the velocities is approx. constant.

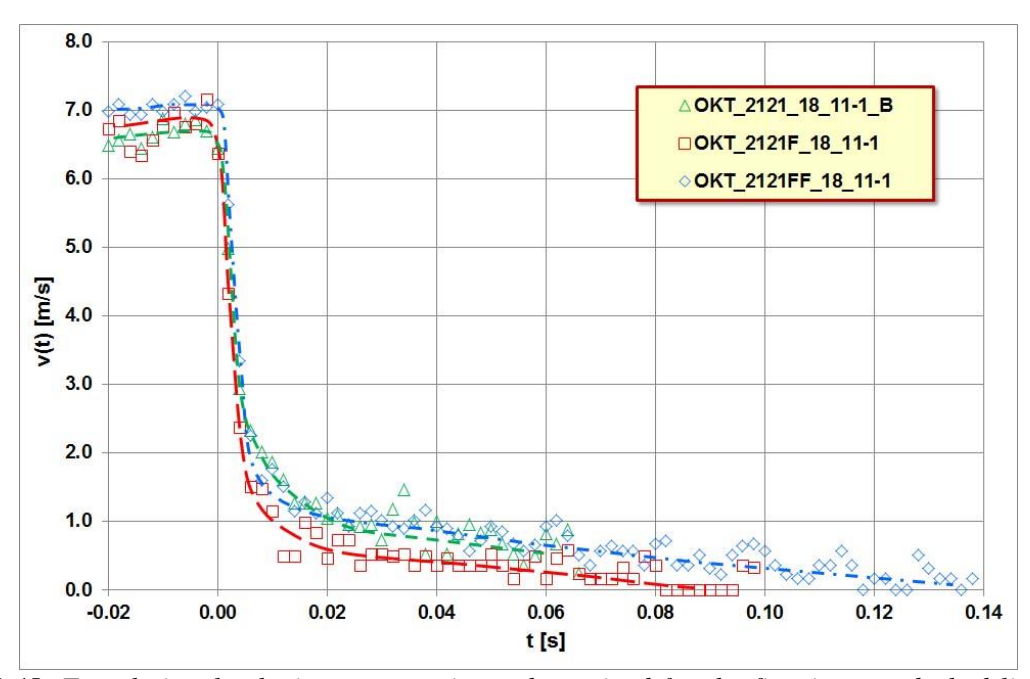


Fig. 3.45: Translational velocity v versus time t determined for the first impact, dashed lines are estimated mean values. The oscillation of the data points in the graphs provides information about the error rate of this kind of measurement.

Assuming the translational velocity at t=0.02 s may be used completely for a vertical lift of the block, this will result in a calculated height of 2 cm for the velocity v=0.6 m/s and 5 cm for the velocity v=1 m/s. The distance impact location to maximum passing height in test OKT_2121FF_18_11-1 is approx. 6.7 cm measured parallel to the slope. Converted to the vertical the value is 5.5 cm. The measured vertical lift in test OKT_2121F_18_11-1 is approx. 1.8 cm. This agrees very well with the values based on the velocities.

Fig. 3.46 shows the decrease of velocity v versus horizontal displacement x of impactor OKT. The largest horizontal movement of block OKT is achieved for the embankment with stones on both sides.

July 2017 58/90 Analysis of Existing Rockfall Embankments of Switzerland (AERES), part C

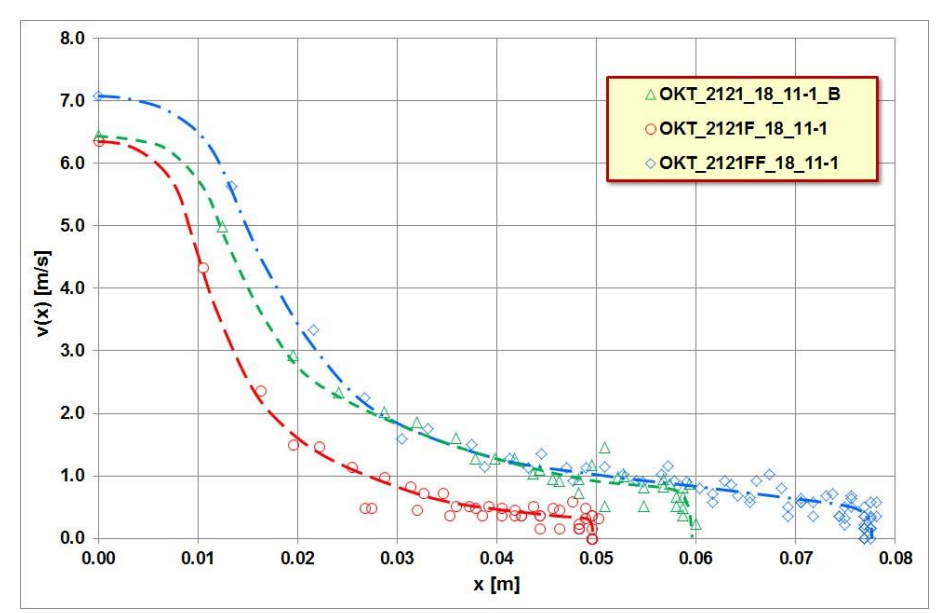


Fig. 3.46: Decrease of velocity v versus horizontal displacement x of impactor OKT at embankments type 2121 without stones on the slopes, with stones placed horizontally at the "uphill" side and stones placed on both slopes of the embankment.

Fig. 3.47 shows the angle of revolution versus time determined during the first impact of the three tests. During the first 0.02 s the curve progression of the three tests are very similar. But then there is a divergence and the block OKT receives a higher angular velocity in test OKT_2121FF_18_11-1 than in the two other tests. So also in the case of a block with edges it seems to be that high rotational block energy leads to less reduction in the translational energy than a lower rotational energy

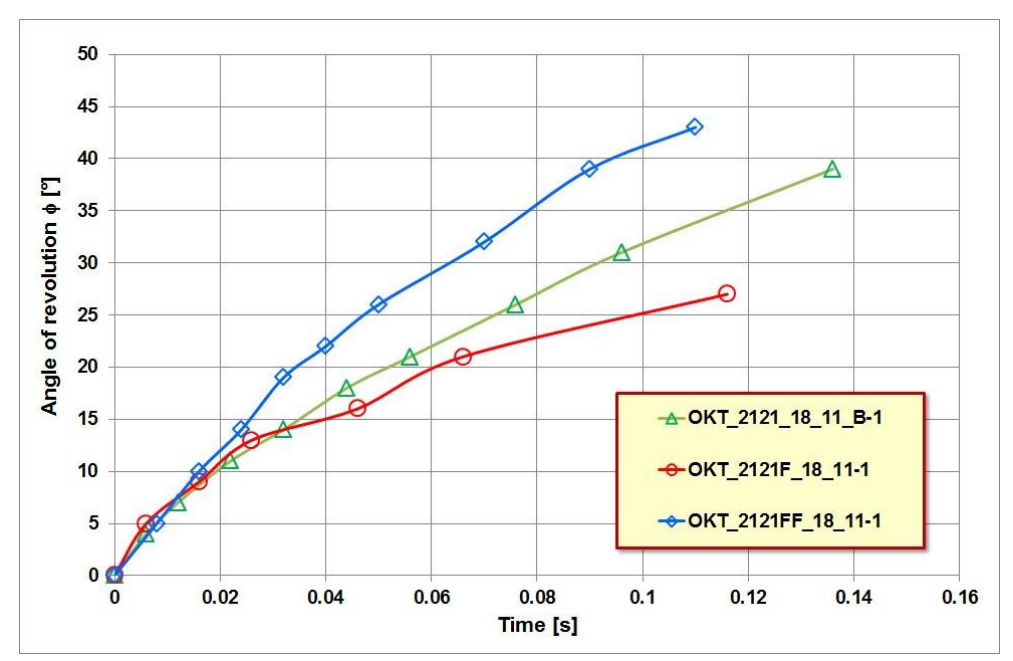


Fig. 3.47: Angle of revolution versus time determined for the first impacts.

July 2017 59/90 Analysis of Existing Rockfall Embankments of Switzerland (AERES), part C

The thickness of the stones used to build the "rockery" is very similar and the slope inclination is the same in the above mentioned tests. So the roughness of the slope does not vary very much for slopes with batter 2:1 (q.v. Fig. 2.17), even though the stones had not been placed at the same position in tests OKT_2121F_18_11-1 and OKT_2121FF_18_11-1. Fig. 3.48 shows the difference in the surface structure as well as a difference in the impact mark.

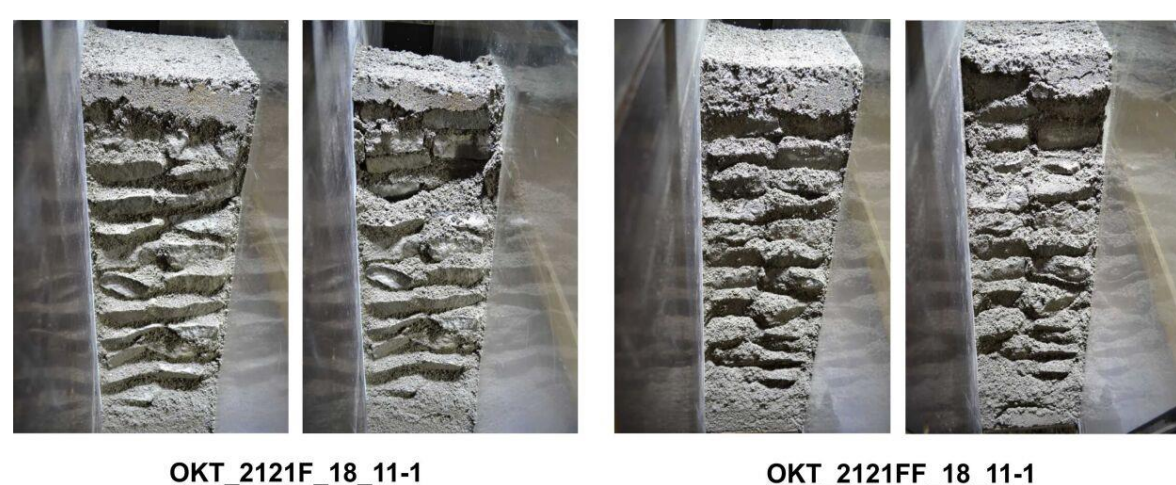


Fig. 3.48: "Uphill" slope before and after the first impact.

OKT_2121FF_18_11-1

The results for the translational velocity v as well as for the rotational velocity ω of the three tests done with the embankment model Gurtnellen are shown in Figures 3.49 and 3.50. The tests had been done with block GS as impactor.

Before the impact the translational velocities of block GS in the tests Gurtnellen 1 (first impact) and Gurtnellen 2 (second impact) are very similar and the mean value is 6.9 m/s (Fig. 3.49). Due to the contact with the embankment the velocity is reduced within a very short period of about 4 ms. Immediately after this period block GS showed a translational velocity v of only approximately 1.5 m/s in test Gurtnellen 1 (impactor hits the uppermost brick course mainly at the front wall and pushed the stones inside the embankment) while v is about 3 m/s in test Gurtnellen 2 (impactor hits the uppermost brick course at the top side). Because the energy goes with the square of velocity v the reduction in translational energy is significantly larger for block GS in test Gurtnellen 1 than in test Gurtnellen 2. Respectively the translational energy of block GS in test Gurtnellen 2 after 4 ms is about 4 times the translational energy of block GS in test Gurtnellen 1 at the same time. This explains why the embankment was surmounted in test Gurtnellen 2, but not in test Gurtnellen 1.

Block GS showed in test Gurtnellen 3 a lower velocity of about 6.1 m/s before the contact, but less energy loss due to the contact than in test Gurtnellen 1 (Fig. 3.49). In both tests the block hit the embankment below the kink of the bi-linear slope. The velocity reduction in test Gurtnellen 1 is approximately 78% while the reduction in test Gurtnellen 3 is only 67%. The higher translational velocity of about 2 m/s allows block GS in test Gurtnellen 3 to reach the crest of the embankment.

Fig. 3.50 shows the decline of the rotational velocity in the tests Gurtnellen 1, 2 and 3. Again the loss of velocity and so also the loss of energy is the largest in test Gurtnellen 1, where block GS hit the embankment just below the kink of the bi-linear slope. The time period to reach a relative constant level for the rotational velocity is approximately 20 ms and therefore significantly larger than for the translational velocity.

July 2017 60/90 Analysis of Existing Rockfall Embankments of Switzerland (AERES), part C

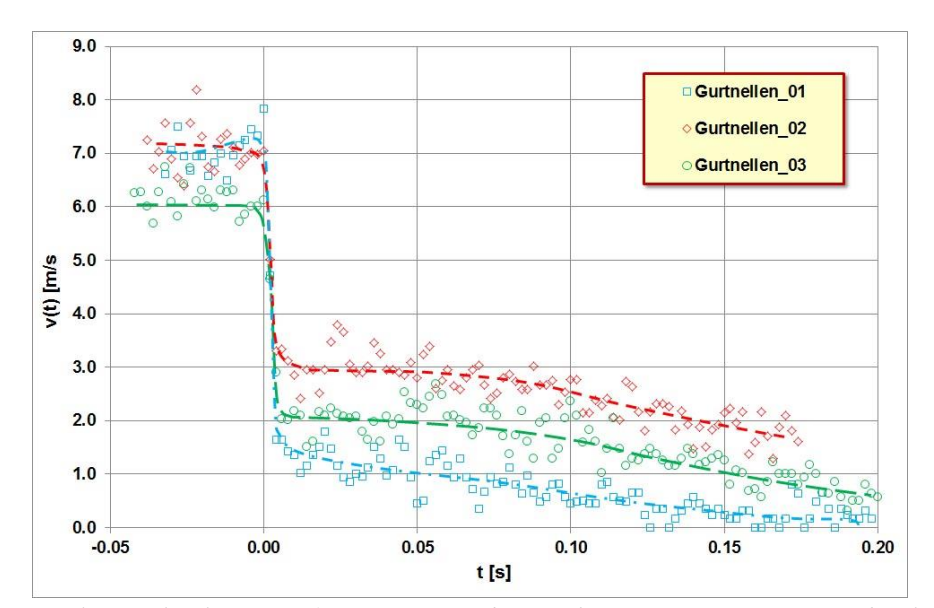


Fig. 3.49: Translational velocity v of impactor GS during the impact process on embankment model Gurtnellen, dashed lines show estimated mean values of velocity v.

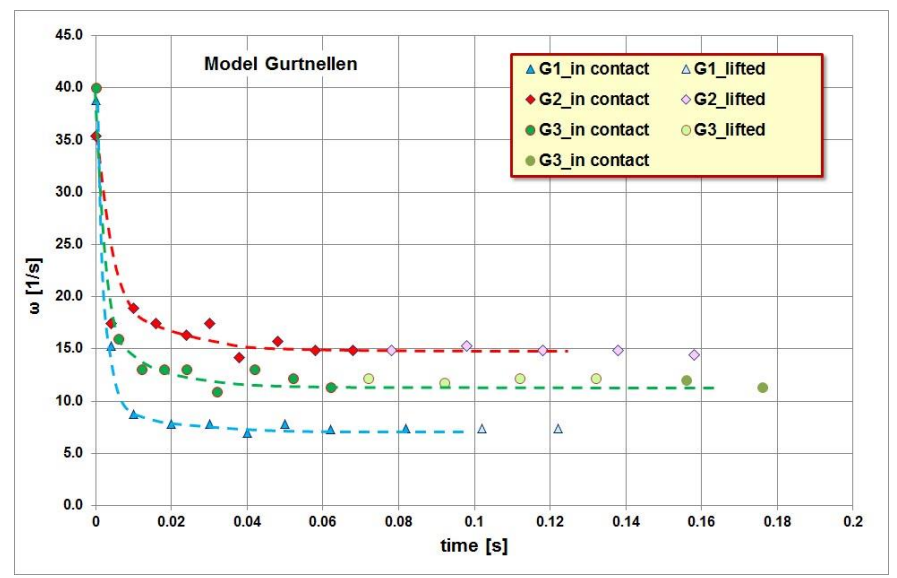


Fig. 3.50: Rotational velocity ω of impactor GS during the impact process on embankment model Gurtnellen

In all three tests the block GS hit the embankment and then it bounced. The period, the block GS was without contact to the slope, is shown in pale colors in the graph in Fig. 3.50.

The three tests done with the model Gurtnellen are insufficient to give a general conclusion, but it can be stated, that the kink of the bi-linear slope plays a significant role for the impact. If the block is rolling or hit the embankment at the lower part of the slope, there is a good chance that the embankment will not be surmounted.

3.4 Drop of energy due to impact

Fig. 3.51 shows the drop of translational energy of block G during the impact onto an embankment with cross section type 2121 for the different types of slope surface conditions in comparison. The data show a tremendous energy drop within the first 10 to 15 ms for all types of slope surface conditions, with and without "rockery". Differences between the four tests are hard to see in Fig. 3.51. After this energy drop the remaining translational energy is reduced with a low gradient.

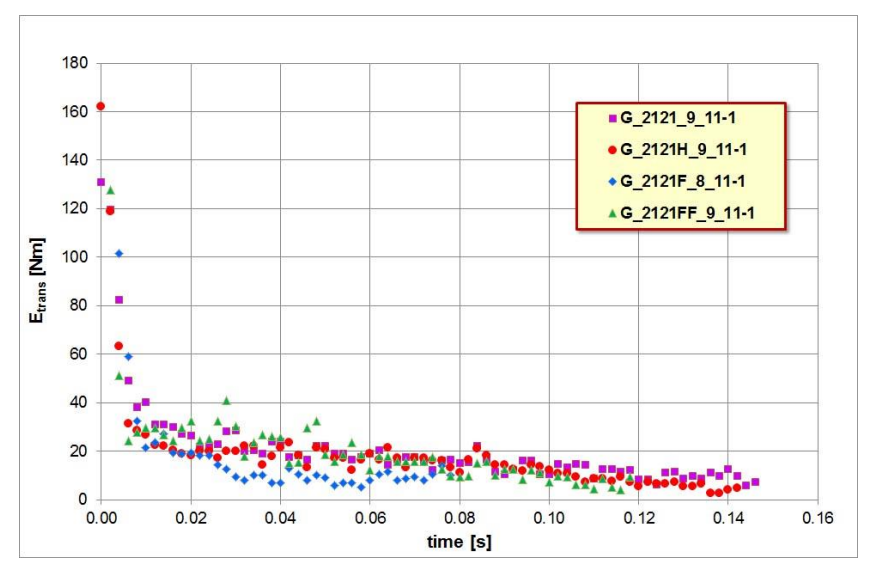


Fig. 3.51: Translational energy versus time of impactor G during the impact process on embankment models with and without rockery at the slopes.

In Fig. 3.52 the energy data is normalized to the respective maximum energy value determined for the test just before the contact (Appendix C1). It is shown that more than 75% of the translational block energy is dissipated within the first 20 ms. A bi-linear upper boundary may be established to describe the energy drop.

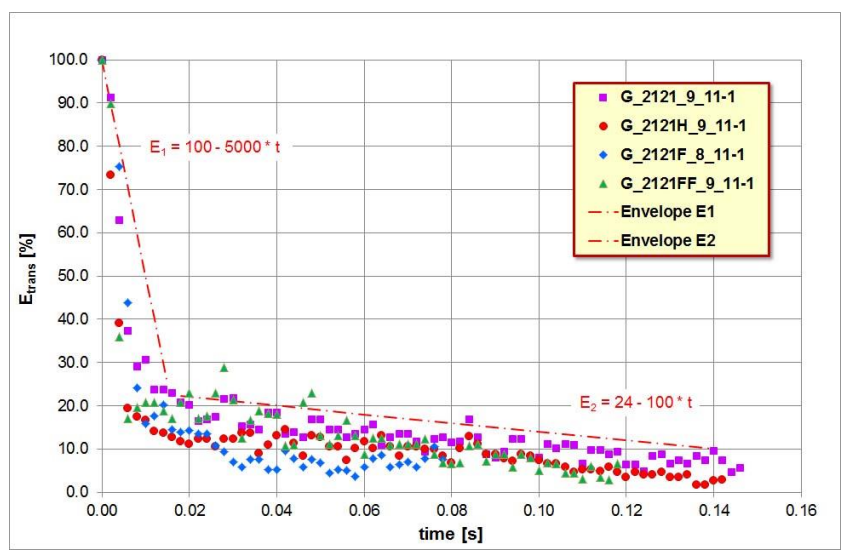


Fig. 3.52: Comparison of the normalized translational energy loss of impactor G, 0.02 s after the first contact between impactor G and the embankment with cross section type 2121 the block has lost at least 75 % of its translational energy.

July 2017 62/90 Analysis of Existing Rockfall Embankments of Switzerland (AERES), part C

The influence of the different slope surfaces in the 4 tests is visible in Fig. 3.53, where the normalized translational energy is shown versus the horizontal movement of block G. The highest resistance is given by the embankment with stones placed horizontally at the slope while the minimal resistance is given by the slope without stones. The test results for the embankment with stone placed parallel to the slope surface lies in between. This behavior was expected physically and is based on the different stiffness of soil and rock material respective the combination of these materials at the slopes.

On the other hand the results of the test with "rockery" on both sides of the embankment is surprisingly, because it shows that the roughness of the slope and the orientation of stones are not solely responsible for the curve progression of the energy drop. The smaller volume of soil between the two layers of "incompressible" stones may be the reason for the difference in the energy drop data here in comparison to the test with only "rockery" at the uphill slope.

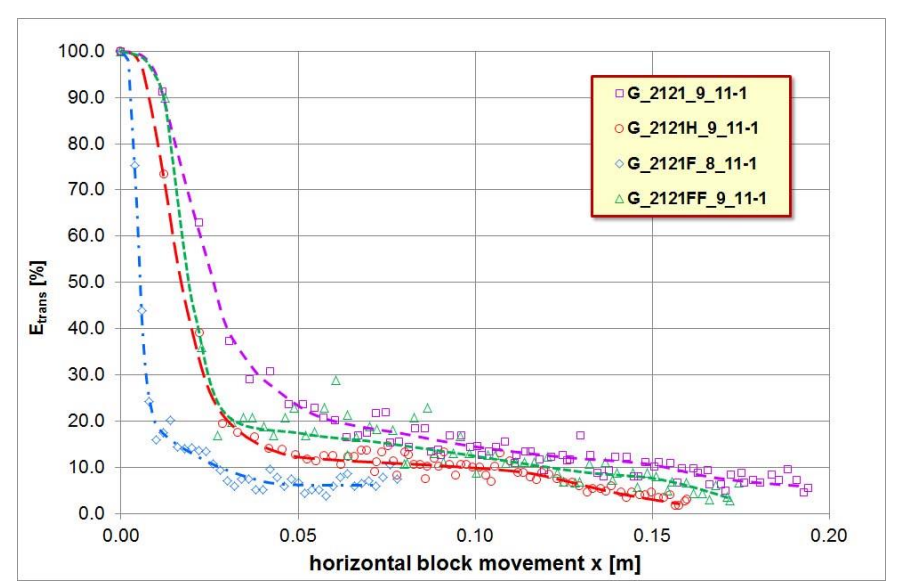


Fig. 3.53: Reduction of the standardized translational energy E_{trans} with horizontal movement x of the block G for the 4 different embankment slope constructions. Dashed lines are estimated mean values.

The reduction of the standardized rotational energy E_{rot} of block G with horizontal block movement x is shown in Fig. 3.54. Again the data show a tremendous energy drop at the start of the impact process for all types of slope surface conditions, with and without "rockery". Differences between the three tests - $G_2121_9_11-1$ without "rockery", $G_2121H_9_11-1$ with stones placed parallel to the slope and $G_2121FF_9_11-1$ with stones placed horizontally at both slopes - are hard to see in Fig. 3.54. Only the data of test $G_2121F_8_11-1$ shows a significant difference in curve progression and is situated above the three other curves.

Fig. 3.54 shows also that the rotational energy had been reduced to a level of 10% or less within the first 5 cm of horizontal block movement. In the aftermath the block rotation and therefore the rotational energy is approximately constant and the data of the 4 tests showing lines running approximately parallel. This phenomenon, that the rotational energy of rotating cylinders will be more or less constant in the later phase of the impact process, had already been found by Kister (2015) for embankments made of pure soil.

July 2017 63/90 Analysis of Existing Rockfall Embankments of Switzerland (AERES), part C

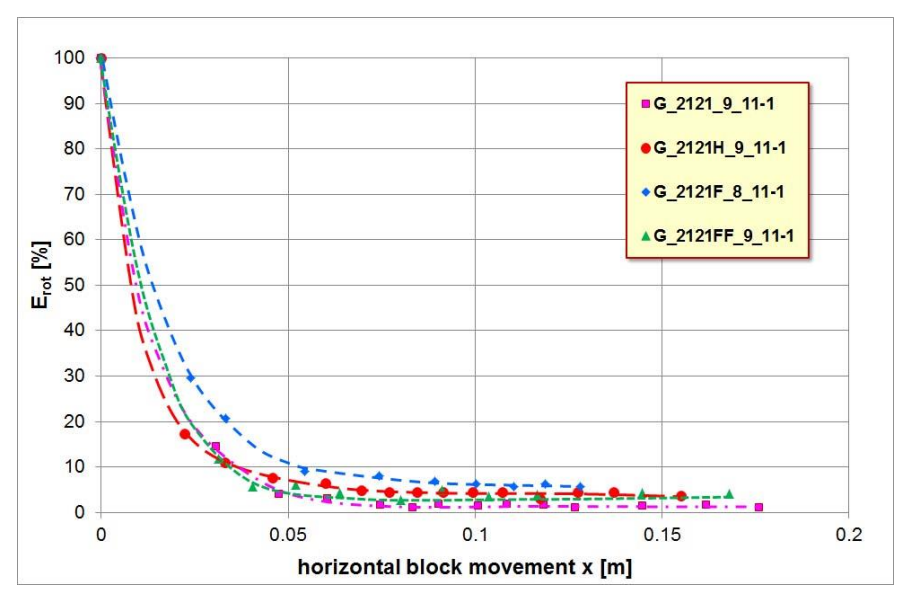


Fig. 3.54: Reduction of the standardized rotational energy E_{rot} with horizontal block movement x of block G for 4 different embankment slope constructions. Dashed lines are estimated mean values.

Figures 3.55, 3.56 and 3.57 are showing the reduction of the standardized translational energy E_{trans} with horizontal movement x of block OKT. All graphs in the three figures have in common that the translational energy had been reduced to a level of 10% or less within the first 3 cm of horizontal block movement during the impact process.

In Fig. 3.55 the results for a crest to block ratio of approx. 0.5 are shown while Fig. 3.56 shows the graphs for the same test arrangement, but for a crest to block ratio of approx. 1.1. Both figures have in common that the embankment only with "rockery" at the uphill slope (2121F) seems to have the largest resistance against the impact of block OKT while the embankment with "rockery" at both slopes (2121FF) seems to have the lowest resistance against the impact of block OKT. The embankment only with "rockery" at the uphill slope (2121F) led also to the smallest values for the maximum horizontal movement of block OKT in the three tests, while the embankment with "rockery" at both slopes (2121FF) led to the largest values for the maximum horizontal movement of block OKT in the three tests (see Figures 3.55 and 3.56). Therefore the "rockery" at the downhill slope may reduce the necessary building ground for an embankment, but does not improve necessarily the resistance against impact.

The influence of the embankment's width is also visible in Figures 3.55 and 3.56. The slender construction led to a larger maximum value of the horizontal block movement. So for example the maximum horizontal movement of about 9.5 cm for embankment type (2121F) for the slender structure with crest width of approx. 8 cm is almost twice the value of 5 cm received for the embankment with crest width of approx. 18 cm. The translational block energy in both tests was identical (142.8 resp. 142.6 Nm, see also Appendix C1).

As already mentioned for Fig. 3.39, velocity v versus horizontal movement x, there is no clear correlation between slope steepness and block stopping (Fig. 3.57).

July 2017 64/90 Analysis of Existing Rockfall Embankments of Switzerland (AERES), part C

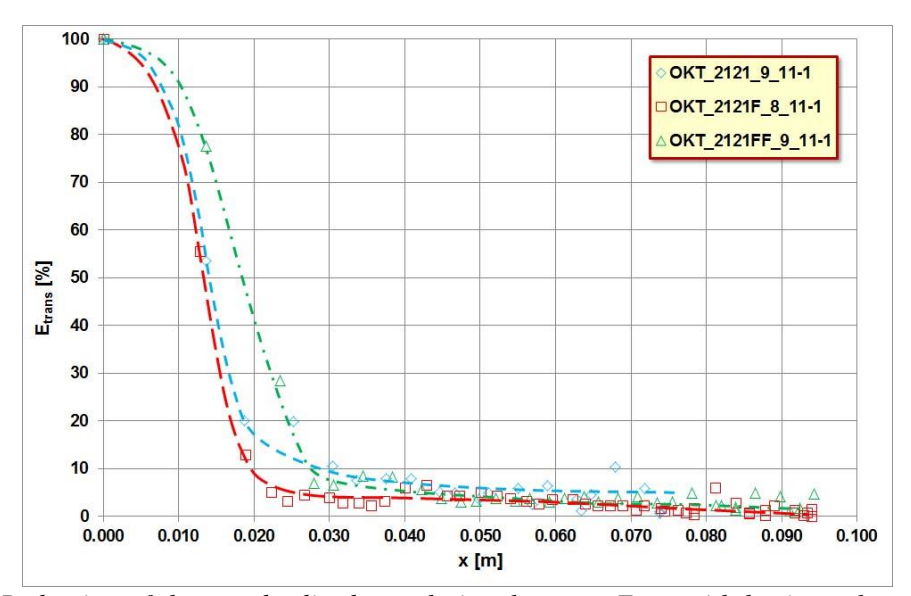


Fig. 3.55: Reduction of the standardized translational energy E_{trans} with horizontal movement x of block OKT for different embankment slope constructions and a crest to block ratio of approx. 0.5. Dashed lines are estimated mean values

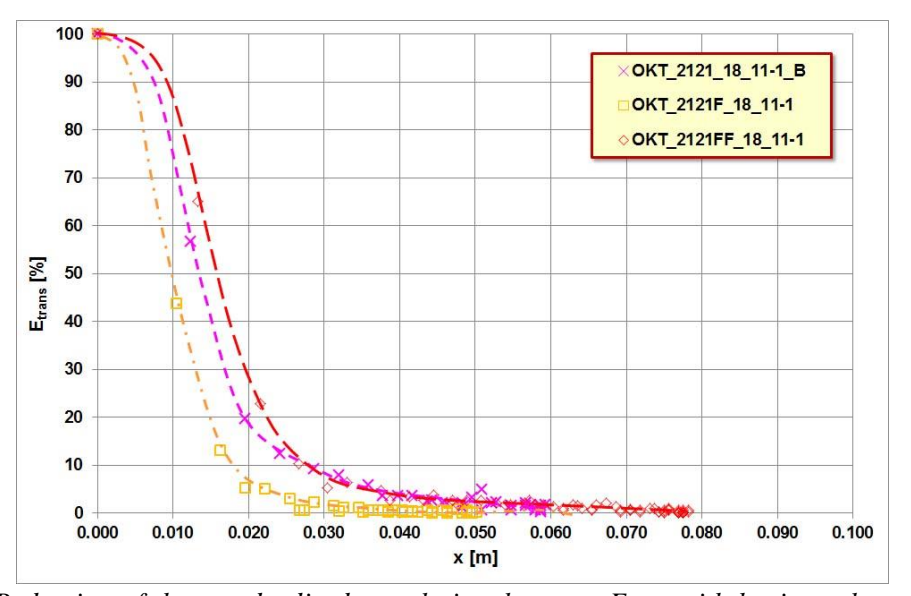


Fig. 3.56: Reduction of the standardized translational energy E_{trans} with horizontal movement x of block OKT for different embankment slope constructions and a crest to block ratio of approx. 1.1. Dashed lines are estimated mean values.

Fig 3.58 shows the standardized translational energy E_{trans} versus time t of the block OKT in the tests. The graph has been limited to a maximum standardized translational energy value of 25% for better visibility. 0.01 s after the first contact the block energy is reduced to a value of 10% or less. So for the time mark 0.02 s after the first contact the block energy of the non-rotating or low-rotating block OKT is much more reduced than for the cylinder G with the higher rotation (Fig. 3.52). The 10%-mark is reached for block G only at 0.14 s after the first contact.

July 2017 65/90 Analysis of Existing Rockfall Embankments of Switzerland (AERES), part C

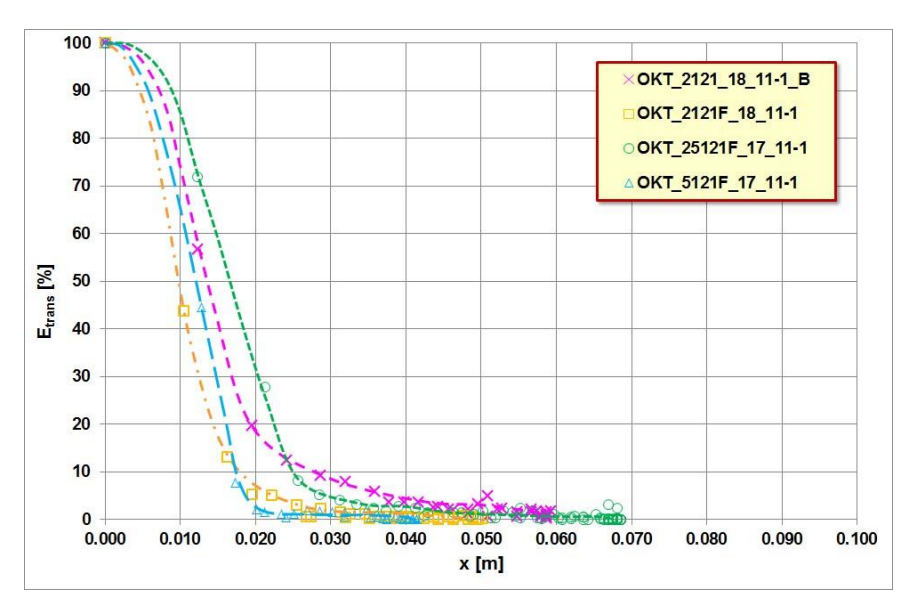


Fig. 3.57: Reduction of the standardized translational energy E_{trans} with horizontal movement x of block OKT for different embankment slope inclination and a crest to block ratio of approx. 1.1. Dashed lines are estimated mean values.

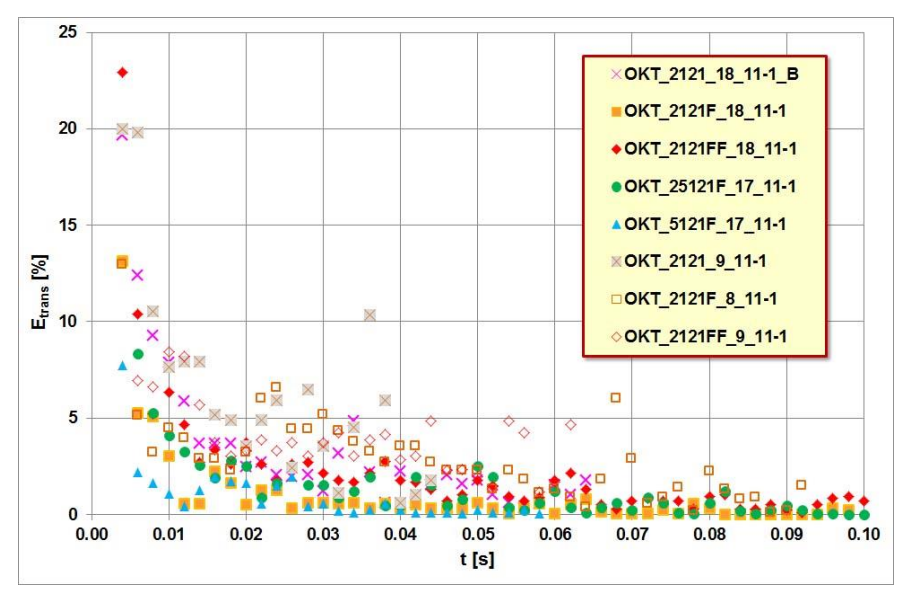


Fig. 3.58: Block OKT, standardized translational energy E_{trans} below the 25% level versus time t.

So the energy loss of translational block energy is much faster for non-rotating or low rotating blocks than for blocks with high rotation. This is the experimental confirmation of the thesis of Plassiard & Donzé (2009), that "the initial rotational kinetic energy favors an increase of the translational kinetic energy during impact". This statement of Plassiard & Donzé was based on results of numerical calculations using the Discrete Element Method (DEM).

3.5 Direct measurement of deceleration

Direct measurement of deceleration during the impact had been done with a triaxial acceleration sensor and a mini data logger placed in block GS (Fig. 2.2). The results of those measurements for the small crest to block diameter ratio of approx. 0.5 and the embankment cross section types 2121 and 2145 are presented in Figure 3.59.

July 2017 66/90 Analysis of Existing Rockfall Embankments of Switzerland (AERES), part C

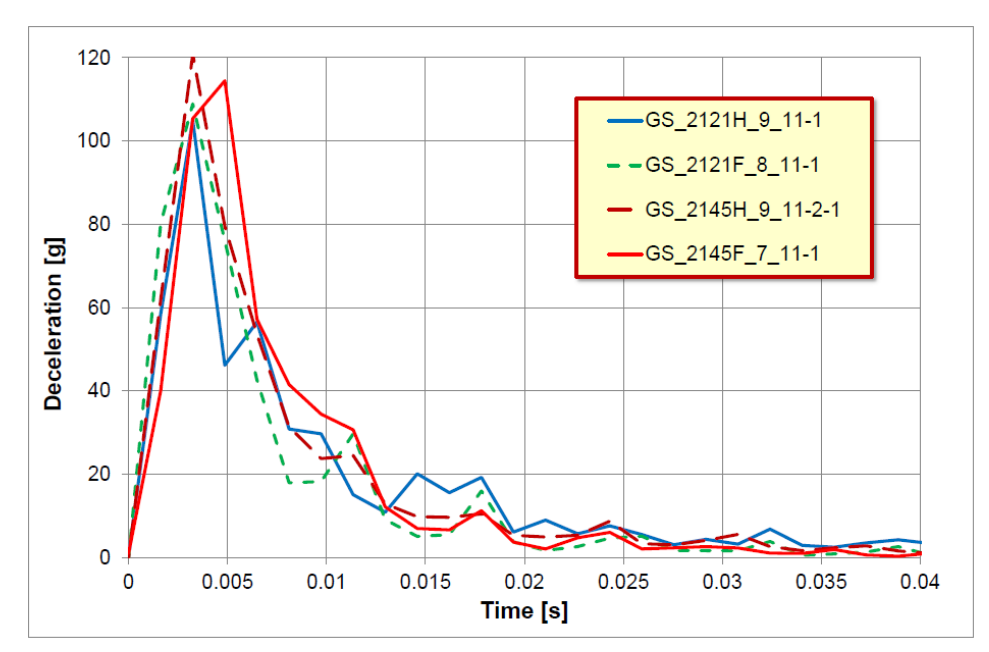


Fig. 3.59: Deceleration versus time of block GS for the small crest to block diameter ratio of approx. 0.5.

In all four tests with stones placed at the "uphill" slope the deceleration reached a maximum value, which is higher than 100g. For the embankments of type 2145 even deceleration values higher than 110g had been measured (121g for index H resp. 114g for index F). For the slender structures of embankment type 2121 smaller maximum values had been determined, 105g for index H resp. 109g for index F. So the maximum deceleration values for the two tests are very similar and the orientation of stones and therefore the roughness of the uphill slope seem to be of minor influence on the block deceleration. On the other hand the graph of test GS_2145F_7_11-1 in Fig. 3.59 differs in its shape in comparison to the other 3 graphs. The maximum value of deceleration is slightly shifted in time compared to the other three graphs and the graph has a broader shape.

Searching for explanation of the differences in the graphs of Fig. 3.59 the impact parameters had been checked. The translational velocity v of block GS before the impact is within the interval 6.5 m/s and 6.7 m/s in the four tests, i.e. the difference in block velocity is less than 4% and therefore may not explain the differences in the graphs. On the other hand the rotational energy in both tests of embankment type 2145 is approx. 15% higher than in both tests of embankment type 2121 (see Appendix C1). This may explain the differences of the maximum deceleration values in Fig. 3.59. The impact angle α in the three tests GS_2121H_9_11-1, GS_2121F_8_11-1 and GS_2145H_9_11-2-1 was determined to 12° resp. 13°. Only for test GS_2145F_7_11-1 a lower impact angle of 8° was determined. So this could be an indication that the impact angle affects the shape of the deceleration graph.

Fig. 3.60 shows the deceleration versus time graphs of block GS for the large crest to block diameter ratio of approx. 1.1 and embankment type 2121 for three cases:

- a) without rockery at the slope,
- b) with stones placed horizontally at the uphill slope and
- c) with stones placed horizontally on both slopes of the embankment.

July 2017 67/90 Analysis of Existing Rockfall Embankments of Switzerland (AERES), part C

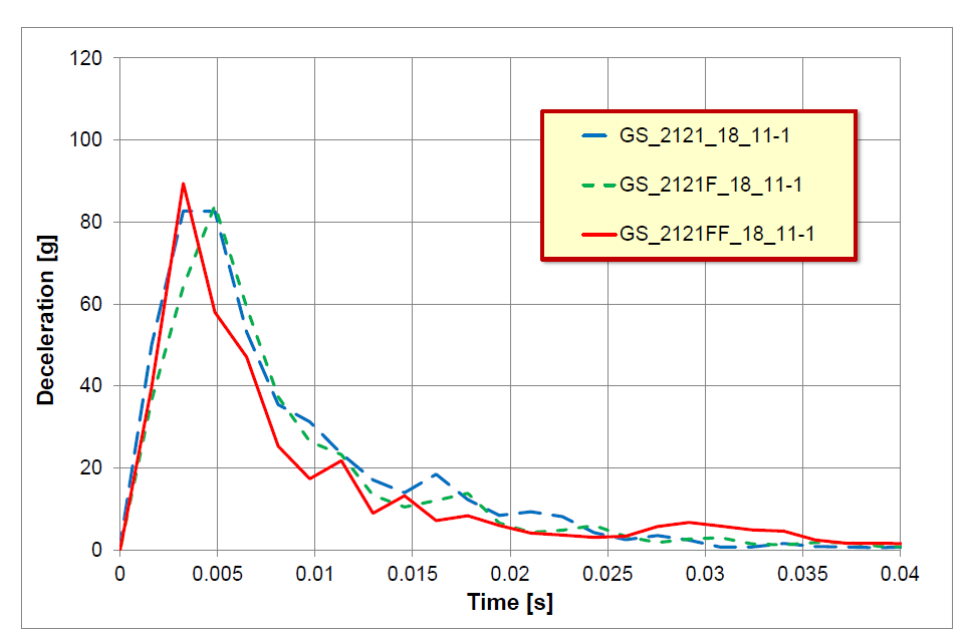


Fig. 3.60: Deceleration versus time of block GS for the large crest to block diameter ratio of approx. 1.1.

The maximum values of the graphs in Fig. 3.60 are very close together, but they are smaller in comparison to those in the graphs in Fig. 3.59 and did not exceed the 90g-level in all three tests. The translational velocities in the three tests had been determined to be in the interval 6.4 m/s to 7.1 m/s, which is in the same range as the velocities determined for the four tests mentioned before. The rotational energy is in the interval 19.7 Nm to 22.4 Nm, which is lower than in the tests shown in Fig. 3.59. So also in this case the smaller values for the deceleration maximum may be explained by differences in rotational energy. But the theory, that the deceleration will reach a larger value in case of a slope covered with stones instead made of pure soil, seems to be disproved due to the tests shown in Fig. 3.60. The maximum deceleration values are very similar for impacts on slopes with stone facing and on a slope made of pure soil. Due to the similarities of the graphs of the tests GS_2121F_18_11-1 and GS_2121_18_11-1 it may be deduced, that the stones placed horizontally and the roughness of the uphill slope seems to be of minor influence on the block deceleration.

Comparing the parameters of the tests presented in the Figures 3.59 and 3.60 for the embankment type 2121, additional to the rotational energy there is another parameter, the crest width, which significantly differs in the two small test series. The crest width in the tests of Fig. 3.59 is just approx. half of the crest width in the tests of Fig. 3.60. But the maximum value of deceleration received in the tests with a smaller crest width is higher than the values achieved for the tests with a larger crest width. This was not expected and therefore had to be checked.

Test	α [°]	E _{trans} [Nm]	E _{rot} [Nm]	E _{total} [Nm]	Deceleration [g]
GS_2121_18_11	14	141.0	22.4	163.5	82.7
GS_2121H_9_11	12	152.1	23.3	175.4	105.0
GS_2121F_8_11	12	149.7	23.6	173.3	108.9
GS_2121F_18_11	10	150.7	21.6	172.3	84.1
GS 2121FF 18 11	13	168.3	19.7	188.1	89.4

Table 3.10: Impact angle, energies and maximum deceleration values of tests done with embankment cross section type 2121.

July 2017 68/90 Analysis of Existing Rockfall Embankments of Switzerland (AERES), part C

To check, if an influence of the crest width on the block deceleration exists, results of tests done by Kister (2015) had been redrawn. In Fig. 3.61 the graphs of deceleration versus time of block GS for three different crest widths named as A, B and D for embankment type 2145 without rockery are presented.

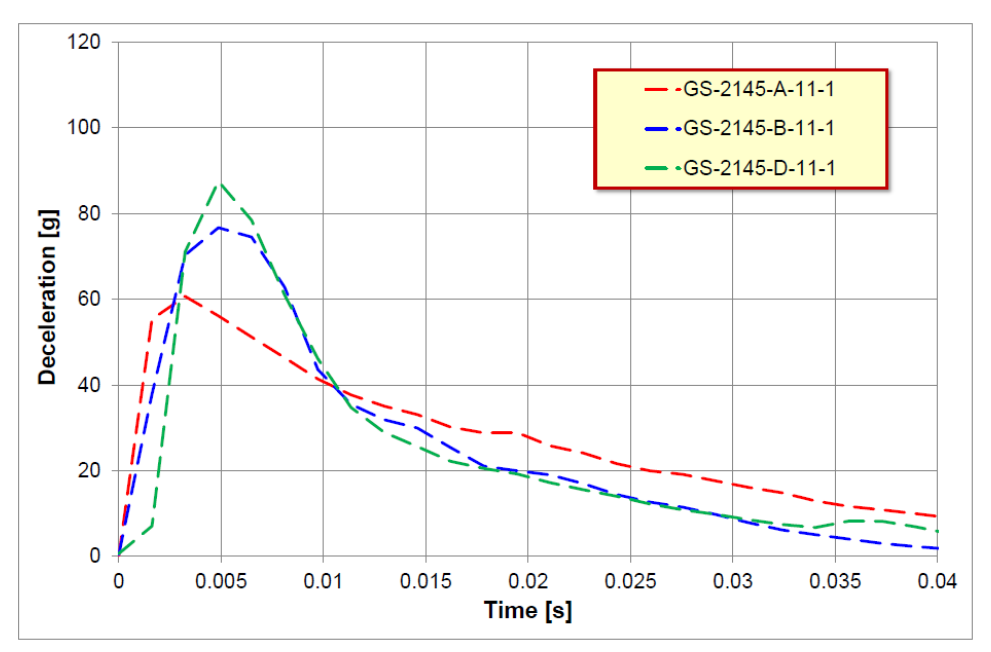


Fig. 3.61: Deceleration versus time of block GS for three different crest widths: A approx. 19 cm, B approx. 9.5 cm, C approx. 2.5 cm.

For the embankment with the largest crest width (index A) the smallest maximum value of deceleration had been achieved in Fig. 3.61. On the other hand, for the embankment with the smallest crest width (index D) the largest maximum value of deceleration had been achieved. The embankment with crest width type B (approx. 9.5 cm) lies in between the crest width types A (approx. 19 cm) and D (approx. 2.5 cm) and so the maximum value for deceleration does in the tests.

The translational velocities in the three tests are 6.3 m/s, 6.1 m/s and 6.1 m/s and therefore there is no large difference in the translational energies (104 Nm ... 109 Nm). The rotational energies are in the interval 38.4 Nm (type D) and 44.3 Nm (type B). The rotational energy in the test with crest type A was 41.2 Nm, which lies in between the two other results. So the gradation in the graphs in Fig. 3.61 cannot be explained by differences in energy.

Also no correlation with the impact angle is visible, because only in test GS-2145-B-11-1 a larger value of 17° was determined for the impact angle. The impact angle in the tests GS-2145-A-11-1 and GS-2145-D-11-1 had been determined to 13°.

So there seems to be a really good chance for a correlation of crest width and block deceleration. To verify this, additional tests done by Kister (2015) had been redrawn.

July 2017 69/90 Analysis of Existing Rockfall Embankments of Switzerland (AERES), part C

Test	α [°]	E _{trans} [Nm]	E _{rot} [Nm]	E _{total} [Nm]	Deceleration [g]
GS-2145-A-01-1	19	86.1	41.1	127.2	82.3
GS-2145-A-11-1	13	109.4	41.2	150.5	60.7
GS-2145-B-01-1	19	75.1	48.4	123.5	88.6
GS-2145-B-11-1	17	105.8	44.3	150.1	76.7
GS-2145-D-01-1	21	83.4	42.2	125.6	71.9
GS-2145-D-11-1	13	104.4	38.4	142.8	87.5
GS_2145F_7_11	8	142.0	27.7	169.7	114.5
GS_2145H_9_11_2	13	145.8	26.7	172.5	120.8

Table 3.11: Impact angle, energies and maximum deceleration values of tests done with embankment cross section type 2145.

Fig. 3.62 shows results of impacts with block GS on an embankment of type 1111, i.e. a symmetric embankment with a slope inclination of approx. 1:1. The results of tests with crest width type A and type D are presented. The largest values of deceleration had been determined for the embankments with crest width type A, the largest crest width in this test series. For the smaller crest width type D the maximum values of deceleration are smaller than in the tests with crest type A. So these tests show a contradictory result in comparison to the tests shown in Fig. 3.61.

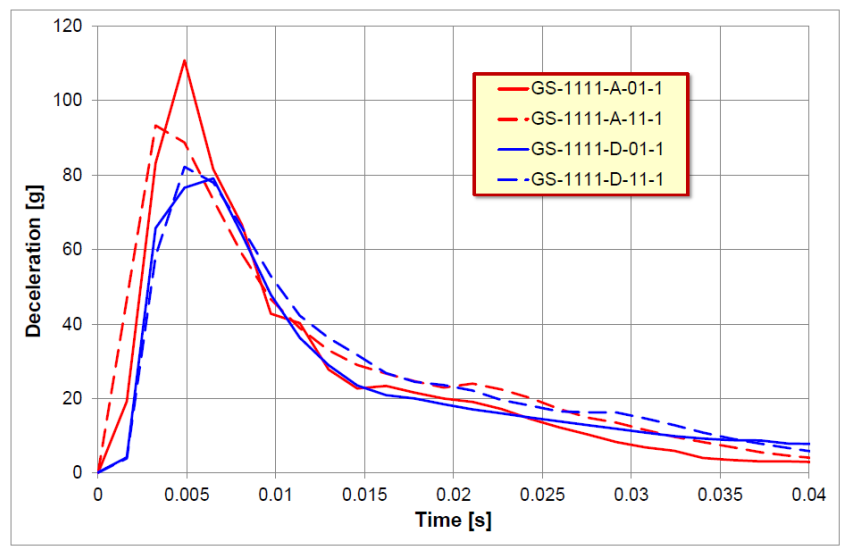


Fig. 3.62: Deceleration versus time of block GS for 2 different crest widths: A approx. 19 cm, C approx. 2.5 cm.

Test	α [°]	E _{trans} [Nm]	E _{rot} [Nm]	E _{total} [Nm]	Deceleration [g]
GS-1111-A-01-1	34	97.6	36.4	134.0	110.8
GS-1111-A-11-1	28	98.8	36.0	134.9	93.3
GS-1111-D-01-1	34	102.9	33.6	136.5	79.1
GS-1111-D-11-1	28	103.6	43.8	147.4	82.2

Table 3.12: Impact angle, energies and maximum deceleration values of tests done with embankment cross section type 1111.

The results of direct measurement of deceleration during the impact may be summarized as follows:

- The graph of deceleration versus time is characterized by a steep and asymmetric curve. With the used measurement device only a limited number of measurement points could be measured. So some details of the deceleration versus time graph may not be detected because of a limited resolution.
- The orientation of stones at the "uphill" slope and therefore the roughness of the "uphill" slope seem to be of minor influence on the block deceleration.
- The impact angle seems to have no influence on the shape of the deceleration versus time graph.
- To explain differences in the maximum value of deceleration the rotational energy of the block has to be taken into account.

Fig. 3.63 shows the total block energy versus the maximum deceleration value. Despite of the data scattering the graph shows increasing maximum deceleration values with increasing total block energy.

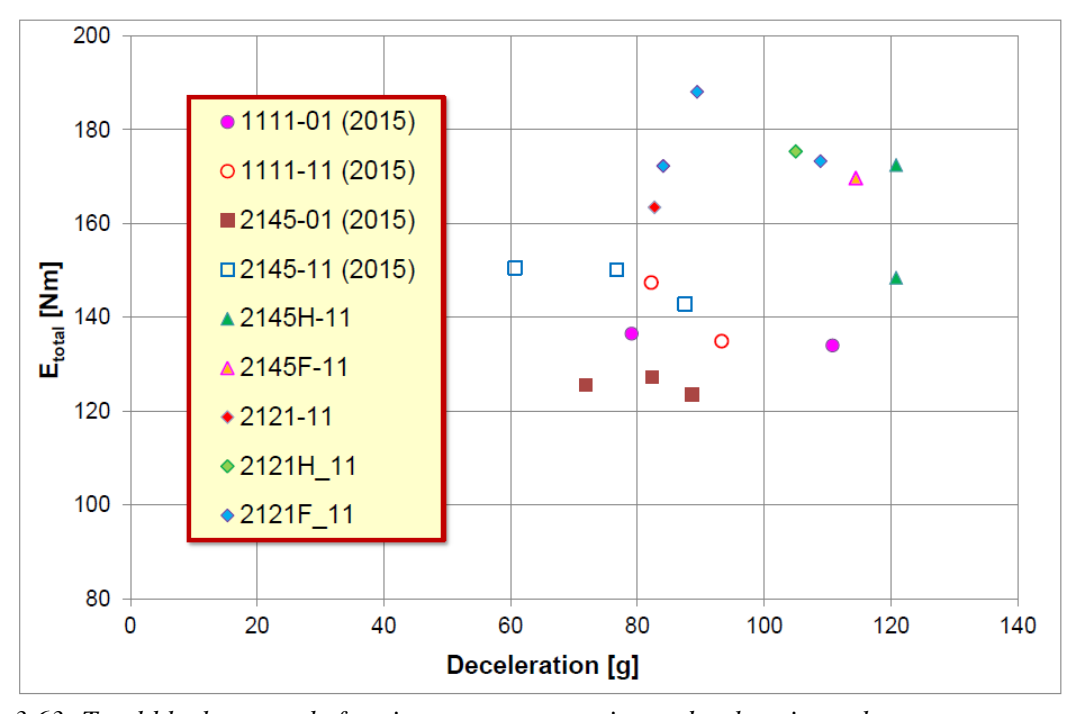


Fig. 3.63: Total block energy before impact versus maximum deceleration value.

3.6 Displacement inside the embankment due to impact

A few tests had been analyzed by the Particle Image Velocimetry method (PIV). This method is a kind of pattern recognition. For the analysis by the PIV method two pictures done at different time steps have to be compared. A time interval of 10 ms was used for these analyses. So time is known and the displacement of a selected area measured in pixels and characterized by a certain pattern can be determined by comparing the two pictures. With this method the velocity of an area with a certain pattern as well as the displacement can be determined. But to use the method successfully the pattern may be slightly deformed but not destroyed. The method and program used for these analyses are described in Kister (2015).

July 2017 71/90 Analysis of Existing Rockfall Embankments of Switzerland (AERES), part C

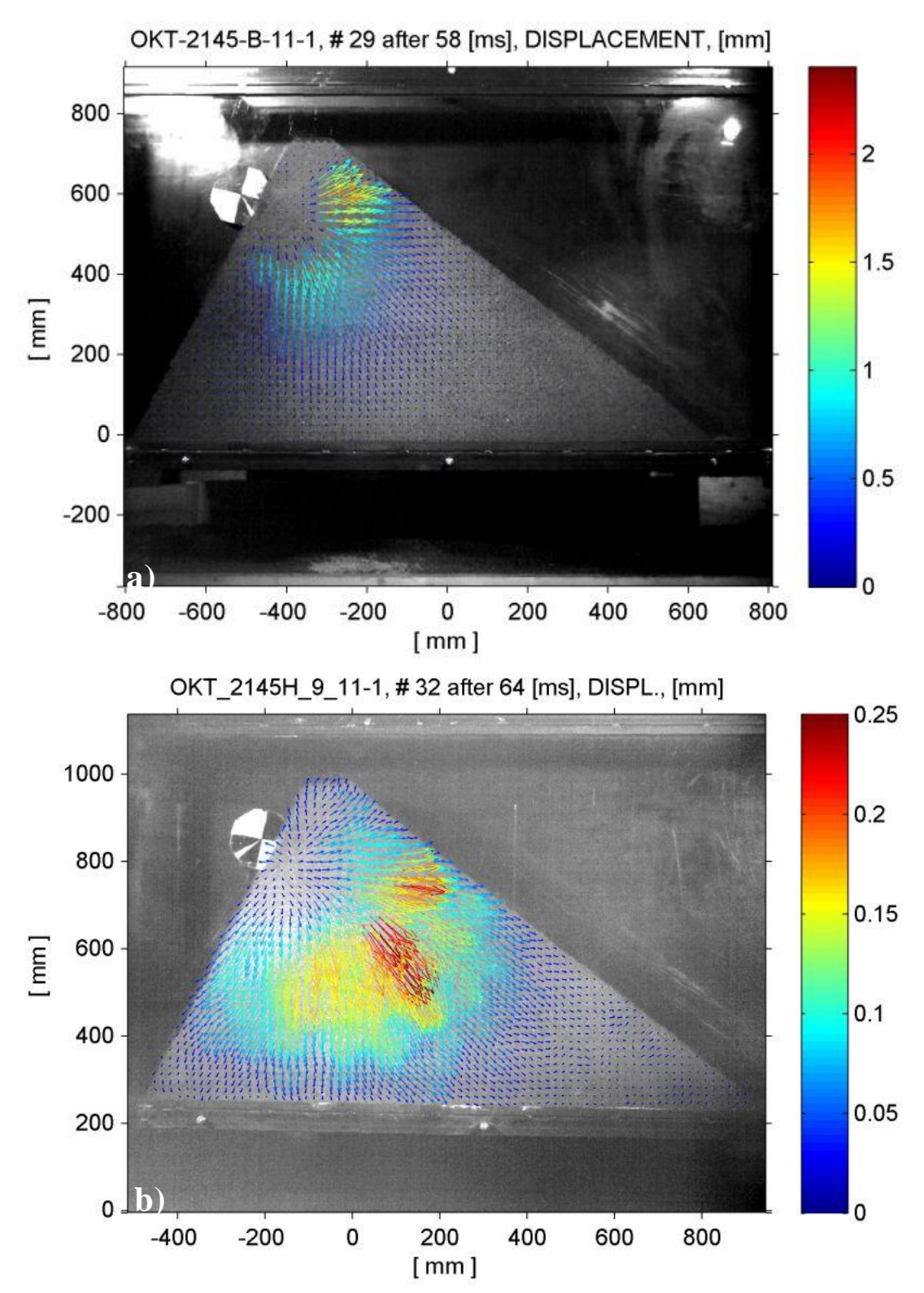


Fig. 3.64: Displacement field determined by PIV at a time 6 ms after the first contact of block and embankment, time interval: 10 ms: a) test OKT-2145-B-11-1 without stones on the "uphill" slope, b) test OKT_2145H_9_11-1 with stones placed parallel to the slope.

July 2017 72/90 Analysis of Existing Rockfall Embankments of Switzerland (AERES), part C

Fig. 3.64 shows the displacement field 6 ms after the first contact of block and embankment determined by PIV for the tests OKT-2145-B-11-1 and OKT_2145H_9_11-1. The test OKT-2145-B-11-1 is a test executed during the first test series (Kister, 2015) and the embankment was constructed without stones on the "uphill" slope. The index B in the test name is used for a crest width of approx. 9 cm. So the embankment geometry is the same as for test OKT_2145H_9_11-1 with stones placed parallel to the slope.

The PIV analysis of test OKT_2145H_9_11-1 led to significant smaller values for the displacements than the analysis done for test OKT-2145-B-11-1. So it is difficult to compare the two results because of the two different scales, which had to be used to present the data.

Additional to the difference of the size of displacements the two pictures in Fig. 3.64 show a significant difference in the alignment of the presented larger displacement arrows. The maximum displacements in test OKT-2145-B-11-1 are aligned more or less horizontally towards the "downhill" slope, while the maximum displacements in test OKT_2145H_9_11-1 with stones placed parallel to the "uphill" slope show a downward direction.

In Fig. 3.65 the further evolution of the displacement field with time is presented for test OKT_2145H_9_11-1. While moving towards the "downhill" slope the values of the displacement field decrease. 28 ms after the contact block - embankment displacements are only visible in a narrow band at the level of the impacting block.

Fig. 3.66 shows the cumulated displacements of the test GS_2121HG_18_11-1 and the test GS_2121FG_18_11-1 determined by PIV at 58 ms after the contact block - embankment. For the slender structure of embankment type 2121 the areas showing the displacement field are looking similar, although in one case the rocks at the slope had been placed parallel to the slope (index H) and in the other the rocks had been placed horizontally (index F). But there is a small difference concerning the size of the displacements. Higher displacement values are achieved for the test with the stones placed parallel to the "uphill" slope, which may be an indication for a higher compaction of the embankment center in this test in comparison to the test with the stones placed horizontally.

Fig. 3.66 shows additional the displacements, which occur at the embankment's bottom at the "downhill" side for slender structures. But those displacements are small and did not impair the embankment's stability.

 $\begin{array}{l} \hbox{July 2017} \\ 73/90 \\ \hbox{Analysis of Existing Rockfall Embankments of Switzerland (AERES), part C} \end{array}$

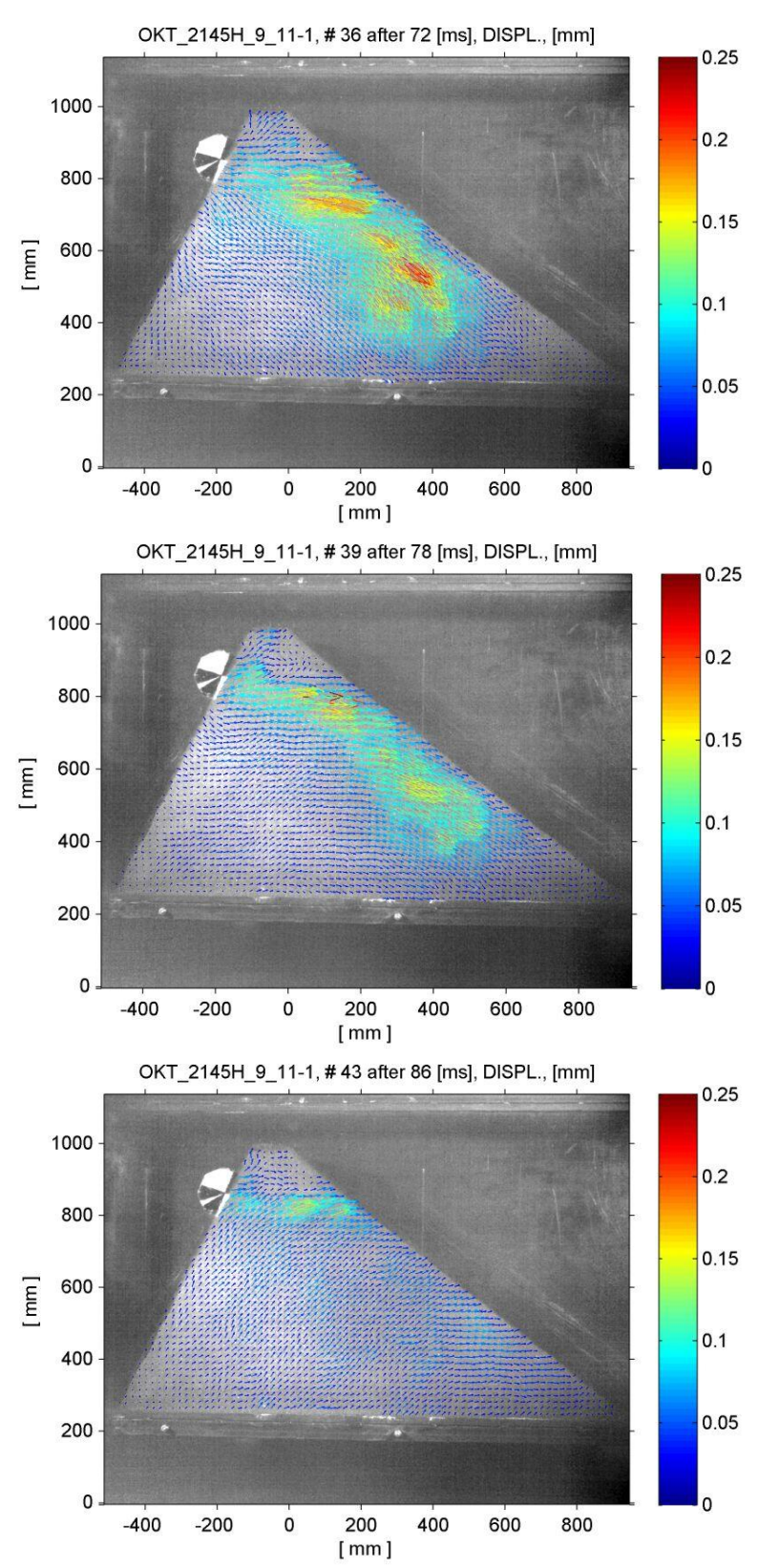


Fig. 3.65: Development of the displacement field determined by PIV of test OKT_2145H_9_11-1: 14 ms, 20 ms and 28 ms after the first contact of block and embankment

July 2017 74/90 Analysis of Existing Rockfall Embankments of Switzerland (AERES), part C

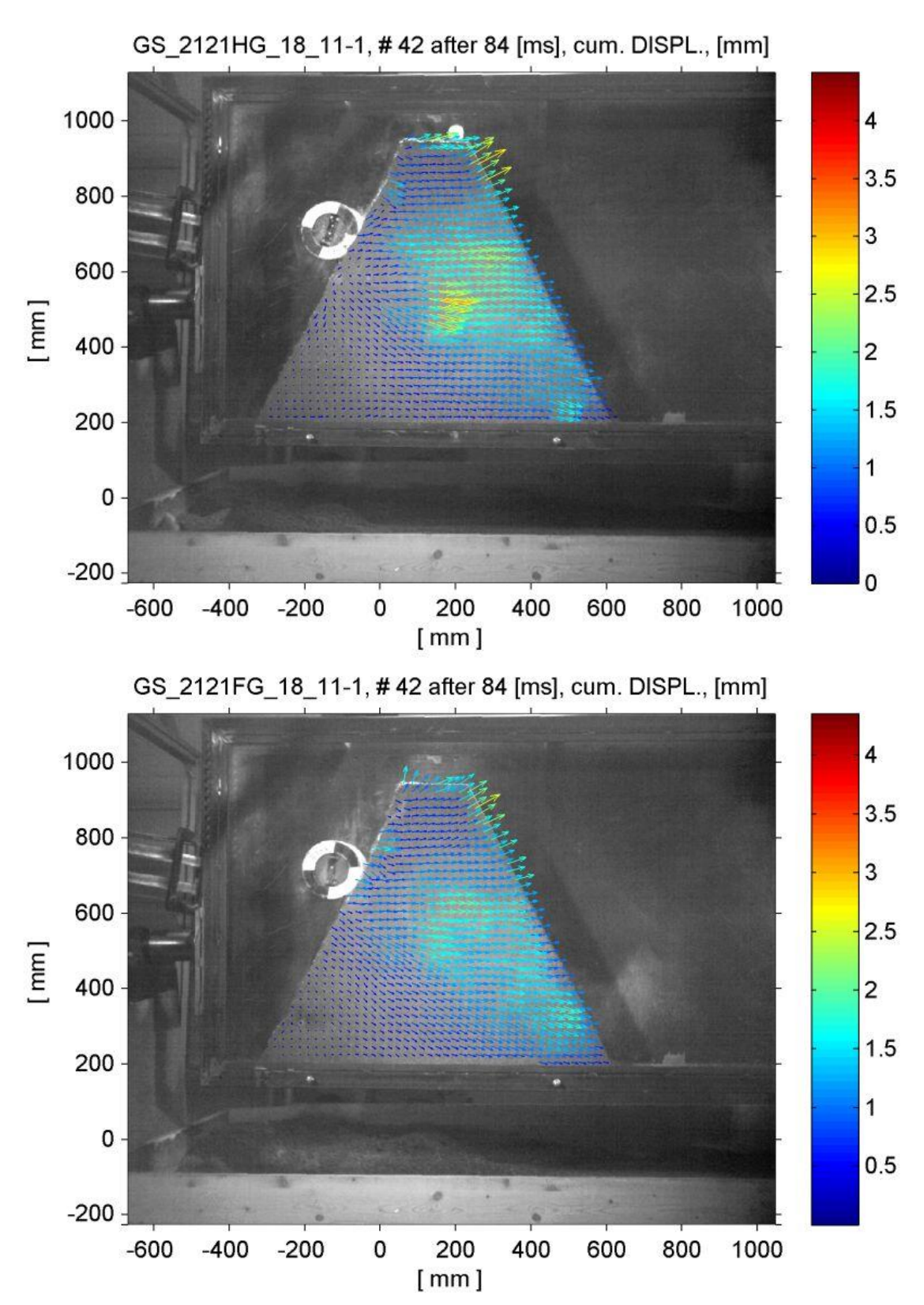


Fig. 3.66: Cumulated displacements determined by PIV: a) test GS_2121HG_18_11-1, b) test GS_2121FG_18_11-1.

4 Conclusions

The idea to combine rockfall protection embankments with natural stone masonry at the uphill side or sometimes at both sides is very common in Switzerland. This combination allows the construction of steep slopes and reduces thereby the place necessary for the embankment. Often material, which is around, can be used for the construction. Furthermore the removal of debris flow relicts is easy. But only little information is available on the behavior of such constructions in case of an impact by a block.

First studies on the influence of so called riprap or rockery at an embankment's surface have been done by Hofmann & Mölk (2012). But the two research reports which have been cited in their paper are not open to the public and the information given in their paper is very limited. So information concerning the roughness profile and the thickness of the used riprap is missing and only two statements are given as results of their tests:

- "Slope angles $\geq 50^{\circ}$ require a freeboard of at least one-time the diameter of the sphere.
- After the impact, the sphere scarcely changes its height, whereas in the case of pure soil embankments and reinforced structures, it tends to jump or roll in the direction of the crest"

To check the experimental results of Hofmann & Mölk (2012) and to study the impact process of blocks impacting rockfall protection embankments with a rockery cover, small scale quasi-2D-experiments have been executed and analyzed at the HSLU during the project AERES. The results of this test series had been described in this report.

4.1 Influence of embankment's uphill slope inclination

To avoid an embankment made of pure soil (slope inclination $\leq 50^{\circ}$) will be surmounted by a block, the Austrian standard ONR 24810:2013 requires a freeboard of at least two block diameter. But the graph used for determining the design parameters according to Hofmann & Mölk (2012) and which is presented also in the appendix of ONR 24810:2013 limits the applicability of the diagram to a block rotational energy $\leq 1\%$ for pure earth embankments (Fig. 4.1).

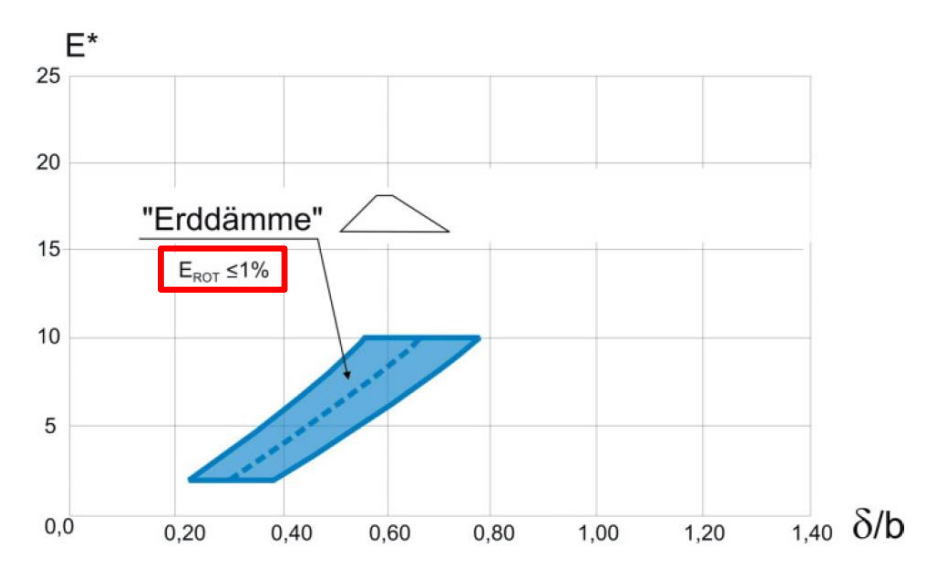


Fig. 4.1: Dimensionless illustration of the test results of Hofmann & Mölk (2012) received for pure earth embankments, relative impact energy E^* versus ratio of penetration depth δ and crest width b, rotational energy E_{ROT} is limited to $\leq 1\%$.

July 2017 76/90 Analysis of Existing Rockfall Embankments of Switzerland (AERES), part C

On the other hand, in-situ tests done by Usiro et al. (2006) showed that the ratio of rotational to translational energy for natural blocks will be in the interval 0.025 to 0.2 respectively 2.5% to 20%, which is significantly higher than the energy limit given by Hofmann & Mölk (2012). Taking into account the results of Usiro et al. (2006) as well as the limit for the diagram presented in the appendix of ONR 24810:2013 no design parameters for the load case impact of natural blocks with real rotational energy on an embankment made of pure soil exist and therefore as a consequence the construction of pure earth embankments with an uphill slope inclination of about 1:1 or less should be omitted.

Kister (2015) showed test results of small-scale quasi-2D-experiments where, even in the case of edged blocks with no or only very low rotation, blocks move upward the embankment's slope during the impact process and reached the crest level, if the impact angle comes up to an appropriate value. Kister (2015) concludes out of this there is a good chance a block with a ratio of rotational to translational energy of 0.1 to 0.2 will surmount an embankment with slope inclination of 50° or less, even if a freeboard of two block diameters has been kept.

Two documented examples of existing rockfall protection embankments underpin the results and the statement presented by Kister (2015). The embankment Halteli-Talmatt, Canton Uri, was damaged during a larger event on 1st October 1983. The embankment, constructed with a slope inclination 1:1 at the uphill side, was neither punched through nor surmounted, but the impacting block reached the crest and caused some damage (Fig. 4.2). Schneider (1984) described the movement of the largest block as follows: "The block overcame the ditch with small jumps and hit the crest at the uphill side. The block produced a large impact crater and radial spreading shear joints, which penetrated the complete embankment. The block stayed at the crest for several hours and then fell down into the ditch." Fig. 4.2 shows the irregular shape of this block, which differs significantly from a sphere or a cylinder. According to Schneider the jumps of the block had been small before it hit the embankment and therefore the block could not directly hit the embankment's crest area because the ditch - crown vertical distance is more than 8 m.



Fig. 4.2: Impact at the embankment Halteli-Talmatt, Canton Uri. The embankment was neither punched through nor surmounted, but the impacting block reached the crest (Schneider, 1984)

July 2017 77/90 Analysis of Existing Rockfall Embankments of Switzerland (AERES), part C

The second example is the embankment Gretla, Canton Graubünden. This rockfall protection embankment was constructed in 2009 due to an event in 2008. The embankment was made of debris with a slope inclination of 2:3 on both sides. The ditch - crown vertical distance of this embankment is 5 m. The embankment was surmounted during events in 2009 and 2010 (2009: block size approx. 1.5 x 2 x 0.6 m³, 2010: block size approx. 1.8 x 1.8 x 0.9 m³). As a consequence a redesign of the embankment had been done and rockery with a batter 5:1 had been placed at the uphill slope. During a new event in 2011 the embankment Gretla, now with rockery, was able to stop 2 blocks with a volume of 4 m³ resp. 6 m³ (Fig. 4.3). Only a rock fragment with a mass of approx. 70 kg was spalled off during the event and reached the roadside behind the embankment (Nänni, 2011). So the redesign of the embankment with rockery in front of the embankment stood the test.



Fig. 4.3: Impacts of two blocks $(4 \text{ m}^3 \text{ resp. } 6 \text{ m}^3)$ in 2011 at embankment Gretla after redesign and implementation of rockery at the uphill slope (Photo: Tiefbauamt Graubünden). The rockery showed only minor damage.

To reduce the probability that an embankment will be surmounted by a block, it was suggested by Kister (2015) to design rockfall protection embankments in general with an uphill slope inclination of at least 60°. This is because the impact angle is essential for the impact process and the impact angle depends on the block trajectory as well as the inclination of the uphill slope of the embankment. But influencing the inclination of the uphill slope of an embankment is easier than influencing the block trajectory and a steep embankment slope will normally reduce the impact angle and with it an upward directed velocity component (Fig. 3.1).

But such a slope inclination of 60° or more cannot be constructed with pure soils. Additional measures have to be used to stabilize such steep slopes. Three different types of stabilization measures had been used in the past for the construction of steep slopes at rockfall protection embankments in Switzerland:

- Reinforcement of the soil structure using old tires
- Stabilization of the embankment slope / embankment body with geogrid reinforcement
- Stabilization of the embankment slope by putting rockery in front of the slope.

July 2017 78/90 Analysis of Existing Rockfall Embankments of Switzerland (AERES), part C

The use of old tires to create steep slopes at rockfall protection embankments was not very often executed in Switzerland. According to the interviews done during the project AERES, only two examples of rockfall protection embankments had been executed in Switzerland, where old tires had been used as supporting measure. Both embankments are located in Canton Lucerne. Unfortunately it was not possible to get information about the construction of these two embankments by the designer. A reason for the low spreading of this stabilization method may be the high effort for the construction.

The use of geogrid reinforcement for rockfall protection embankments is very new in Switzerland. Up to now only few embankments of this type have been constructed or are under construction in Switzerland. As an example the embankment Riemenstalden is shown in Fig. 4.4, which is mainly constructed to protect against snow avalanche, but also for protection of rockfalls.



Fig. 4.4: Embankment Riemenstalden, Canton Schwyz, constructed with geogrid reinforcement, (Photo: B. Kister, 2015)

The design of such embankments is mainly based on the experiments done by Professor Peila and his staff (see part A of the report). To fulfill the fitness for purpose of a rockfall protection embankment with geogrid reinforcement and a slope angle of at least 60° , Hofmann & Mölk (2012) stated: "For geogrid reinforced structures, a freeboard of 1.5 times the sphere diameter can be considered as being on the safe side." This statement was also transferred to the standard ONR 24810:2013 and the applicability of the design diagram is limited to a block with a rotational energy $E_{ROT} \leq 15\%$ for embankments with geogrid reinforcement.

A common measure used in Switzerland to stabilize steep slopes of rockfall protection embankments is the use of riprap or rockery. According to the interviews done with employees of canton departments as well as with design engineers the rockery used in the past at the uphill slope of an embankment was constructed with a batter between 60° to 80°. But in general only less attention had been paid on the behavior of such natural stone walls during the impact of a block. The main reasons to use rockery was to limit the area, which is necessary for embankment construction and/or to stop rolling blocks.

July 2017 79/90 Analysis of Existing Rockfall Embankments of Switzerland (AERES), part C

In the project AERES small-scale quasi-2D-experiments had been done with embankments with stones placed parallel to the slope and stones placed horizontally. The batter of this "rockery" was chosen to be 2:1 (62.6°), 5:2 (68.6°) and 5:1 (79.5°) (Fig. 2.17). The experiments showed that rotating cylinders acting as impactors may surmount an embankment with batter 2:1, if the freeboard is less than 1 block diameter. For the "rough" rockery surface, where the stones had been placed horizontally, the climbing height of the hollow cylinder GS was 1.8 x the block diameter for the first impact and 1.55 x the block diameter for the second impact (Fig. 3.15). For the "smooth" rockery surface a smaller climbing height had been achieved. But for the first impact the climbing height was still 1.3 x the block diameter and for the second impact 1 x the block diameter (Fig. 3.14). According to these results a smooth rockery surface may help to reduce the climbing height of a block in comparison to a rough slope surface. But a slope with an inclination of 60° and equipped with rockery or riprap in general does not guarantee that a free board of 1.5 block diameter will be sufficient, if the block has the shape of a sphere or a cylinder and has rotational energy.

Also for a batter of 5:2 and with a rough slope surface the rotating cylinder was able to surmount the embankment. The freeboard in this test was chosen to be 0.6 x the block diameter, but the trajectory of the block in Fig. 3.18 allows the conclusion that even a freeboard of one block diameter would not be sufficient in this case. On the other hand an embankment with a batter of 5:1 and stones placed horizontally was able to stop the rotating cylinder (Fig. 3.20). The cylinder G showed still an upward movement in this test even though the impact angle was negative. But a freeboard of 0.4 x the block diameter was sufficient to avoid the embankment was surmounted by the block.

4.2 Influence of block rotation

As already shown by Kister (2015) the block rotation plays a very significant role in the impact process. This could be verified by the test series done during the AERES project and the results described before. Model embankments in the tests had been surmounted by cylinder G with rotation in most cases. But as already mentioned by Kister (2015) the test arrangement used in these tests led to a ratio of rotational to translational energy for cylinder G, which exceed the ratio of rotational to translational energy of natural blocks (see Usiro et al., 2006).

A ratio of rotational to translational energy, which is in the same range as for natural blocks, was achieved for the new cylinder GS with a steel lining (Fig. 3.5). For a freeboard of about 0.5 x the block diameter embankments with a batter of 2:1 had been surmounted by the block GS. This occurred irrespective to the construction of the slope with or without rockery. As already mentioned before the embankment with batter 2:1 and "rough" rockery surface was not surmounted by the block GS for a freeboard chosen to 1.9 x the block diameter.

On the other hand block OKT with no or only very low rotation was not able to surmount embankments with the same cross section in the tests. Block OKT with edges showed a significant different behavior. There was still an upward movement of the block OKT during the impact, but the climbing height was significant less. For slender structures, where the thickness of the embankment at the impact point was less than two times the block diameter, the embankment crest was damaged or even totally destroyed, but the block OKT was not able to surmount the embankment (Fig. 3.11). If the thickness of the embankments had been increased, there occurred still significant damage due to the first impact, but for embankments with rockery the penetration depth of the block was limited to less than the half block diameter (Fig. 3.13 c and d). Even for an embankment without rockery and for the second impact block OKT was not able to surmount the embankment and the penetration depth was less than one block diameter (Fig. 3.13 b).

4.3 Influence of block shape and freeboard

As already shown by Kister (2015) an impactor with edges (impactor OKT) may reach the crest level of an embankment with a slope inclination of approx. 1:1, even though the block rotation is very low and the freeboard was chosen to be two times the block diameter (Fig. 4.5). But this occurred for large impact angles. The test series done in the project AERES showed on the other hand, if the impact angle is small because of a steep slope of the embankment, the block OKT with no or low rotation was not able to surmount an embankment with a freeboard of about 0.8 x the block diameter.

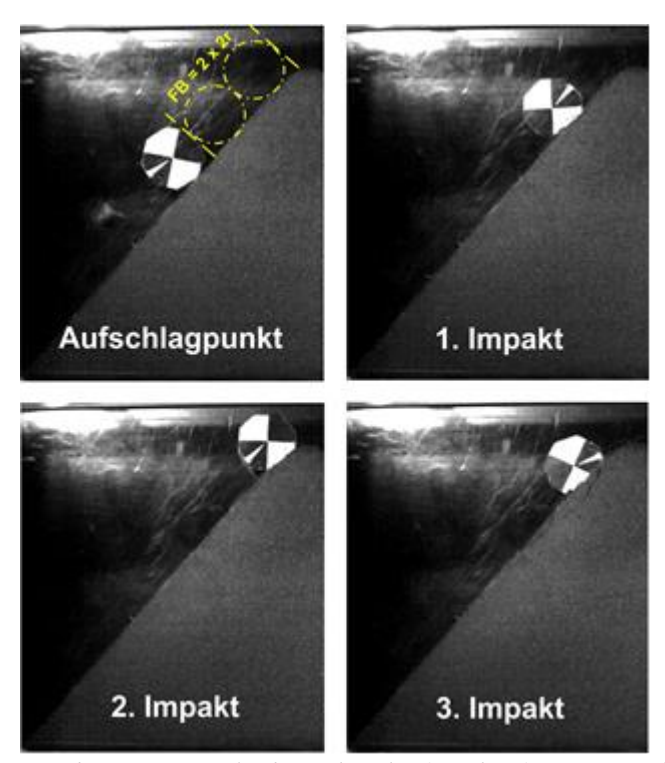


Fig. 4.5: Impact point and maximum climbing height for the first, second and third impact of impactor OKT onto a slope with inclination 1:1, rotational velocity of the block: 1.3 Hz (Kister, 2015).

On the other hand a ratio of rotational to translational energy, which is in the same range as for natural blocks and was achieved for the new cylinder GS with a steel lining, is not sufficient to avoid the embankment will be surmounted by a block. So also the shape of the block is of significant influence for the dimension of the freeboard.

Unfortunately with the existing experimental set-up it is not possible to increase the rotation of block OKT with edges or to define a special rotational block velocity. So the parameters block shape and block rotation are bound together for the existing experimental set-up and cannot be studied separately.

4.4 Embankments with rockery on both slopes

Sometimes in Switzerland rockfall protection embankments had been constructed with rockery on both slopes. As an example embankment Botegh, Canton Graubünden, is shown in Fig. 4.6. The reason for this type of construction very often is a very limited space for the construction of an embankment as shown for example in Fig. 4.6.

July 2017 81/90 Analysis of Existing Rockfall Embankments of Switzerland (AERES), part C



Fig. 4.6: Embankment Botegh, Canton Grisons, 2015 (Photo: Tiefbauamt Graubünden)

Some tests with model embankments of this type had been executed in the project AERES and the test results showed a probability for secondary rockfall at certain circumstances. Because no compression work will be done at the stones of the rockery, so these stones act approximately like a Newton pendulum and transfer the impact energy directly towards the soil behind the rockery. If the volume of soil between the two stone walls is small, the capability to dissipate energy by compression is very limited and a high quota of energy is transferred to the downhill rockery and may cause secondary rockfall (Fig. 4.7). The problem may be reduced, if the soil volume between the two stone walls has a horizontal extent of more than one block diameter (Fig. 3.13 d).

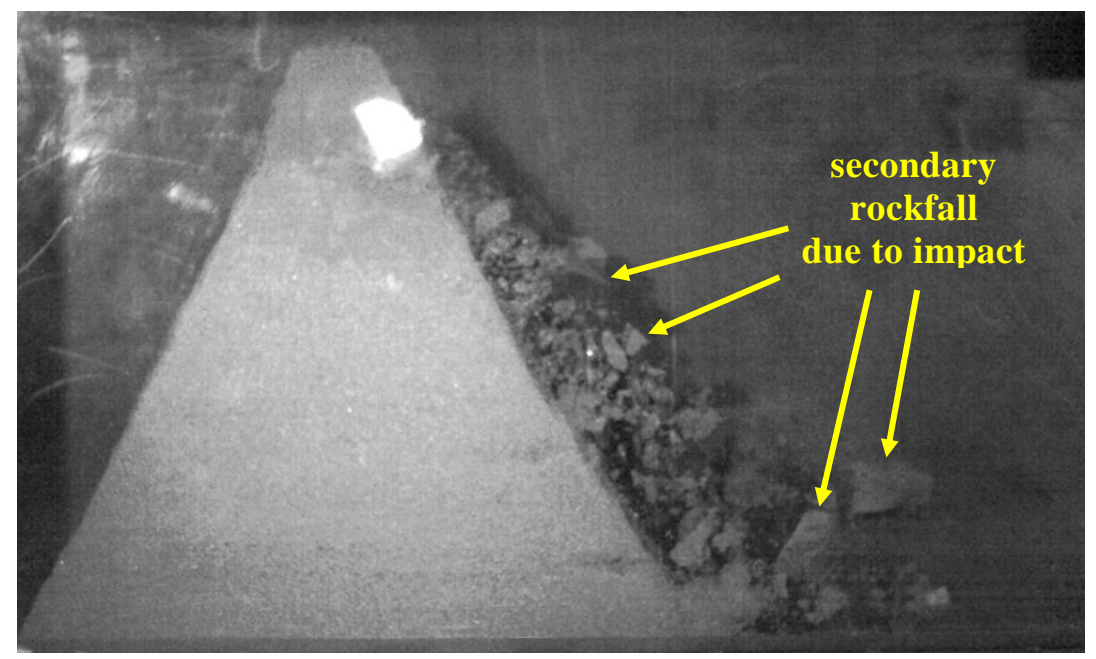


FIG. 4.7: Test OKT_2121FF_9_11-1: Secondary rockfall due to impact of block OKT, embankment was not surmounted by the block, but crest was destroyed.

To avoid the problem of secondary rockfall and construct nevertheless steep slopes at the downhill side of the embankment a construction with geogrid reinforcement is suggested. Such a construction prevents the downhill slope to act as a free boundary because the geogrids will bind back the embankment's soil material (see tests of Peila et al., 2007). Examples of such a construction with geogrids are shown in Fig. 4.8 and Fig. 4.9. With the existing experimental set-up it was not possible to do tests with such a type of embankment, because the lateral fixing of geogrids in a quasi-2D-model is not possible.

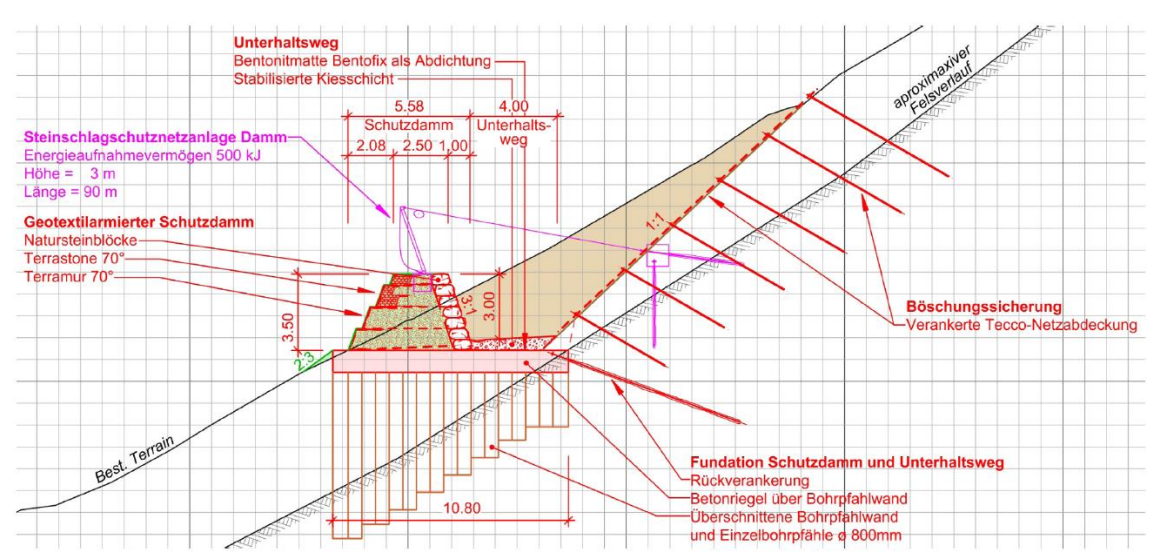


Fig. 4.8: Profile of the planned protection dam at Laugneri East with rockery at the uphill side and geogrid reinforcement and gabions at the downhill side of the embankment (Weggis, 2016).



Fig. 4.9: Example of an embankment constructed with geogrid reinforcement on both slopes nearby Lecco, Italy (Photos: B. Kister).

July 2017 83/90 Analysis of Existing Rockfall Embankments of Switzerland (AERES), part C

4.5 Dissipation of energy

The dissipation of energy has been studied by

- simple physical models (see for example Kister & Fontana, 2011)
- numerical calculations (see for example Ronco et al., 2009) and
- evaluation of experiments in the research project AERES.

According to those studies based on different methods and approaches at least 75% to 85% of the block total kinetic energy will be transformed into compression work, wave energy and heat when the block hits the embankment.

The evaluation of test data received in the project AERES showed that the main part of energy dissipation occurs during the first 6 ms of the impact process. During this period the block translational velocity is reduced to less than the half value for all three types of impactors (Table 3.7). Differences in loss of block velocity and block energy of the three used impactors mainly occur after the large drop of velocity and energy (Fig. 3.22).

A comparison of the velocity time diagram with the pictures made by the high-speed camera shows furthermore the heaviest damage at the embankment occurred at a time, when the translational energy was already dropped to a significant low level (G and GS: less than 15%, OKT: less than 5%, Figures 3.24, 3.25 and 3.26). It may be concluded due to this, that the heaviest damage is not directly produced by the block itself but by the wave, which is a product of the impact process.

4.6 General remarks

A rockfall protection embankment is a geotechnical structure and therefore in Switzerland it has to fulfill the requirements for structural safety for static load conditions as described in the standard specification SIA 267 and the standards referred in SIA 267. General remarks concerning the construction of an embankment can be found for example in Floss (2011) and had been described also by Kister (2015).

Additional the rockfall protection embankment has to withstand an impact of the design block. This means the embankment may be heavily damaged, but not punched-through by the design block in this load case. Up to now there is no standard specification available in Switzerland for this load case. To avoid that a rockfall protection embankment will be punched-through by a block, Kister (2015) suggested a thickness of the embankment at the impact point of at least three times the block diameter. This suggestion had been done due to the results of small and half scale impact tests on embankments made of pure soil. The test series described in this report was mainly based on embankments with rockery at the "uphill" slope. Because the density of stones is significantly higher than the density of soil, a lower embankment thickness at the impact point may be taken into account to achieve the same mass at the impact level of the embankment. On a physical view and taking into account that natural blocks hardly will receive translational velocities higher than 30 m/s, it seems to be unlikely a block will be able to punch-through an embankment, if the counteracting part of the embankment has a mass which is at least 2.5 times that one of the block. This does not mean that such a block will not be able to surmount the embankment due to its rotational energy, a large impact angle and a freeboard, which is undersized.

The fitness for purpose of a rockfall protection embankment is fulfilled, if the embankment will neither be punched-through nor the block will be able to surmount the embankment. The last requirement is much more complicated to fulfill than the former as shown before. Four main parameters have been found, which are dominating this process:

July 2017 84/90 Analysis of Existing Rockfall Embankments of Switzerland (AERES), part C

- the total block energy,
- the ratio of rotational to translational block energy,
- the impact angle, which is a function of block trajectory and slope inclination, and
- the shape of the block.

The experiments had shown that there are some interactions between these parameters, which could not be solved in detail with the existing experimental set-up. So for large impact angles (and slopes with low inclination) the edges of a block may help to move the block towards the crest level, because they act as a kind of crampon. On the other hand a block with edges but only low or no rotation will not be able to surmount an embankment's uphill slope, if the impact angle is small (and the embankment's slope is steep), even then a short freeboard of less than one block diameter has been chosen. Whereas a cylinder with steel lining and a ratio of rotational to translational energy like natural blocks exceeds the freeboard dimension given by Hofmann & Mölk (2012) for a slope with riprap significantly.

4.7 Need for further research

With the existing experimental set-up it is possible to produce rotating cylinders as impactors. With the steel lining placed on a cylinder it was possible to reduce the ratio of rotational to translational energy in such a way that the values are similar to those of natural blocks. But the experiments showed also a significant influence of the block shape. With the block OKT a block with edges had been used in the tests, but only with no or very low rotation. Several efforts had been undertaken to increase the rotation of the block OKT, but with no significant success.

The use of the Austrian standard ONR 24810:2013 is based on experiments with a small steel sphere and may induce large values for the freeboard which result in embankments with enormous heights (Fig. 1.2). The tests with block OKT showed that the freeboard for a block with edges will be less than for a sphere or a cylinder, if the impact occurs on a steep slope and with a small impact angle.

The full size tests done by Peila et al. (2007) and Mongiovì et al. (2014) had been executed with the same type of impactor as it is used for tests on rockfall net fences (Fig. 4.10). In both test series a funicular railway was used. But the use of a funicular railway to accelerate the impactor does not allow block rotation. So indeed in those tests a block with edges had been used, but without taking into account block rotation.



Fig. 4.10: Full size test done by Mongiovì et al. (2014): The block used for the tests complies with the ETAG 027 standard and has a total mass of 13'357 kg. The block was accelerated with a funicular railway therefore block rotation could not be taken into account.

July 2017 85/90 Analysis of Existing Rockfall Embankments of Switzerland (AERES), part C

Analyses of the movies made during the tests done by Peila et al. (2007) show additional an impact angle which is negative (Fig. 4.11). Therefore no velocity component parallel to the slope surface in upward direction is produced in those tests.



Fig. 4.11: Full size test done by Peila et al. (2007). Result of an analysis with the program Tracker of a movie presented by Tenax Geosynthetics. The test shows a negative impact angle.

So the significant question concerning the behavior of a block with edges and with a ratio of rotational to translational energy like natural blocks during the impact process is unsolved. And therefore the question concerning the dimension of the freeboard and by this the necessary height of a rockfall protection embankment could not be solved definitively up to now.

Therefore it is suggested to do tests with a more realistic block shape than a sphere or a cylinder for the impacting block and well defined ratios of rotational and translational energy. This may be able to clarify the question about a realistic freeboard and the fitness for purpose of a rockfall protection embankment. First tests for a new type of experimental set-up, which may fulfill the demands to use an impactor with the same shape as the impactors used for testing rockfall net fences as well as to adjust separately translation and rotation of such an impactor have been done at the HSLU.

July 2017 86/90

Analysis of Existing Rockfall Embankments of Switzerland (AERES), part C

References

- Blovsky, S.: Bewehrungsmöglichkeiten mit Geokunststoffen, PhD thesis, TU Wien, 2000
- **Floss, R.**: ZTVE-StB, Zusätzliche Technische Vertragsbedingungen und Richtlinien für Erdarbeiten im Strassenbau, Ausgabe 2009, Kommentar und Leitlinien mit Kompendium Erdund Felsbau, 4. Auflage, Kirschbaum Verlag, Bonn, 2011
- **Hofmann, R., Mölk, M.:** Bemessungsvorschlag für Steinschlagschutzdämme. Geotechnik, Vol. 35, pp. 22-33, 2012
- JRA, Japanese Road Association: Japanese Rockfall Protection Handbook, 2000
- **Kälin, A.:** Steinschlagverbauung Wilerwald, Gurtnellen, Bauprojekt, Projektbasis und statische Berechnungen, 07.09.2006
- **Kister, B.:** Development of basics for dimensioning rock fall protection embankments in experiment and theory (in German, with abstracts in English and French), research project FEDRO 2012/003, FEDRO report 1524, 2015
- **Kister, B.; Fontana, O.**: On the evaluation of rock fall parameters and the design of protection embankments a case study, Interdisciplinary Rockfall Workshop 2011, Innsbruck-Igls, 2011
- Mongiovi, L.; Bighignoli, M.; Danzi, A.; Recalcati, P.: An impact test on a reinforced earth embankment. Proceedings of the interdisciplinary workshop on rockfall protection Rocexs, Lecco, Italy, 2014
- **Nänni**, C.: Dokumentation des Felssturzes in Caltgeras vom 22.03.2011, Aktennotiz, Tiefbauamt Graubünden, Canton Gaubünden, 2011
- **ONR 24810:** Technischer Steinschlagschutz Begriffe, Einwirkungen, Bemessung und konstruktive Durchbildung, Überwachung und Instandhaltung, ASI Austrian Standards Institute (Österreichisches Normungsinstitut), Ausgabe 15.01.2013.
- **Peila, D.; Oggeri, C.; Castiglia, C.:** Ground reinforced embankments for rockfall protection: design and evaluation of full scale tests, Landslides, 4, pp 255–265, 2007.
- **Plassiard, J.P.; Donzé, F.-V.:** Rockfall impact parameters on embankments: A Discrete Element Method Analysis, Structural Engineering International, 3, 2009.
- Ronco, C.; Oggeri, C.; Peila, D.: Design of reinforced ground embankments used for rockfall protection, Natural Hazards and Earth System Sciences, 9, 2009
- **Schneider, T. R.:** Der Felssturz von Bristen am 1. Oktober 1983, Schweizer Ingenieur und Architekt, Heft 46, 102, 1984
- **Smith, D. D.; Duffy, J. D.:** Field tests and evaluation of rockfall restraining nets, Report No. CA/TL-90/05, Transportation Materials and Research, California Department of Transportation, Final Report, 1990
- **TRB, Transportation Research Board:** Estimating stiffness of subgrade and unbound materials for pavement design a synthesis of highway practice, National Cooperative Highway Research Program, NCHRP Synthesis 382, 2008
- Usiro, T.; Kusumoto, M.; Onishi, K.; Kinoshita, K.: An experimental study related to rockfall movement mechanism, Doboku Gakkai Ronbunshu FVOL. 62, No. 2, pp 377-386, 2006
- Weggis: Risk management in the municipality of Weggis, Excursion Guide Weggis EX1, 13th Congress Interpraevent, 2016
- Yoshida, H.: Movement of boulders on slope and its simulation, in: Recent Studies on Rockfall Control in Japan, 1998

Appendix C1: Block data

			_		1
Test	α	V	E _{trans}	ω	E _{rot}
1001	[°]	[m/s]	[Nm]	[1/s]	[Nm]
G_2121H_9_11	13	6.60	162.0	78.5	73.4
G_2145H_9_11	12	6.50	157.2	76.6	69.8
G_2145H_4K_11	13	6.88	176.2	80.0	76.3
G_2121F_8_11	14	6.08	134.7	80.9	76.3
G_2121_9_11	12	6.00	131.0	80.7	75.8
G_2121FF_9_11	9	6.25	142.2	80.1	74.8
G_2121F_9_11_G	14	5.70	118.3	76.3	67.8
GS_2145H_9_11	12	5.57	86.8	73.8	61.7
GS_2145F_7_11	8	6.48	142.0	43.6	27.7
GS_2145H_9_11_2	13	6.57	145.7	42.9	26.7
GS_2121H_9_11	12	6.71	152.1	40.0	23.3
GS_2121F_8_11	12	6.65	149.7	40.3	23.6
GS_2121F_18_11	10	6.68	150.7	38.5	21.6
GS_2121_18_11	14	6.46	141.0	39.3	22.4
GS_2121FF_18_11	13	7.06	168.3	36.8	19.7
GS_2121FF_18_11_B	10	6.89	160.5	36.8	19.7
GS_2121FG_18_11	14	6.92	161.8	38.5	21.6
GS_2121HG_18_11	15	6.75	154.1	36.3	19.2
OKT_2145H_9_11	14	6.17	128.7	9.9	1.0
OKT_2121H_7_11	14	6.14	127.7	0.0	0.0
OKT_2145H_6K_11	14	6.43	140.1	8.7	0.8
OKT_2121F_8_11	11	6.61	147.8	7.5	0.6
OKT_2121_9_11	13	6.56	142.8	10.2	1.1
OKT_2121FF_9_11	12	6.81	154.2	1.6	0.0
OKT_2121F_18_11	10	6.55	142.6	13.1	1.8
OKT_2121_18_11-B	13	6.63	145.8	10.9	1.2
OKT_2121FF_18_11	11	6.97	161.6	8.7	0.8
G_25121F_17_11	8	5.90	126.7	76.8	68.6
OKT_25121F_17_11	8	6.35	136.3	3.4	0.1
G_5121F_17_11	-4	5.97	129.7	79.0	72.8
OKT_5121F_17_11	-5	6.70	152.0	8.1	0.7

 α : impact angle

v: mean value of translational block velocity just before impact

E_{trans}: translational block energy

ω: mean value of rotational block energy just before impact

E_{rot}: rotational block energy

Appendix C2

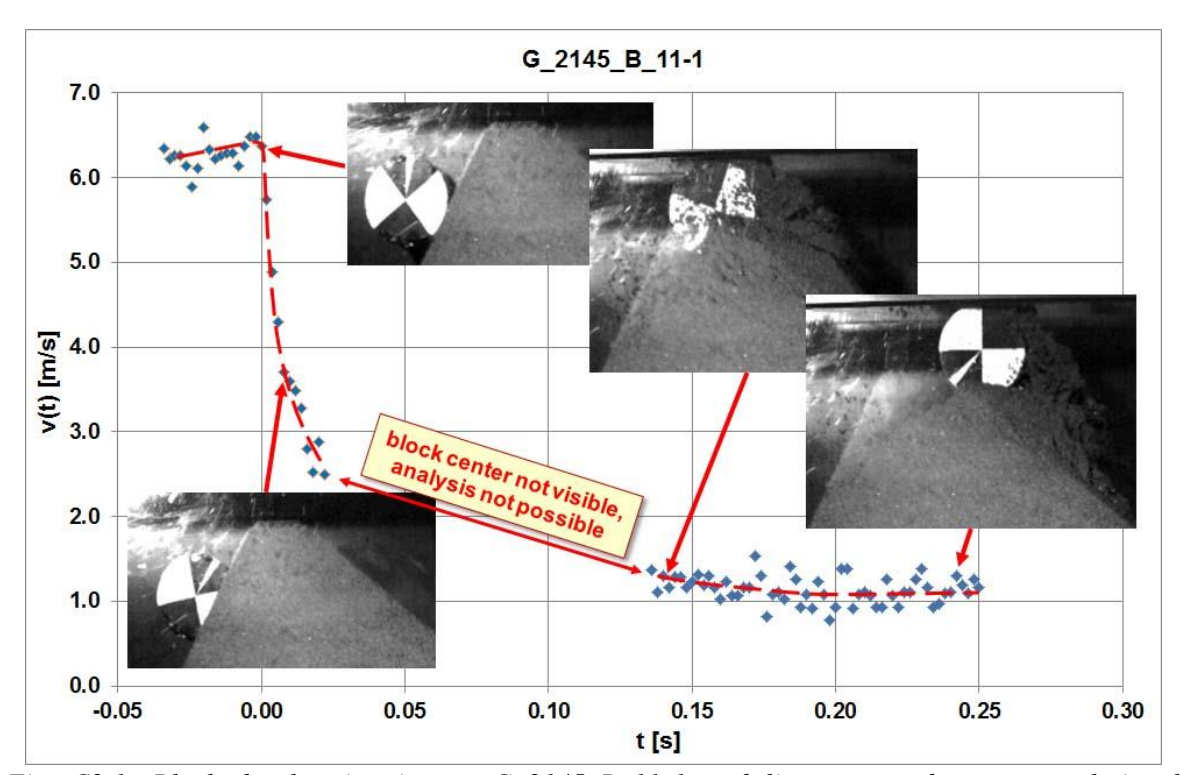


Fig. C2.1: Block deceleration in test $G_2145_B_11-1$, red line: assumed mean translational velocity.

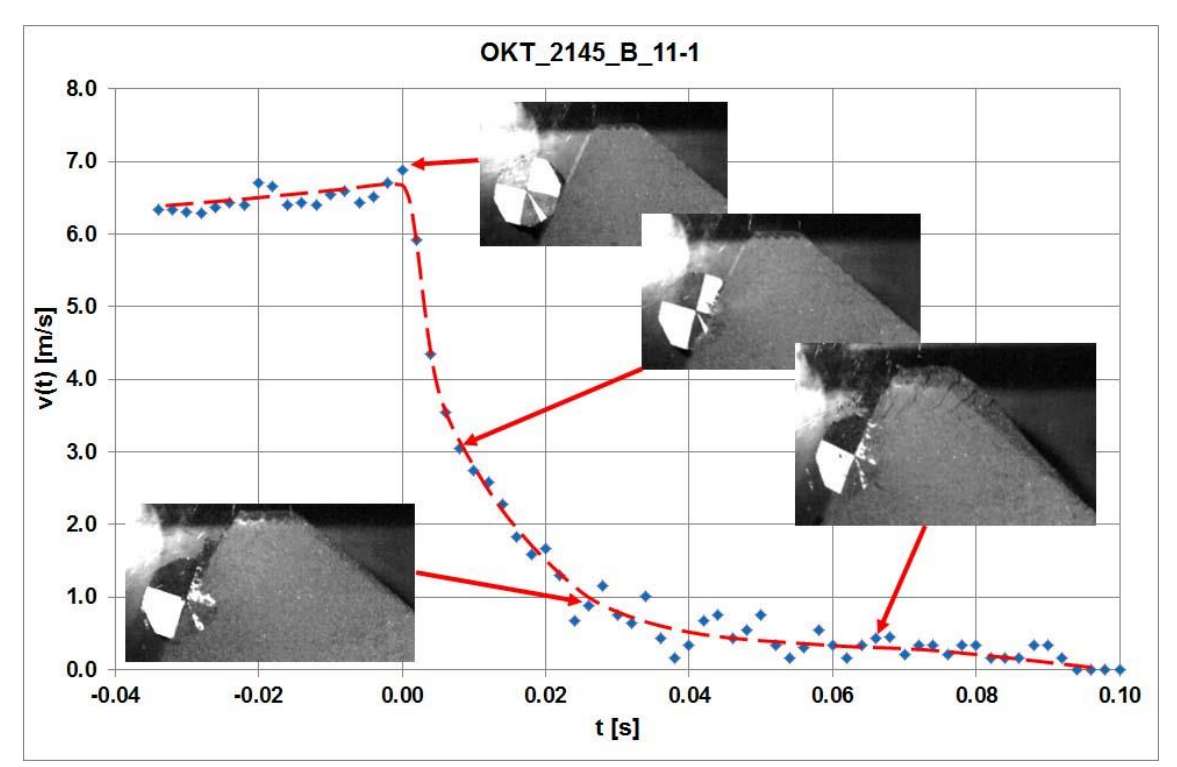


Fig. C2.2: Block deceleration in test OKT_2145_B_11-1, red line: assumed mean translational velocity.

July 2017 89/90 Analysis of Existing Rockfall Embankments of Switzerland (AERES), part C

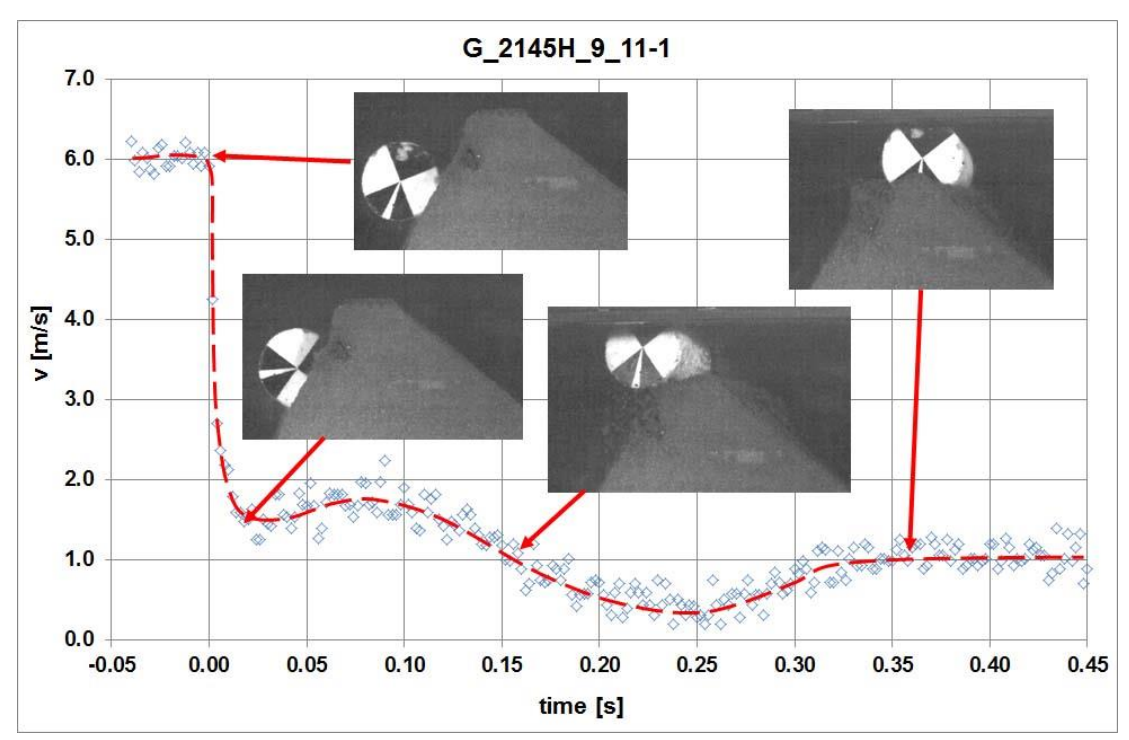


Fig. C2.3: Block deceleration in test $G_2145H_9_11-1$, red line: assumed mean translational velocity.

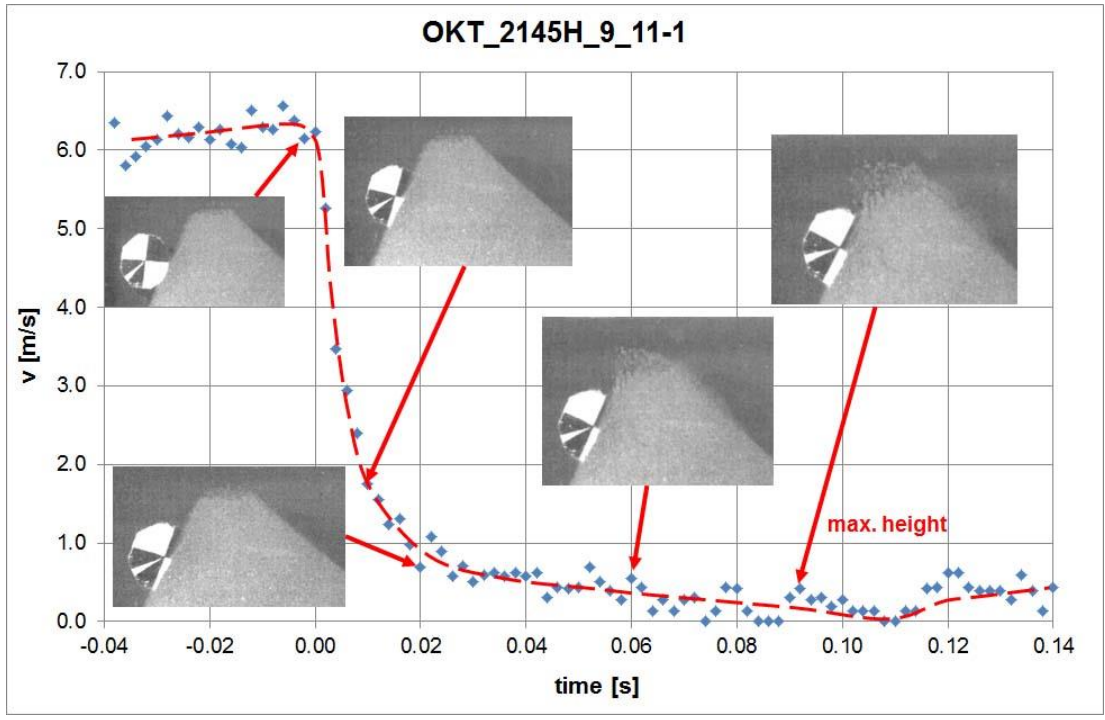


Fig. C2.4: Block deceleration in test OKT_2145H_9_11-1, red line: assumed mean translational velocity.

July 2017 90/90 Analysis of Existing Rockfall Embankments of Switzerland (AERES), part C

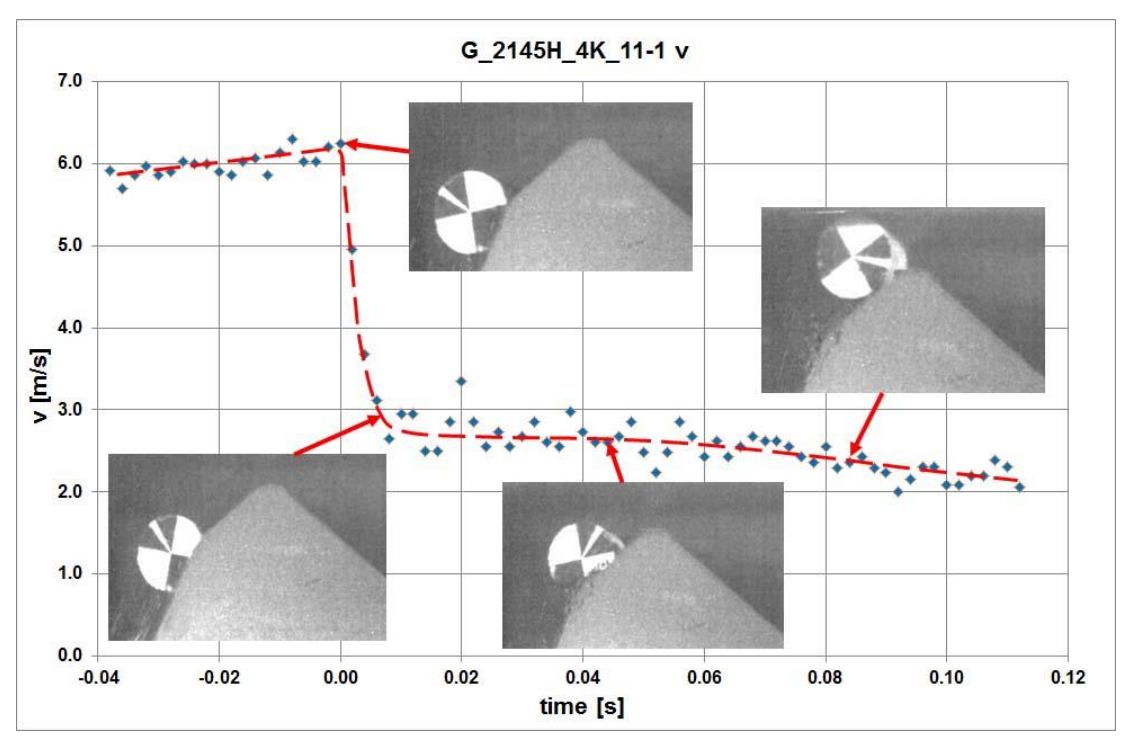


Fig. C2.5: Block deceleration in test $G_2145H_4K_11-1$, red line: assumed mean translational velocity.

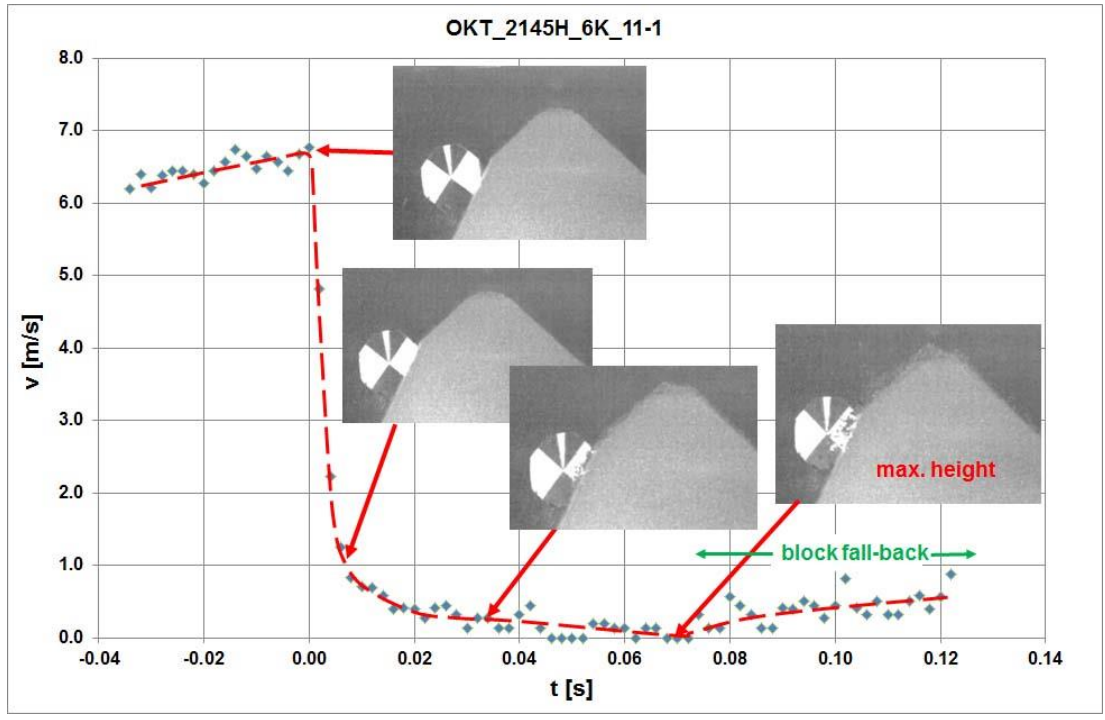


Fig. C2.6: Block deceleration in test OKT_2145H_6K_11-1, red line: assumed mean translational velocity.